Attitude estimation & control of autonomous aerial vehicles

Lotfi Benziane

UNIVERSITÉ DE VERSAILLES SAINT-QUENTIN

ECOLE DOCTORALE STV

SCIENCES ET TECHNOLOGIES DE VERSAILLES

THÈSE

pour obtenir le titre de

DOCTEUR
de l'Université de Varsailles Saint-Quentin

Mention: Automatique, Informatique et Traitement de Signal

Présentée par

Lotfi BENZIANE

CONTRIBUTIONS À L'ESTIMATION ET À LA COMMANDE D'ATTITUDE DE VÉHICULES AÉRIENS AUTONOMES

Thèse préparée au Laboratoire d'Ingénierie des Systèmes de Versailles

Dirigée par

Abdelaziz BENALLEGUE, Professeur, LISV-UVSQ
Abdelhafid El Hadri, Maître de conférence, LISV-UVSQ

Soutenue publiquement le 15 Juin 2015 devant le jury composé de :

Président :	Pascal MORIN, Professeur, ISIR, Paris, FRANCE
Rapporteurs :	Nicolas MARCHAND, Directeur de Recherche, GIPSA-lab, Grenoble, FRANCE
	Maruthi R. AKELLA, Professeur, DAEEM, U-Texas at Austin, Texas, USA
Examinateurs :	Yacine CHITOUR, Professeur, LSS-SUPELEC, Gif-sur-Yvette, FRANCE
	Mustapha HAMERLAIN, Directeur de recherche, CDTA, Alger, ALGERIE
Invité :	Kamel REMILI, Directeur de Recherche, CRD, Réghaïa, ALGERIE

VERSAILLES SAINT-QUENTIN UNIVERSITY

DOCTORAL SCHOOL STV

SCIENCE AND TECHNOLOGY OF VERSAILLES

THESIS

This dissertation is submitted for the degree of

DOCTOR
of Varsailles Saint-Quentin University

Discipline: Control, Computers and Signal Processing

By

Lotfi BENZIANE

ATTITUDE ESTIMATION & CONTROL OF AUTONOMOUS AERIAL VEHICLES

Prepared at Versailles Systems Engineering Laboratory

Supervised by

Abdelaziz BENALLEGUE, Professor, LISV-UVSQ
Abdelhafid El Hadri, Associate Professor, LISV-UVSQ

Publicly defended June 15, 2015 in front of the dissertation committee:

President:	Pascal MORIN, Professor, ISIR, Paris, FRANCE
Reviewers:	Nicolas MARCHAND, Research Director, GIPSA-lab, Grenoble, FRANCE
	Maruthi R. AKELLA, Professor, DAEEM, U-Texas at Austin, Texas, USA
Examiners:	Yacine CHITOUR, Professor, LSS-SUPELEC, Gif-sur-Yvette, FRANCE
	Mustapha HAMERLAIN, Research Director, CDTA, Alger, ALGERIE
Invited:	Kamel REMILI, Research Director, CRD, Réghaïa, ALGERIE

To the memory of my daughter, my angel ALÄA and the memory of my father
To the one that taught me the meaning of life, my mother
To my loving wife Nadia, without her I could never achieve this work
To my children and all my familly and in-laws familly

My daughter Lili, was born in May 15, 2009 at 00:40 Algiers-Algeria, died July 26, 2013 at 19:45 Antony-France

Declaration

I hereby declare that except where specific reference is made to the work of others, the contents of this dissertation are original and have not been submitted in whole or in part for consideration for any other degree or qualification in this, or any other University. This dissertation is the result of my own work and includes nothing which is the outcome of work done in collaboration, except where specifically indicated in the text. This dissertation contains fewer than 65,000 words including appendices, bibliography, footnotes, tables and equations and has less than 150 figures.

Lotfi BENZIANE
2015

Acknowledgements

My thanks and appreciation to my thesis supervisor Prof. A. BENALLEGUE. I am in debt to him for all his teachings, his advices, his invaluable discussions and especially for giving me support throughout the duration of this work. I am grateful as well to PROF. Y. CHITOUR and PROF. A. TAYEBI, they were always humble and I appreciate their help, their guidance, their contribution, their helpful comments and their recommendations. A special thanks to my associate thesis supervisor Ass. PROF. A. EL HADRI and my friend A. SEBA for their help, their presence, the work we have accomplished together.

I owe many thanks to RESEARCH DIRECTOR. M. N. MARCHAND and ASS. PROF. M. R. AKELLA for taking the time to review my thesis report and providing useful comments and suggestions to further improve this dissertation. Thanks also to all members of my dissertation committee, PROF. P. MORIN, PROF. Y. CHITOUR, RESEARCH DIRECTOR M. HAMERLAIN and RESEARCH DIRECTOR K. REMILI for given me generously their time and expertise to better my work. I thank them for their patience and for the honor that gave me by accepting to judge this work.

I must acknowledge as well the director of Versailles Engineering Systems Laboratory - LISV PROF. L. CHASSAGNE and the former director PROF. Y. ALAILI for their help, their welcome and support. Thanks also to all laboratory staff and all those people whose names are not listed here for their assistance and helpful discussions on the subject matter.

It is important for me to mention the significant and huge work done every day by all staff of Versailles Science and Technology doctoral School, my special thanks to his director PROF. C. LARPENT and the School manager MS. V. DELAHAYE.

I am grateful to many friends, colleagues, neighbors, brothers, sisters, all my familly and my in-laws familly in Algeria and France who emotional supported me and help through the painful and enormous loss of my beloved daughter Lili. I mention especially ZEBIDA, ZAHIA, LE GRAND, NAGIB, WAHAB, OLIVIER'S, BRAHIM'S, MANAL, NAZIM, EMMANUEL, H'MED'S, FARID'S, ADEL, FRANCOIS, SOFIANE, JUGURTHA, CHAMSSEDDINE, LILA, ELIZABETTE, RIAD, MAGID'S, DOMINIQUE'S, AHMED'S, LIZA, RAFIK'S, TAKFARINAS, HOSSINE, MOKHTAR, JACQUES, FOUAD'S, REDA, REDHA, MIMICHA, NACER, ODILE, YAMINA, RACHED, PATRICIA, MOUFIDA, WALID'S, ZOUAOUI, HAMA, MOHAMMED AND

Mohamed's, Lambert, Aissa, Fafi, Nabil, Asma, Fred, Farouk's, Abdelaali, Athman, Mohammed Abdellah, Boubaker's, Wahiba, Wissem, Omar, Ali's, Yacine's and Yassine's, Abdelrahmen, Lokmane, Larbi, Foufa, Luc, Samira, Hiba, Bachir's, Naima, Malek, Amine's, Fawzi's, Sidou, Taher, Smail, Karima, Kamel's, Karim's, Abdelsalam, Lotfi, William, Youcef's, Naafa, Yasser, Abdelnour, M'barka, Tarek's, Azou, Samir's, Samer, Khaled's, Khalid, Akram, Messaoud and Messaoud's, Eric, Aziz's, Abdel's, Hichem's, Tuyet, Kadour, Saadi, Abdelkader, Zouhir and many others. Please forgive me if I forgot someone...

Abstract

Nowadays, we see a growing popularity of the use of Unmanned Aerial Vehicles (UAV) of especially Vertical Take-Off and Landing (VTOL) type. One of the most known VTOL is the quadrotor or Quadcopter which is probably the most used one as a research platform. This thesis deal with attitude control and estimation techniques applied to a rigid body moving in 3D space such as Quadcopter VTOL. The first contribution of this thesis is the design of a new class of complementary linear-like filters allowing the fusion of inertial vector measurements with angular velocity measurements and combined with algebraic algorithms as TRIAD, QUEST etc. to give an efficient attitude estimation solution. This class of filters allows several possibilities of implementation such as the order of the filters which can be chosen high in order to reduce more the measurement noise and the form of the filters that can be direct or passive and the ability to take into account the possible gyro bias. Lyapunov analysis shows the global asymptotic convergence of the estimation errors to zero. The same principle of data fusion is used for the proposed new attitude control law in which the complementary filters were included to reduce the effect of measurement noise. The obtained controller ensures almost global stability of the desired equilibrium point; it represents the second contribution of this thesis. The third contribution takes into consideration an interesting special case, where instantaneous measurements of attitude and angular velocity are unavailable. A first order linear auxiliary system based directly on vector measurements is used in an observer-like system to handle the luck of angular velocity. The proposed controller ensures almost global asymptotic stability of the trajectories to the desired equilibrium point. Detailed sets of experiments were done to validate the obtained results.

Résumé

Les drones ou systèmes de drones aériens jouent un rôle de plus en plus important dans tous les domaines, spécialement les drones à décollage et atterrissage verticaux. L'un des plus connus est le Quadrotor et, sans doute, il est la plateforme de recherche la plus utilisée. Cette thèse traite le problème de l'estimation et de la commande d'attitude appliqué à un corps rigide se déplaçant dans l'espace 3D tel que le Quadrotor. La première contribution de cette thèse est la conception et l'implémentation d'une solution d'estimation d'attitude. Celle-ci est basée sur un ensemble de filtres complémentaires combinés avec un algorithme algébrique tel que TRIAD, QUEST, etc. avec la possibilité de choisir deux formes différentes des filtres: la première dénommée forme Directe, et la seconde dénommée forme Passive. Les filtres proposés ont une flexibilité dans le choix de l'ordre qui peut être pris grand afin de bien réduire l'effet du bruit de mesure et permettent d'aboutir à un estimateur qui peut prendre en compte le biais éventuel des gyromètres. L'analyse par la théorie de Lyapunov prouve que les erreurs d'estimation tendent globalement et asymptotiquement vers zéro. Une suite logique de cette première contribution est la proposition d'une solution pour la commande d'attitude qui constitue la deuxième contribution de cette thèse. Elle se traduit par le développement d'une nouvelle loi de commande d'attitude d'un corps rigide dans l'espace 3D, dans laquelle seulement les vecteurs de mesures inertiels avec les mesures des gyromètres sont utilisés. Elle utilise le principe de fusion des données à travers un filtre complémentaire permettant l'élimination des bruits des mesures tout en assurant une stabilité presque globale de l'équilibre désiré. La troisième contribution est une loi de commande pour la stabilisation d'attitude sans mesure de vitesse angulaire, ni mesure d'attitude. Pour cela, un système linéaire auxiliaire basé sur les mesures des vecteurs inertiels a été introduit. Ce dernier se substitue au manque de l'information de la vitesse angulaire. L'analyse de stabilité du contrôleur proposé est basée sur la théorie de Lyapunov couplée avec le théorème de LaSalle. Elle permet de conclure sur la stabilité presque globale de l'équilibre désiré. Les performances des solutions proposées ont été validées par un ensemble de tests expérimentaux.

Contents

List of Figures

List of Tables

Nomenclature

Roman Symbols

b, b_i Vectors $\in \mathbb{R}^3$ expressed in mobile frame $\{\mathscr{B}\}$

r, r_i Vectors $\in \mathbb{R}^3$ expressed in inertial frame $\{\mathscr{I}\}$

$\{\mathscr{B}\}$ Mobile reference frame

$\{\mathscr{I}\}$ Inertial reference frame

$\{n\}$ Navigation reference frame

$\mathbb{R}^{(n\times m)}$ The set of real matrices of n rows and m columns

$\mathbb{R}^n$ N-dimensional vector space over the field of the real numbers

$\mathbb{R}_+$ The set of positive real numbers

$\mathbb{R}_+^*$ The set of strictly positive real numbers

$\mathbb{S}^2$ The two unit sphere definded on $\mathbb{R}^3$

$\mathbb{S}^3$ The three unit sphere definded on $\mathbb{R}^4$

$\mathscr{R}$ The mapping from $\mathbb{S}^3$ to $SO(3)$

$\mathfrak{so}(3)$ Lie algebra of $SO(3)$

$a_{\mathscr{B}}(t)$ Accelerometer vector measurements expressed in $\{\mathscr{B}\}$

$C(s)$, $H(s)$ Transfert functions, where s is Laplace variable

g Gravitational earth vector magnitude $g = 9.81\,(m/s^2)$

J Rigid body moment of inertia or inertia matrix expressed in $\{\mathscr{B}\}$

$m_{\mathscr{B}}(t)$ Magnetometer vector measurements expressed in $\{\mathscr{B}\}$

Q, $Q(t)$ Unit Quaternion belonging to $\mathbb{S}^3$

R Rotation matrix of the mobile frame $\{\mathscr{B}\}$ relative to the inertial fixed frame $\{\mathscr{I}\}$

$S(\cdot)$ Lie algebra isomorphism from $\mathbb{R}^3 \rightarrow \mathfrak{so}(3)$

$SO(3)$ Special Orthogonal Group

$v(t)$ Linear velocity belonging to $\mathbb{R}^3$ expressed in $\{\mathscr{I}\}$

x_{pq} The pure quaternion of $x \in \mathbb{R}^3$ such that $x_{pq} = (0, x)$

Constant Symbols

$0_{3n\times 3}$ 3n by 3 zero matrix

0_{3n} 3n by 1 zero vector

0_3 3 by 3 zero matrix

$\mathbf{0}$ 3 by 1 zero vector

I_d 3 by 3 identity matrix

I_k k by k identity matrix

Greek Symbols

(ϕ, θ, ψ) Euler angles (roll, pitch, yaw)

$\omega(t)$ The real angular velocity belonging to $\mathbb{R}^3$ expressed in $\{\mathscr{B}\}$

$\omega_m(t)$ Rate gyros vector measurements expressed in $\{\mathscr{B}\}$

$\tau(t)$ The torque $(N.m)$ expressed in $\{\mathscr{B}\}$

$\xi(t)$ The position belonging to $\mathbb{R}^3$ expressed in $\{\mathscr{I}\}$

Other Symbols

$\|\cdot\|$ The l^2 norm or the Euclidean norm

$\odot$ The quaternion product

$\otimes$ The Kronecker product

$\times$ The vector cross product

$x^T y$ The scalar product of x by y

Acronyms / Abbreviations

AGAS Almost Global Asymptotic Stability

CCW Counter ClockWise

COM Center Of Mass

CW ClockWise

DCM Direction Cosine Matrix

ECEF Earth Centered Earth-Fixed

ECI Earth Centred Inertial

ENU East, North, Up

ESC Electronic System Control

GPS Global Positioning System

IMU Inertial Measurement Unit

LTP Local Tangent Plane

NED North, East, Down

PWM Pulse Width Modulation

RPAS Remotely Piloted Aircraft Systems

VTOL Vertical Take Off and Landing

Introduction

Traditionally, Unmanned Aerial Vehicles (UAV) or Remotely Piloted Aircraft (RPA) or Remotely Piloted Aircraft Systems (RPAS) have been developed and used in military applications. Nowadays, we see a growing popularity of the use of UAV in civilian fields, especially type Vertical Take-Off and Landing (VTOL) vehicle (for instance, see Figure 0.0.3 for UAVs Categories [15]). Indeed, their immense potential and the multiplication of applications open new perspectives in many sectors of industry. Some applications are already being considered such as Photography and Mapping, parcel delivery services, inspection of railway lines or power lines, Search and Rescue, observation of the pipeline network, visual support in emergency interventions, etc. (for instance, see the excellent survey paper [51]). The outcome of these applications will depend on the reliability of the emerging technologies. In this context, the challenge is to develop systems that offer a higher degree of autonomy and ability for performing complex tasks.

Generally, the degree of autonomy of an UAV depends on how much systems are embedded onboard vehicle. To execute a given mission, onboard systems can be classified as illustrated in Figure 0.0.1. The very low level is the "Vehicle" system, where actuators and sensors are placed. Actuators receive the appropriate control signals from "Vehicle Control" system in which, the vehicle state and reference trajectories are taken in consideration to generate controls for both translational and rotational motions. The vehicle state and references trajectories are generated by "Estimation & Localization" and "Navigation" systems respectively. The outputs generated by these two last systems are based on the behavior of the vehicle, which can be expressed by sensor measurements. The very high level mission description is done in "Mission" systems, where the current available technologies do not allow to limit the degree of human intervention. To guarantee a minimum degree of autonomy two systems must be embedded. The first one is "vehicle control" system and the second is "Estimation & Localization" system. Several techniques ensuring the efficient operation of these two systems exist in the literature and the three main contributions of this thesis belongs to these techniques. They constitute solutions to the attitude estimation and control problems.

Attitude estimation is definitely one of the most studies problem in literature. Various

attitude parametrizations [63, 85, 91] have been used to propose variety of solutions for the attitude determination. The widely used techniques are based on Kalman filter (KF) or Extended Kalman filter (EKF) [24, 25, 49, 88], and his many variants such as Multiplicative Extended Kalman Filter (MEKF) [37, 83, 84], Robust Extended or Unscented Kalman filter (REKF or RUKF) [46, 90], Cascaded Kalman–Particle Filter (C-KPF) [80], Cubature Kalman filter (CKF) [115] or Square-Root Cubature–Quadrature Kalman Filter (SR-CQKF) [52]. The effectiveness of Kalman based solutions is due to its ability to fuse heterogeneous signals. Some recent techniques like linear or nonlinear complementary filters [9, 31, 54, 61, 65, 66, 94, 107] have the same property. A comparison between complementary and Kalman filtering can be found in [39]. Generally, the above mentioned results are based on the assumption that the used reference vectors are constant. Other class of techniques take into consideration the time-varying reference vectors aspect when vehicles equipped with INS/GPS sensors are subjected to strong accelerations, by using linear velocity measurements from Global Positioning System (GPS) such as in [4, 34, 42, 64, 79] or by using the linear velocity measured in the mobile frame such as in [41]. Some other results proposed a simultaneous estimation of attitude and angular velocity, like in [47] where the authors use Lagrange-D'Alembert principle and two or more non-collinear vector measurements to propose an observer for both attitude and angular velocity. In [71], only one vector measurement and the angular velocity have been used to estimate the attitude.

As claimed in [6], there exist two attitude estimation approaches : The first one considers the existence of attitude measurements determined usually by algebraic methods, after these noisy measurements will be filtered, see Figure 0.0.2-(a). The drawback of this approach is the distortion of noise characteristics due to existing nonlinear operations in algebraic methods. Thus, Batista *et al.* [6] proposed a reverse strategy, see Figure 0.0.2-(b), where the noisy measurements are first filtered and after attitude are determined. This solution leads to a globally asymptotically stable filters, that designed as a Kalman filter using Linear Time Variant (LTV) representation of the nonlinear kinematic equation. The theoretical drawback of this solution is the fact that observability analysis was done on the obtained LTV system and mathematically it doesn't mean that the initial non linear system is observable. Inspired by this approach, a new class of linear-like complementary filters are proposed in this thesis. The proposed filters can have *Direct* and *Passive* form, similarly to the work presented in [61]. Moreover, it is shown using Lyapunov theory that the errors converge globally asymptotically to the desired equilibrium point for a general n-order filters. In addition, the estimation of the rate gyro biases are considered. This constitutes the first contribution of this dissertation. The proposed solution is validated by experimental results using a Quadrotor test-bench. As a logical sequel, the second contribution of this thesis deals with the problem of attitude control

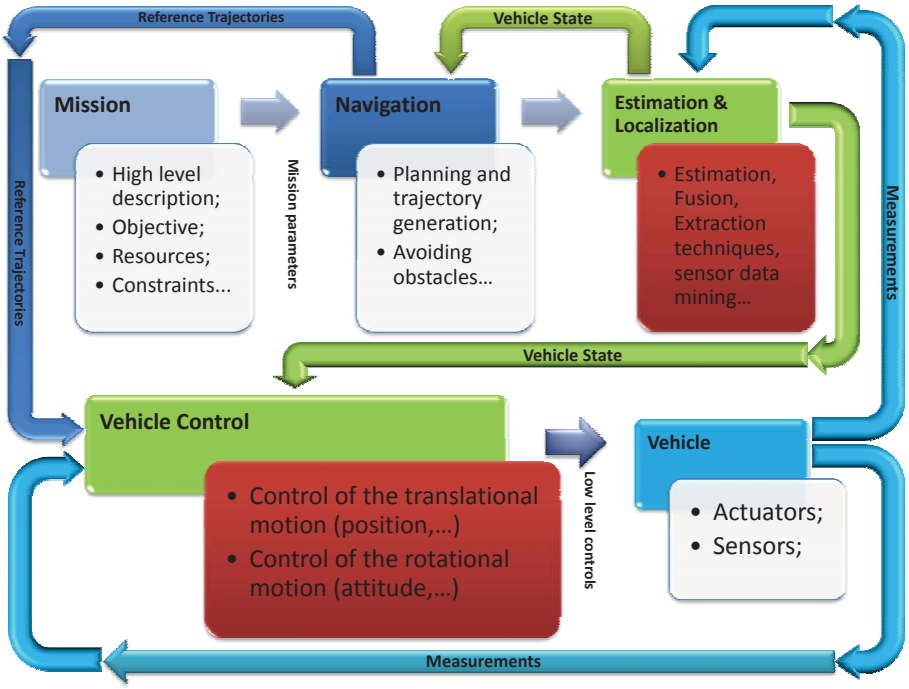

Figure 0.0.1: The structure of navigation, guidance and control systems for mission execution of a VTOL

of a rigid body moving in 3D space such as Quadrotor VTOL type.

Many works on attitude control apply their research results on VTOL aircraft type, such as in [36] where a global asymptotic stabilizing control law with bounded inputs was proposed. A second order and high-order sliding mode techniques were successfully used to control a quadcopter in [8, 27]. Others make use of a full state backstepping technique as in [59, 60] or adaptive fuzzy control technique in [113] for trajectory tracking of a quadcopter. Some works take into consideration the aerodynamic drag forces, such that in [43], where nonlinear feedback control laws were proposed to stabilize VTOL reference trajectories. An excellent review of basic control design and feedback control for underactuated VTOL can be found in [44]. A quaternion-based feedback was used in [98] to stabilize the attitude of a VTOL and in [35] a quaternion-based feedback for the attitude stabilization based on nested saturation approach was experimentally tested on a quadrotor. Also, Vision and rate gyro were used as information source to stabilize a VTOL to the equilibrium pose, like in [74]. In [77, 78] authors proposed a control law for attitude stabilization of a flapping wing micro aerial vehicle. A more recent work proposed a full actuation position and attitude control law for an augmented VTOL with complementary thrust-tilting capabilities [45]. All of these solutions can be included in "Vehicle control" systems, as depicted in Figure 0.0.1.

Despite the significant existing number of solutions to the attitude control problem, it

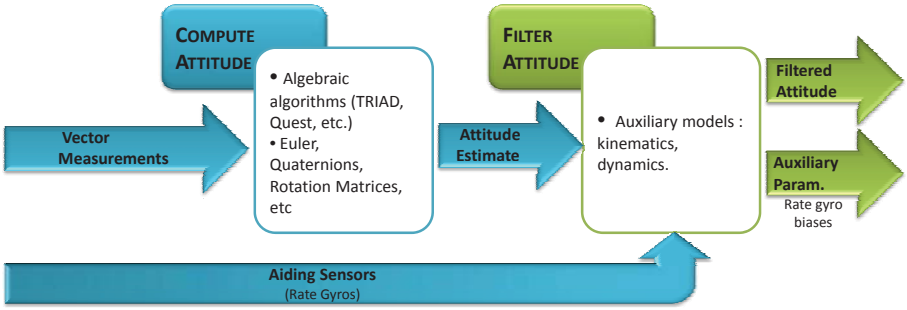

(a) Classic attitude estimation solution

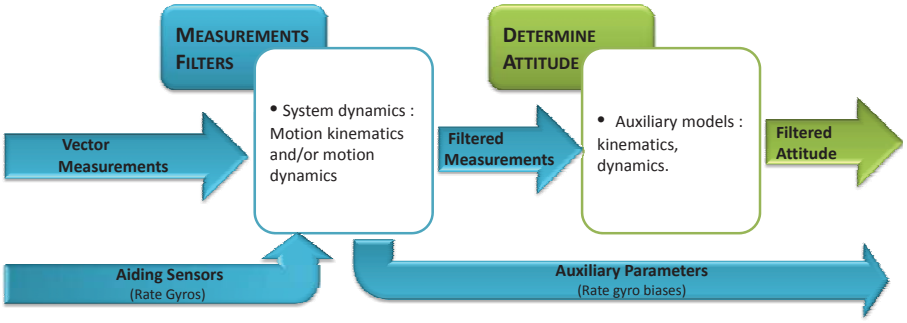

(b) Sensor-based attitude estimation approach

Figure 0.0.2: Attitude estimation approaches [6]

remains an attractive research topic [20, 110]. Many recent work deal with this problem (see for instance, [11, 45, 55, 101]). Almost all VTOL attitude control laws use measurement data from an embedded Inertial Measurement Unit (IMU). Most of them first estimate the attitude and after control it. In this thesis, a new control law that uses only the inertial vector measurements and angular velocity to track attitude trajectories is proposed. Presented results show the effectiveness and performances of the proposed solution even if the measurements are corrupted by noise. This is due to the introduction of a new complementary-like filter in the control law design. Using Lyapunov theory coupled with LaSalle's theorem, it is shown that almost all trajectories of the closed loop dynamics are asymptotically globally stable. The notion of "*almost global asymptotic stability*" is used in the sense that a dense and open set belonging to the Special Orthogonal Group $SO(3)$ exists, where all trajectories are stable. This notion was used, since it was shown that it is impossible to achieve a global asymptotic stabilization using continuous time invariant state feedback [14]. Although unit quaternion are used in stability analysis, the unwinding phenomena is avoided. This constitutes the second contribution of this thesis.

The third and last contribution of this thesis deals also with the problem of attitude control of a rigid body moving in 3D space, but with taking into consideration a special interesting case where no rate gyros measurements are available. Indeed, in [95, 100] authors propose a

new class of attitude controllers, in which neither the angular velocity nor the instantaneous measurements of the attitude are used in the feedback control. This solution uses only raw vector measurements to perform attitude stabilization of a rigid body. In the same context, a new "velocity-free" control law is proposed, in which a new auxiliary system was introduced to handle the luck of angular velocity. This can be used as main or backup controller in applications where prone-to-failure and expensive gyroscopes are used. The "*almost global asymptotic stability*" of the closed loop system is shown and a comparison with existing work illustrates the effectiveness and performances of the proposed solution. Also, a detailed procedure for gain tuning is used, where a constrained nonlinear optimization technique is adapted to evaluate the adequate values of all parameters.

This thesis is organized as follow :

In Chapter 1, some mathematical tools and attitude representations are presented. Especially, the used attitude parametrization, such as rotation matrix, unit quaternion and Euler angles. After, the attitude kinematics and dynamics are detailed. Since Quadcopter are used in experimental results, the different levels of its modeling are presented briefly. The chapter is ended by stating the different assumptions used in this thesis.

In Chapter 2, simple and efficient algorithms for attitude estimation based on data fusion using complementary linear-like filters are presented. First of all, a globally asymptotic complementary linear-like filters are proposed and combined with TRIAD algorithm to give an attitude estimation solution. The solution leads to several possibilities for implementation as either in direct form or passive form and also by choosing the adequate *n-order* of the filter. The adaptive estimation of gyro bias is also considered. Lyapunov analysis results for the proposed direct and passive complementary filters show global asymptotic convergence of estimation errors to zero. The chapter is ended by validation and comparison simulations.

In Chapter 3, The same principle of data fusion is used to address the problem of attitude control and stabilization. Then, instead of using direct raw measurements in the control law we propose a new solution that includes the principle of complementary filters. The stability analysis of the tracking error based on Lyapunov theory coupled with LaSalle's invariance theorem prove that almost all trajectories converge asymptotically to the equilibrium point. The effectiveness of the proposed solution is validated by simulation results.

In Chapter 4, we address the problem of attitude stabilization of a rigid body, in which neither the angular velocity nor the instantaneous measurements of the attitude are used in the feedback control, only raw vector measurements are needed. The design of the controller is based on an angular velocity observer-like system, where a first order linear auxiliary system based directly on vector measurements is introduced. The introduction of gain matrices provide more tuning flexibility and better results compared with existing works. The proposed

controller ensures almost global asymptotic stability. The performance and effectiveness of the proposed solution are illustrated via simulation results where the gains of the controller are adjusted using non linear optimization.

In Chapter 5, the proposed solutions for attitude estimation and control are validated using experimental results. The designed test-bench based on open-hardware and open-software multirotor projects is presented with its components and the different steps needed to turn on the platform. Thus, some results related to calibration operations and inertia matrix determination are exposed. The obtained experimental results illustrate the effectiveness and performance of the proposed solutions presented in previous chapters.

(a) Nano, Micro and Mini drones

(b) Mini drones

(c) Close Range drones

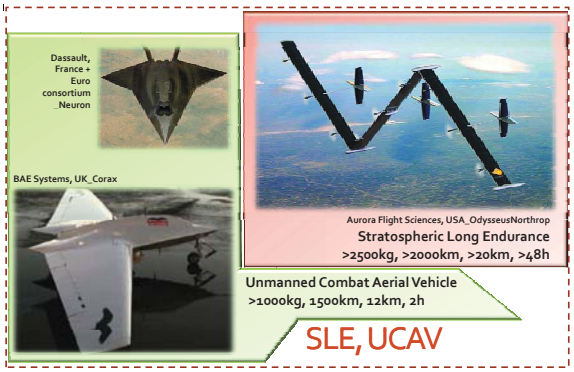

(d) Stratospheric Long Endurance and Combat drones

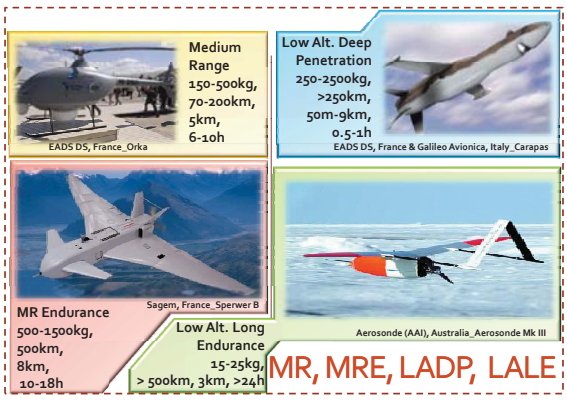

(e) Medium Range, Low Altitude, Long Endurance drones

(f) Short Range Drones

(g) Medium and High Altitude, Long Endurance drones

Figure 0.0.3: Categories of UAVs[15]

Chapter 1

Mathematical Background and Quadrotor Modeling

1.1 Introduction

At the beginning of the 21st century, the evolution of aerial robotics has allowed a wide range of applications fields [51]. One of the most known aerial robot is the Quadrotor or Quadcopter and probably the most used one as a research platform. Mainly, this is due to its simple structure and low cost. Many universities have designed their own quadrotor and an interesting open source projects are growing [51, 57]. The quadrotors are belonging to "VTOL" vehicles family. They are equipped with a set of sensors allowing the measurements of the position, linear and angular velocities, and other physical quantities used to estimate crucial information such as attitude. These data are required to control the motion of the quadrotors and it is clear that the modeling of the quadrotor is also needed. The quadrotor modeling is well studied in the literature [13, 26, 62, 76] and different levels of modeling can be considered.

The motion of quadrotor, considered as a rigid body, is decomposed into a translational and rotational motions. The study of the rotational motion brings us back to the mathematical parametrization of attitude [85], but also to the study of attitude kinematics and dynamics [20, 21, 63, 91]. Since the quadrotor is an underactuated system (which mean that the number of actuators are less then the number of degrees of freedom), the "attitude measurements" is very important. Unfortunately, it is well known that the attitude is not physical measurable quantity. Therefore, other information are used to estimate it, such as the acceleration vector measured by accelerometers, the earth magnetic field vector measured by magnetometers and the angular velocity vector measured by rate gyros.

Although this chapter contains many well-known concept and available in countable ref-

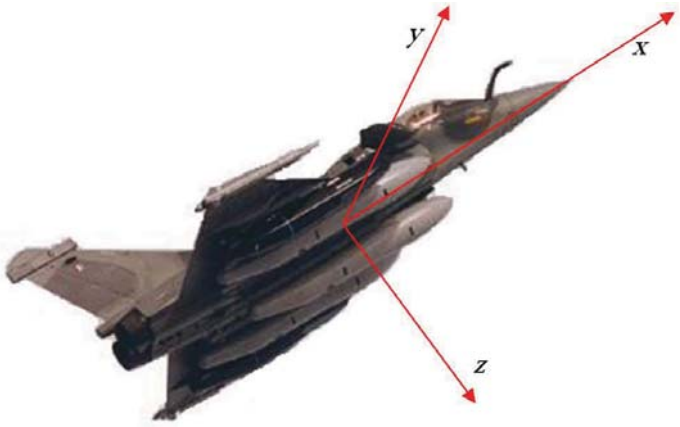

Figure 1.2.1: Mobile frame

erences, it constituted a corpus of information that I wanted to find in a single Chapter, in which mathematical preliminaries that will be used in the present work are presented. Firstly, reference used systems are recalled. Secondly, all attitude parametrization used in this work are presented. Finally, attitude kinematics and dynamics are elaborated in the goal to give a mathematical model to the quadrotor. The presented quadrotor modeling are based on the distinction between various modeling levels, where rigid body modeling constitutes the highest level.

1.2 Reference systems

1.2.1 Mobile reference system $\{\mathscr{B}\}$

This reference is associated to the vehicle (the specific reference to the mobile), with its origin at the Center Of Mass (COM) of the mobile as illustrated in Figure 1.2.1. The axes of this frame are :

- $(x-axis)$: directed along the longitudinal axis oriented from the rear towards the front
- $(y-axis)$: directed along the transverse axis oriented from left to right
- $(z-axis)$: completes the Direct Cartesian coordinate following the rule of the right hand.

1.2.2 The navigation reference system $\{n\}$

Defined in the "Local Tangent Plane" (LTP), its origin is always at the current position of the mobile and the xy plane is tangent to the surface of the earth. Two conventions LTP systems

are common in navigation:

- NED: North, East, Down (down or to the gravity vector), see Figure 1.2.2
- ENU: East, North, Up (up)

In this work, the NED frame was chosen.

1.2.3 The ECI (Earth Centered Inertial) reference system $\{\mathscr{I}\}$

This is a system in which Newton's laws are applicable. It does not follow the rotation of the earth and therefore do not rotate relative to the stars. The origin of this system is the center of the Earth. The corresponding coordinate system is a coordinate system with axes marked :

- $(x-axis)$: to the "Vernal Equinox" (distant star)
- $(y-axis)$: north pole,
- $(z-axis)$: to complete the direct reference system.

1.2.4 The ECEF (Earth Centered Earth-Fixed) reference system $\{e\}$

It follows the rotation of the earth and the origin of this system is the center of the earth, therefore this system coincides with the inertial system once a complete revolution of the earth on itself, see Figure 1.2.2.

- $(x-axis)$: to the Greenwich meridian (longitude = O)
- $(y-axis)$: north pole,
- $(z-axis)$: to complete the direct reference system.

1.2.5 Geodetic Coordinates system (The WGS-84 standard)

Several problems arise when we wish to get absolute position of an object on the globe.

- The earth is not actually a volume of regular shape. It is usually treated as a geoid or ellipsoid.
- The geoid is an equipotential surface coinciding with the "mean sea level" and at each point perpendicular to the direction of the "local vertical" (direction of gravity).

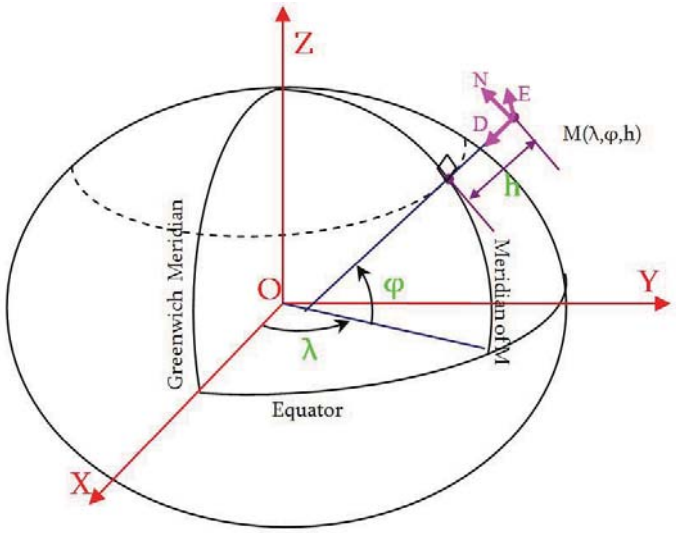

Figure 1.2.2: ECEF, NED and Geodetic Coordinates systems

- The ellipsoid is a mathematical surface coinciding as well as possible with the "geoid" and usually characterized by its "semi-major axis" and "flattening". Depending on the location of the globe where there is some local ellipsoid models that are more accurate than others.

The "WGS 84" is a three-dimensional terrestrial reference system expressing the position in terms of latitude, longitude and altitude. These are based on a reference ellipsoid which is an approximation of the shape of the Earth, see Figure 1.2.2.

The latitude φ : is the angle between the equatorial plane and the normal to the surface of the Earth (ellipsoid) at the point in question. It is zero at the equator and is counted positive for the northern hemisphere, negative for the southern hemisphere.

The longitude λ : is the angle between the Greenwich meridian and the desired point. It is counted positively towards the East.

The height h : "ellipsoidal height - not to be confused with altitude", is the difference in meters between that point and the reference ellipsoid measured normal to the ellipsoid. This value is set in a geodetic system and may differ from the altitude of several tens of meters. It should be noted that in general the satellite positioning systems provide ellipsoidal height and not an altitude.

The altitude of a point M of a topographic surface is an approximation of the distance between the point and the reference surface known as the geoid.

Attitude parametrization	Globality	Uniqueness
Rotation matrices	yes	yes
Axis-angle	yes	no
Quaternions	yes	no
Euler angles	no	no

Table 1.3.1: Global and unique properties of attitude parametrization

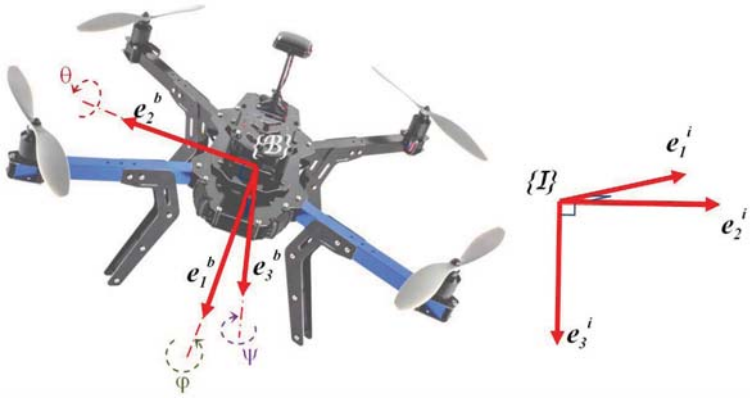

Figure 1.3.1: Rotation Matrix and Euler Angles

1.3 Attitude Representation

The orientation of a rigid body in space is often crucial, especially in aerospace applications. In this section, we provide a description of various attitude parametrizations [85]. Especially, four type of attitude representations are detailed, as described in Table 1.3.1. The natural parametrization of rigid body attitude is the set of orthogonal matrices whose determinant is one [20], named rotation matrix or Direction Cosine Matrix (DCM). It is a unique and global mathematical parametrization. All others are either only global, such as the Axis-Angle and unit quaternion representations, or singular and not unique, such as Euler angles. Axis-Angle and unit quaternions use four parameters to represent the attitude. Usually, the singularity is due to the fact that only three parameters are used, which is the case of Euler angles. Two other singular minimal parametrization are derived from unit quaternions, Rodrigues Parameters and Modified Rodrigues Parameters [63].

1.3.1 Rotation Matrices and Axis-angle representations

We call a rotation matrix or Direction Cosine Matrix (DCM) [91], denoted R every rotation of the mobile frame $\{\mathscr{B}\}$ relative to the inertial fixed frame $\{\mathscr{I}\}$ (see Figure 1.3.1). Let e_1^{bi}, e_2^{bi},

$e_3^{bi} \in \mathbb{R}^3$ be the principal axis of $\{\mathscr{B}\}$ expressed in $\{\mathscr{I}\}$, then

$$R = [\ e_1^{bi} \quad e_2^{bi} \quad e_3^{bi}\ ], \tag{1.3.1}$$

where e_1^{bi}, e_2^{bi}, e_3^{bi} are column vectors forming the columns of R.

Remark 1.1. Another definition of the rotation matrix is used where e_1^{bi}, e_2^{bi}, e_3^{bi} are column vectors forming the rows of R.

The correspondence between a vector $b \in \mathbb{R}^3$ expressed in $\{\mathscr{B}\}$ and a vector $r \in \mathbb{R}^3$ expressed in $\{\mathscr{I}\}$ can be written as

$$r = Rb \tag{1.3.2}$$

Rotation matrices form a group under the operation of matrix multiplication called the *Special Orthogonal* Group $SO(3) \subset \mathbb{R}^{3\times3}$. The abbreviation SO refers to the properties of rotation matrices :

$$SO(3) = \{R \in \mathbb{R}^{3\times3} \mid R^T R = RR^T = I_d, det(R) = 1\} \tag{1.3.3}$$

Properties of the rotation matrix R

According to Euler's theorem, for every rotation matrix R, there exist an invariant vector a such that $Ra = a$. Which mean that the vector a is an eigenvector of R corresponding to the eigenvalue $\lambda = 1$. In this case a line βa is called rotation axis of R and the eigenvalues of R are $\{1, e^{i\beta}, e^{-i\beta}\} = \{1, cos(\beta) + isin(\beta), cos(\beta) - isin(\beta)\}$, where β is the angle of Euler axis βa and i is the standard imaginary unit ($i^2 = -1$). Then,

1. The sum of eigenvalues of R define it's trace :

$$trace(R) = 1 + 2cos(\beta) \tag{1.3.4}$$

2. Since for every $\beta \in \mathbb{R}$ we have $-1 \leq cos(\beta) \leq 1$. Therefore :

$$-1 \leq trace(R) \leq 3 \tag{1.3.5}$$

3. The product of eigenvalues of R define it's determinant :

$$det(R) = 1, \tag{1.3.6}$$

due to this property, the group of rotation matrices is called $'Special'$.

4. Since e_1^{bi}, e_2^{bi}, e_3^{bi} form an orthonormal basis, then the matrix R is real and orthogonal matrix. This means that
$$R^T R = RR^T = I_d, \tag{1.3.7}$$
due to this property, the group of rotation matrices is called $'Orthogonal'$.

Lie algebra of $SO(3)$

It will be shown that the study of the rotation of a rigid body around a given unit vector $a \in \mathbb{R}^3$ with a given angle $\theta \in \mathbb{R}$ conducts directly to the notion of the Lie algebra of $SO(3)$. Consider a point $p(t) \in \mathbb{R}^3$ of a rigid body rotating around the axis a with an initial condition denoted $p(0) \in \mathbb{R}^3$, the time derivative of $p(t)$ can be written as

$$\frac{d}{dt}(p(t)) = a \times p(t) = \mathscr{A}\, p(t), \tag{1.3.8}$$

where $\times$ stands for the vector cross product and $\mathscr{A} \in \mathbb{R}^{3\times 3}$. Note that the cross product $a \times p(t)$ can be written as a product of a matrix $\mathscr{A}$ and a vector $p(t)$. The properties of the matrix $\mathscr{A}$ will be detailed later.

The unique solution of differential equation (1.3.8) is well known to be $p(t) = p(0)e^{\mathscr{A}t}$, which means that the matrix exponential $e^{\mathscr{A}t}$ is nothing rather than a rotation of the point p from the initial position $p(0)$ to a new position $p(t)$. Therefore, the rotation matrix R can be given by

$$R = e^{\mathscr{A}\theta} \tag{1.3.9}$$

Remark 1.2. The uniqueness of the existence of the matrix R can be derived from the fact that $p(t) = p(0)e^{\mathscr{A}t}$ is a unique solution of (1.3.8). Also, this equation is verified for every physical point $p(t)$ which means that R is global.

The matrix $\mathscr{A}$ if formed by the elements of the vector a. In general, for any two vectors $x, y \in \mathbb{R}^3$, we can denote $x \times y = S(x)y$, where $S(x)$ is a skew-symmetric matrix given by

$$S(x) = \begin{bmatrix} 0 & -x_z & x_y \\ x_z & 0 & -x_x \\ -x_y & x_x & 0 \end{bmatrix} \text{ and } x = \begin{bmatrix} x_x \\ x_y \\ x_z \end{bmatrix} \tag{1.3.10}$$

With this notation, the relation between the unit vector a (which specify the direction of the rotation), the angle of rotation θ and the rotation matrix R can be given by

$$R(a,\theta) = e^{S(a)\theta} \tag{1.3.11}$$

The set of skew symmetric matrices $S(x)$, $x \in \mathbb{R}^3$ is called the Lie algebra of $SO(3)$ and denoted $\mathfrak{so}(3)$, defined by

$$\mathfrak{so}(3) = \{A \in \mathbb{R}^{3\times 3} \mid A^T = -A\}$$

and S is the Lie algebra isomorphism from $\mathbb{R}^3 \to \mathfrak{so}(3)$ which associates to $x \in \mathbb{R}^3$ the skew-symmetric matrix $S(x)$.

For every $x, y \in \mathbb{R}^3$ and a given $R \in SO(3)$, the following identities can be verified

$$\begin{aligned}
S(x)y &= -S(y)x && (1.3.12)\\
S(x)x &= \mathbf{0} && (1.3.13)\\
S(x)S(y) &= yx^T - x^T y I_d && (1.3.14)\\
S^2(x) &= xx^T - x^T x I_d && (1.3.15)\\
S^3(x) &= -x^T x S(x) && (1.3.16)\\
S(S(x)y) &= S(x)S(y) - S(y)S(x) && (1.3.17)\\
S(Rx) &= RS(x)R^T && (1.3.18)\\
S(x)^T &= -S(x) && (1.3.19)
\end{aligned}$$

For every $x, y \in \mathbb{R}^3$ and any constant matrix $A \in \mathbb{R}^{3\times 3}$, the following partial derivative can be verified

$$\begin{aligned}
\frac{\partial [S(x)y]}{\partial x} &= S(y) && (1.3.20)\\
\frac{\partial \left[x^T Ax\right]}{\partial x} &= \left(A + A^T\right)x && (1.3.21)\\
\frac{\partial [S(x)Ax]}{\partial x} &= S(x)A + S(Ax) && (1.3.22)\\
\frac{\partial \left[S^2(x)y\right]}{\partial x} &= S(y)S(x) - 2S(x)S(y) = x^T y I + xy^T - 2yx^T && (1.3.23)\\
\frac{\partial \left[S(x)^2 Ax\right]}{\partial x} &= S(x)^2 A + x(Ax)^T - 2(Ax)x^T + x^T(Ax)I && (1.3.24)
\end{aligned}$$

Rotation matrix R from Axis-Angle (a, θ) : Exponential map $\mathfrak{so}(3) \longrightarrow SO(3)$

Let a be a unit vector representing the direction of a rotation with an angle of rotation θ, corresponding to a rotation matrix R. Therefore, the matrix R can be expressed in function of

(a, θ) by equation (1.3.11). Using Taylor expansion, one can get

$$R(a,\theta) = e^{S(a)\theta} = I_d + S(a)\theta + \frac{S^2(a)}{2!}\theta^2 + \frac{S^3(a)}{3!}\theta^3 + \cdots, \tag{1.3.25}$$

At first time, equation (1.3.25) seem to be unusable since it is an infinite series. In what follows, we show that it is possible to get a closed form of (1.3.25). Before, let us state the following lemma.

Lemma 1.1. *Let $x \in \left(\mathbb{R}^3\right)^*$ and $S(x) \in \mathfrak{so}(3)$. Then, for any integer $n \geq 3$, the following identities can be verified*

Note.

$$S^n(x) = \begin{cases} \frac{1}{\|x\|}(-1)^k \|x\|^{2k+1} S(x) & if\ n = 2k+1 \mid k \geq 1 \\ \frac{-1}{\|x\|^2}(-1)^k \|x\|^{2k} S^2(x) & if\ n = 2k \mid k \geq 2 \end{cases} \tag{1.3.26}$$

Proof. The proof is very simple and the n power of $S(x)$ can be calculated recursively using property (1.3.15) and (1.3.16). □

Using (1.3.26), the Taylor expansion (1.3.25) can be rewritten as

$$R(a,\theta) = I_d + \frac{S(a)}{\|a\|}\left(\sum_{n=0}^{\infty} \frac{(-1)^n}{(2n+1)!}(\|a\|\,\theta)^{2n+1}\right) + \frac{S^2(a)}{\|a\|^2}\left(1 - \sum_{n=0}^{\infty} \frac{(-1)^n}{(2n)!}(\|a\|\,\theta)^{2n}\right),$$

using expansion Taylor theorem for *sin* and *cosine* functions, one can get

$$R(a,\theta) = I_d + \frac{S(a)}{\|a\|} sin(\|a\|\,\theta) + \frac{S^2(a)}{\|a\|^2}(1 - cos(\|a\|\,\theta)), \tag{1.3.27}$$

finally, using the fact that a is a unit vector, one can obtain Rodrigues formula given by

$$R(a,\theta) = I_d + S(a)sin(\theta) + S^2(a)(1 - cos(\theta)), \tag{1.3.28}$$

Angle-Axis (a, θ) from Rotation Matrix R

As mentioned before, angle-axis representation is global but not unique. To show these properties, it suffices to express the angle-axis parametrization in function of rotation matrix. Given a rotation matrix $R \in SO(3)$ as follow

$$R = \begin{bmatrix} r_{11} & r_{12} & r_{13} \\ r_{21} & r_{22} & r_{23} \\ r_{31} & r_{32} & r_{33} \end{bmatrix}, \tag{1.3.29}$$

and using the properties of rotation matrices detailed before, one can verify that for every matrix $R(a,\theta) = e^{S(a)\theta}$ we have

$$\theta = arccos\left(\frac{1}{2}(trace(R)) - 1\right), \tag{1.3.30}$$

and

$$a = \frac{1}{2sin(\theta)}\begin{bmatrix} r_{32} - r_{23} \\ r_{13} - r_{31} \\ r_{21} - r_{12} \end{bmatrix}, \; if\, \theta \neq 0 \tag{1.3.31}$$

where $arccos = cos^{-1}$. Note that if $\theta = 0$ and using (1.3.28) one can get that $R(a,0) = I_d$ and a can be chosen arbitrary. Observing (1.3.30) one can conclude that for one value of R there are two corresponding values of θ $\{\theta + 2k\pi, -\theta + 2k\pi\}$ which give us two directions of rotations $\{a, -a\}$. This means that the couple (a, θ) can represent R globally, but not uniquely. The proof of (1.3.30) and (1.3.31) can be found in chapter 2 of [91].

1.3.2 Quaternion parametrization

Generally, the Euler axis-angle attitude representation is not trivial for the mathematical manipulation point of view. For this and to give another global parametrization using only four parameters [63, 85, 91] (against nine in rotation matrix parametrization), Euler extend his theorem of angle-axis representation by introducing a rotation around a unit vector a considered as imaginary complex part with an angle θ considered as scalar part, which gives

$$Q = e^{\frac{\theta}{2}(a_x i + a_y j + a_z k)} = cos\left(\frac{\theta}{2}\right) + sin\left(\frac{\theta}{2}\right)(a_x i + a_y j + a_z k), \tag{1.3.32}$$

where $i^2 = j^2 = k^2 = -1$. This is a generalization of complex numbers. Using $1, i, j, k$ as a basis, we can note $Q = (q_0, q)$, thus

$$Q = \begin{bmatrix} q_0 \\ q \end{bmatrix} = \begin{bmatrix} cos\left(\frac{\theta}{2}\right) \\ sin\left(\frac{\theta}{2}\right) a \end{bmatrix}, \tag{1.3.33}$$

where $q_0 \in \mathbb{R}$ and $q \in \mathbb{R}^3$. This notation conducts us to the fact that in general $Q \in \mathbb{R}^4$, but since a is a unit vector, therefore

$$\|Q\| = Q^T Q = q_0^2 + q_1^2 + q_2^2 + q_3^2 = 1, \tag{1.3.34}$$

where $q = \begin{bmatrix} q_1 \\ q_2 \\ q_3 \end{bmatrix}$.

Which means that the set of unit quaternions define the unit sphere $\mathbb{S}^3$ such that :

$$\mathbb{S}^3 = \{Q \in \mathbb{R}^4 \mid Q^T Q = 1\} \tag{1.3.35}$$

.

Using (1.3.32), one can conclude that the multiplication of two quaternions $P = (p_0, p)$ and $Q = (q_0, q)$ is a quaternion and if we denoted it by "$\odot$", then

$$P \odot Q = \begin{bmatrix} p_0 q_0 - p^T q \\ p_0 q + q_0 p + p \times q \end{bmatrix}, \tag{1.3.36}$$

and the inverse of a quaternion $Q = (q_0, q)$ is also a quaternion defined by $Q^{-1} = (q_0, -q)$.

Angle-Axis (a, θ) from Unit Quaternion Q

Using (1.3.33) and given a unit quaternion $Q \in \mathbb{S}^3$, one can get the angle-axis representation $(a(Q), \theta(Q))$ corresponding to Q as follow

$$\theta = 2arccos(q_0), \tag{1.3.37}$$

and

$$a = \begin{cases} \frac{1}{sin\left(\frac{\theta}{2}\right)} q & if\ \theta \neq 0, \\ 0 & otherwise, \end{cases} \tag{1.3.38}$$

Rotation matrix R from Unit Quaternion Q : The mapping $\mathbb{S}^3 \to SO(3)$

Denote the mapping from $\mathbb{S}^3$ to $SO(3)$ as $\mathscr{R} : \mathbb{S}^3 \to SO(3)$. Given a quaternion $Q \in \mathbb{S}^3$, the goal is to find the corresponding matrix rotation R, such that $R = \mathscr{R}(Q)$. Using the fact that $1 - cos(\theta) = 2\left(sin\left(\frac{\theta}{2}\right)\right)^2$ and $sin(\theta) = 2sin\left(\frac{\theta}{2}\right) cos\left(\frac{\theta}{2}\right)$ together with (1.3.37), (1.3.38), one can get from Rodrigues formula (1.3.28) the Euler-Rodrigues rotation formula as

$$R = \ \mathscr{R}(Q) = I_d + 2q_0 S(q) + 2S^2(q), \tag{1.3.39}$$

where $Q \in \mathbb{S}^3$. It is easy to verify that $\mathscr{R}(Q) = \mathscr{R}(-Q)$, where $-Q = (-q_0, -q)$, which means that $\mathscr{R}$ defines a double covering map of $SO(3)$ by $\mathbb{S}^3$, i.e., for every $R \in SO(3)$ the equation $\mathscr{R}(Q) = R$ admits exactly two solutions Q_R and $-Q_R$. As a consequence, a vector field f of

$\mathbb{S}^3$ projects onto a vector field of $SO(3)$ if and only if, for every $Q \in \mathbb{S}^3$, $f(-Q) = -f(Q)$ (where we have made the obvious identification between $T_Q\mathbb{S}^3$ the tangent space of $\mathbb{S}^3$ at Q and $T_{-Q}\mathbb{S}^3$ the tangent space of $\mathbb{S}^3$ at $-Q$) (for more details see [38, 70]).

Unit Quaternion Q from Rotation Matrix R : The mapping $SO(3) \to \mathbb{S}^3$

Given a rotation matrix $R \in SO(3)$ defined by (1.3.29) and using the Euler-Rodrigues rotation formula (1.3.39) one can have

$$R = \begin{bmatrix} r_{11} & r_{12} & r_{13} \\ r_{21} & r_{22} & r_{23} \\ r_{31} & r_{32} & r_{33} \end{bmatrix} = \begin{bmatrix} 2(q_0^2+q_1^2)-1 & 2(q_1q_2-q_0q_3) & 2(q_0q_2+q_1q_3) \\ 2(q_0q_3+q_1q_2) & 2(q_0^2+q_2^2)-1 & 2(q_2q_3-q_0q_1) \\ 2(q_1q_3-q_0q_2) & 2(q_0q_1+q_2q_3) & 2(q_0^2+q_3^2)-1 \end{bmatrix}, \quad (1.3.40)$$

where $Q = (q_0, q) = \begin{bmatrix} q_0 \\ q_1 \\ q_2 \\ q_3 \end{bmatrix}$.

Note that from (1.3.40) one can get Q from R in different way, depending on which element of R we want to use. The easiest one is to use only the diagonal of R. Let us first determine the value of q_0. Using the first property of R (1.3.4) and the fact that $cos(\theta) = 2\left(cos\left(\frac{\theta}{2}\right)\right)^2 - 1$, it is straightforward to obtain

$$q_0 = \pm\frac{1}{2}\sqrt{1+trace(R)}, \quad (1.3.41)$$

Thus, using (1.3.40), (1.3.41) and (1.3.34), one can get

$$\begin{aligned} q_1 &= \pm\sqrt{\frac{1}{2}(r_{11}+1)-q_0^2} = \pm\frac{1}{2}\sqrt{2r_{11}+1-trace(R)}, \\ q_2 &= \pm\sqrt{\frac{1}{2}(r_{22}+1)-q_0^2} = \pm\frac{1}{2}\sqrt{2r_{22}+1-trace(R)}, \\ q_3 &= \pm\sqrt{\frac{1}{2}(r_{33}+1)-q_0^2} = \pm\frac{1}{2}\sqrt{2r_{33}+1-trace(R)}, \end{aligned}$$

note that if $R = I_d$, then $Q = (\pm 1, 0)$.

Vector Rotation using Unit Quaternions

Let $b \in \mathbb{R}^3$, $r \in \mathbb{R}^3$ be vectors expressed in $\{\mathscr{B}\}$ and $\{\mathscr{I}\}$ respectively. The rotation of a vector b needs two quaternions Q and it's inverse Q^{-1} as follow

$$r_{pq} = Q \odot b_{pq} \odot Q^{-1}, \tag{1.3.42}$$

where r_{pq} and b_{pq} are the pure quaternions of r and b such that $r_{pq} = (0, r)$ and $b_{pq} = (0, b)$. Let us proof that (1.3.42) is equivalent to (1.3.2). Using (1.3.42) and (1.3.36) the vector part of r_{pq} can be written as

$$\begin{aligned} r &= qq^T b + q_0^2 b + 2q_0 S(q)b - S(S(q)b)q, \\ &= qq^T b + q_0^2 b + 2q_0 S(q)b - S^2(q)b, \end{aligned}$$

where the property (1.3.17) was used. Now, using (1.3.15) and (1.3.34), one can get $qq^T = S^2(q) + (1 - q_0^2)I$. Replacing this last expression in the above equality and after some manipulations, it is straightforward to obtain

$$r = (I_d + 2q_0 S(q) + 2S^2(q))b,$$

which is equivalent to (1.3.2).

1.3.3 Euler Angles parametrization

In Euler angles representation, the rotation from frame $\{\mathscr{I}\}$ to frame $\{\mathscr{B}\}$ is formed by three successive rotations using the right hand rule. A rotation around the axis e_3^i (see Figure 1.3.1) with an angle ψ called "yaw angle", which transforms the basis $\{e_1^i, e_2^i, e_3^i\}$ to $\{e_1^{i'}, e_2^{i'}, e_3^i\}$. The corresponding rotation matrix is

$$R_z = \begin{bmatrix} cos(\psi) & -sin(\psi) & 0 \\ sin(\psi) & cos(\psi) & 0 \\ 0 & 0 & 1 \end{bmatrix} \tag{1.3.43}$$

A rotation around the axis $e_2^{i'}$ with an angle θ called "pitch angle", which transforms the

basis $\{e_1^{i'}, e_2^{i'}, e_3^{i}\}$ to $\{e_1^{i''}, e_2^{i'}, e_3^{i''}\}$. The corresponding rotation matrix is

$$R_y = \begin{bmatrix} cos(\theta) & 0 & sin(\theta) \\ 0 & 1 & 0 \\ -sin(\theta) & 0 & cos(\theta) \end{bmatrix} \tag{1.3.44}$$

A rotation around the axis $e_1^{i''}$ with an angle ϕ called "roll angle", which transforms the basis $\{e_1^{i''}, e_2^{i'}, e_3^{i''}\}$ to $\{e_1^{b}, e_2^{b}, e_3^{b}\}$. The corresponding rotation matrix is

$$R_x = \begin{bmatrix} 1 & 0 & 0 \\ 0 & cos(\phi) & -sin(\phi) \\ 0 & sin(\phi) & cos(\phi) \end{bmatrix} \tag{1.3.45}$$

The total rotation $R(\psi, \theta, \phi)$, which transforms $\{\mathscr{I}\}$ (defined by $\{e_1^{i}, e_2^{i}, e_3^{i}\}$) to$\{\mathscr{B}\}$ (defined by $\{e_1^{b}, e_2^{b}, e_3^{b}\}$) is given by

$$R(\psi,\theta,\phi) = R_x R_y R_z = \begin{bmatrix} c(\theta)c(\psi) & s(\phi)s(\theta)c(\psi) - c(\phi)s(\psi) & c(\phi)s(\theta)c(\psi) + s(\phi)s(\psi) \\ c(\theta)s(\psi) & s(\phi)s(\theta)s(\psi) + c(\phi)c(\psi) & c(\phi)s(\theta)s(\psi) - s(\phi)c(\psi) \\ -s(\theta) & s(\phi)c(\theta) & c(\phi)c(\theta) \end{bmatrix}, \tag{1.3.46}$$

where $c(\cdot) = cos(\cdot)$ and $s(\cdot) = sin(\cdot)$. The angles (ϕ, θ, ψ) are called Euler angles.

Euler angles(ϕ, θ, ψ) from Rotation Matrix R

Given a rotation matrix $R \in SO(3)$ defined by (1.3.29) and using (1.3.46) one can have

$$\theta = arcsin(-r_{31}), \tag{1.3.47}$$
$$\phi = atan2(r_{21}, r_{11}), \tag{1.3.48}$$
$$\psi = atan2(r_{32}, r_{33}), \tag{1.3.49}$$

where "$atan2(y,x)$ computes $tan^{-1}(\frac{y}{x})$ but uses the sign of both x and y to determine the quadrant in which the resulting angle lies" [91].

1.4 Attitude kinematics and dynamics

1.4.1 Attitude kinematics

The study of attitude kinematics [13, 63, 91] is based on the time derivative of a vector in a rotating coordinate system. Let us rewrite (1.3.8) for a derivative of the principal axis $e_1^{bi}(t)$, $e_2^{bi}(t)$, $e_3^{bi}(t) \in \mathbb{R}^3$ of $\{\mathscr{B}\}$ expressed in $\{\mathscr{I}\}$

$$\frac{d}{dt}\left(e_1^{bi}(t)\right) = S(\omega_I(t))e_1^{bi}(t), \tag{1.4.1}$$
$$\frac{d}{dt}\left(e_2^{bi}(t)\right) = S(\omega_I(t))e_2^{bi}(t), \tag{1.4.2}$$
$$\frac{d}{dt}\left(e_3^{bi}(t)\right) = S(\omega_I(t))e_3^{bi}(t), \tag{1.4.3}$$

where ω_I is the vector of angular velocity of $\{\mathscr{B}\}$ expressed in $\{\mathscr{I}\}$ and $S(\omega_I(t))$ is the skew symmetric matrix defined by (1.3.10).

Attitude Kinematics on $SO(3)$

To get attitude kinematics using rotation matrix as parametrization of attitude it suffices to calculate the expression of the derivative of R using the elementary definition (1.3.1). Thus, the derivative of (1.3.1) in view of (1.4.1), (1.4.2) and (1.4.3) gives

$$\begin{aligned}\dot{R}(t) &= \left[\begin{array}{ccc} \dot{e}_1^{bi}(t) & \dot{e}_2^{bi}(t) & \dot{e}_3^{bi}(t) \end{array}\right], \\ &= S(\omega_I(t))\left[\begin{array}{ccc} e_1^{bi}(t) & e_2^{bi}(t) & e_3^{bi}(t) \end{array}\right],\end{aligned} \tag{1.4.4}$$

using the fact that the corresponding angular velocity vector $\omega_I(t)$ to $\omega(t)$ (where $\omega(t)$ is expressed in $\{\mathscr{B}\}$ and $\omega_I(t)$ is expressed in $\{\mathscr{I}\}$) can be written using (1.3.2) as $\omega_I(t) = R(t)\omega(t)$. Therefore, one can get from (1.4.4)

$$\dot{R}(t) = R(t)S(\omega(t)), \tag{1.4.5}$$

where property (1.3.18) was used.

Reduced Attitude Kinematics on $\mathbb{S}^2$

Consider a vector $b_i(t) \in \mathbb{R}^3$ expressed in $\{\mathscr{B}\}$ and a fixed vector $r_i \in \mathbb{R}^3$ expressed in $\{\mathscr{I}\}$, $i = 1, ..., m$, then from (1.3.2) one can write

$$b_i(t) = R^T(t) r_i, \tag{1.4.6}$$

where R is the rotation matrix of the mobile frame $\{\mathscr{B}\}$ relative to the inertial fixed frame $\{\mathscr{I}\}$. Since R preserves distances, therefore if r_i is a unit vector, then b_i is also a unit vector. In this case, $b_i(t) \in \mathbb{S}^2$ such that

$$\mathbb{S}^2 = \{x \in \mathbb{R}^3 \mid x^T x = 1\} \tag{1.4.7}$$

Using the fact that r_i is constant, differentiating (1.4.6) with respect to time in view of (1.4.5) gives

$$\dot{b}_i(t) = -S(\omega(t)) b_i(t), \tag{1.4.8}$$

It is clear from (1.4.8) that the reduced attitude vector evolves in $\mathbb{S}^2$, which can be verified by the evaluation of the time derivative of $b_i^T(t) b_i(t)$, see [20].

Attitude Kinematics on $\mathbb{S}^3$

The evaluation of the equivalent attitude kinematics (1.4.5) using unit quaternions, can be done by using the basic definition of a function derivative as described in page 71 of [63]. The unit quaternion kinematics is given by

$$\dot{Q}(t) = \begin{bmatrix} \dot{q}_0(t) \\ \dot{q}(t) \end{bmatrix} = \frac{1}{2} Q(t) \odot \overline{\omega}(t) = \frac{1}{2} \begin{bmatrix} -q^T(t) \\ q_0(t) I_d + S(q(t)) \end{bmatrix} \omega(t), \tag{1.4.9}$$

where $\overline{\omega}$ is the pure quaternion of ω, such that $\overline{\omega} = (0, \omega)$. It is possible to write the quaternion kinematics (1.4.9) as a product of a matrix and the quaternion. Consider a matrix $M(\omega(t))$ defined by

$$M(\omega(t)) = \begin{bmatrix} 0 & -\omega^T(t) \\ \omega(t) & -S(\omega(t)) \end{bmatrix}, \tag{1.4.10}$$

then,

$$\dot{Q}(t) = \frac{1}{2} M(\omega(t)) Q(t) \tag{1.4.11}$$

Euler angles kinematics on $\mathbb{R}^3$

Consider a rotation matrix $R(t) \in SO(3)$ defined by (1.3.29) and using (1.4.5), one can get

$$\dot{R}(t) = \begin{bmatrix} \dot{r}_{11} & \dot{r}_{12} & \dot{r}_{13} \\ \dot{r}_{21} & \dot{r}_{22} & \dot{r}_{23} \\ \dot{r}_{31} & \dot{r}_{32} & \dot{r}_{33} \end{bmatrix} = \begin{bmatrix} (r_{12}\omega_z - r_{13}\omega_y) & (r_{13}\omega_x - r_{11}\omega_z) & (r_{11}\omega_y - r_{12}\omega_x) \\ (r_{22}\omega_z - r_{23}\omega_y) & (r_{23}\omega_x - r_{21}\omega_z) & (r_{21}\omega_y - r_{22}\omega_x) \\ (r_{32}\omega_z - r_{33}\omega_y) & (r_{33}\omega_x - r_{31}\omega_z) & (r_{31}\omega_y - r_{32}\omega_x) \end{bmatrix}, \tag{1.4.12}$$

where $\omega(t) = \begin{bmatrix} \omega_x & \omega_y & \omega_z \end{bmatrix}^T \in \mathbb{R}^3$ is the angular velocity vector expressed in $\{\mathscr{B}\}$.

Now, using (1.3.46), (1.4.12), (1.3.47), (1.3.48) and (1.3.49), together with the fact that $\frac{d}{dt}(arcsin(x)) = \frac{\dot{x}}{\sqrt{1-x^2}}$ and $\frac{d}{dt}(arctan(x)) = \frac{\dot{x}}{1+x^2}$, and after some manipulations, one can have

$$\begin{aligned} \dot{\theta}(t) &= cos(\phi)\omega_y - sin(\phi)\omega_z, \\ \dot{\phi}(t) &= \omega_x + sin(\phi)tan(\theta)\omega_y + cos(\phi)tan(\theta)\omega_z, \\ \dot{\psi}(t) &= \frac{sin(\phi)}{cos(\theta)}\omega_y + \frac{cos(\phi)}{cos(\theta)}\omega_z, \end{aligned}$$

which means that the attitude kinematics using the minimal Euler angles parametrization is not always defined, as can be verified when $\theta = \pm\frac{\pi}{2} + 2k\pi$.

The discrete-time unit quaternion propagation

For implementation purpose and to avoid the integration of the continuous quaternion kinematics (1.4.9) or (1.4.11), the discrete-time quaternion propagation [63] will be used in this work and it is given by

$$Q_{k+1} = exp\left(\frac{T_s}{2}M(\omega_k)\right)Q_k, \tag{1.4.13}$$

where $M(\omega_k)$ is defined by (1.4.10), T_s is the sample time and

$$exp\left(\frac{T_s}{2}M(\omega_k)\right) = cos\left(\frac{T_s}{2}\|\omega_k\|\right)I_4 + \frac{sin\left(\frac{T_s}{2}\|\omega_k\|\right)}{\|\omega_k\|}M(\omega_k),$$

where $I_4 \in \mathbb{R}^{4\times4}$ is the identity matrix.

1.4.2 Attitude dynamics

Consider a rigid-body moving in 3D space with orthonormal body-frame $\{\mathscr{B}\}$ fixed to its *COM* and denote by $\{\mathscr{I}\}$ the inertial fixed reference, as illustrated in Figure 1.3.1. The angular momentum [63] can be expressed in $\{\mathscr{I}\}$ as

$$L(t) = R(t)J\omega(t), \tag{1.4.14}$$

where $R(t)$ is the matrix of rotation defined by (1.3.1), J is the moment of inertia or inertia matrix of the rigid body expressed in $\{\mathscr{B}\}$ and $\omega(t)$ is the vector of angular velocity expressed in $\{\mathscr{B}\}$. Using the Newton's law of motion, one can get

$$\frac{d}{dt}(L(t)) = R(t)(\tau(t) + \tau_{ext}(t)), \tag{1.4.15}$$

where $\tau(t)$ is the torque generated by actuators and $\tau_{ext}(t)$ all others external torques applied about the center of mass of the rigid body expressed in $\{\mathscr{B}\}$. Using (1.4.14) and (1.4.15), the simplified attitude dynamics [62] can be expressed as

$$J\dot{\omega}(t) = -S(\omega(t))J\omega(t) + \tau(t), \tag{1.4.16}$$

where external torque $\tau_{ext}(t)$ was neglected.

1.5 Quadrotor Modeling

The quadrotor modeling is well studied in the literature [18, 21, 50, 62, 76]. In this section, a brief resume of the different quadrotor modeling levels are given. As described in [13], modeling of quadrotor can be divided into four levels with a fifth level dedicated to sensors modeling. The quadrotor modeling levels are depicted in Figure 1.5.1.

1.5.1 Rigid body modeling level

The quadrotor motion consists of translation and rotation. The rotation kinematics and dynamics were detailed in Section 1.4. In this subsection, we detail the modeling of the translational motion of a rigid body and a simplified model of quadrotor considered as a rigid body is presented.

First, let us consider that the translation motion of quadrotor is described by its position $\xi(t)$, its linear velocity $v(t) = \dot{\xi}(t)$ and its linear acceleration $a(t) = \dot{v}(t)$, all expressed in the inertial reference $\{\mathscr{I}\}$. We assume that the total thrust generated by the quadrotor in $\{\mathscr{B}\}$ at

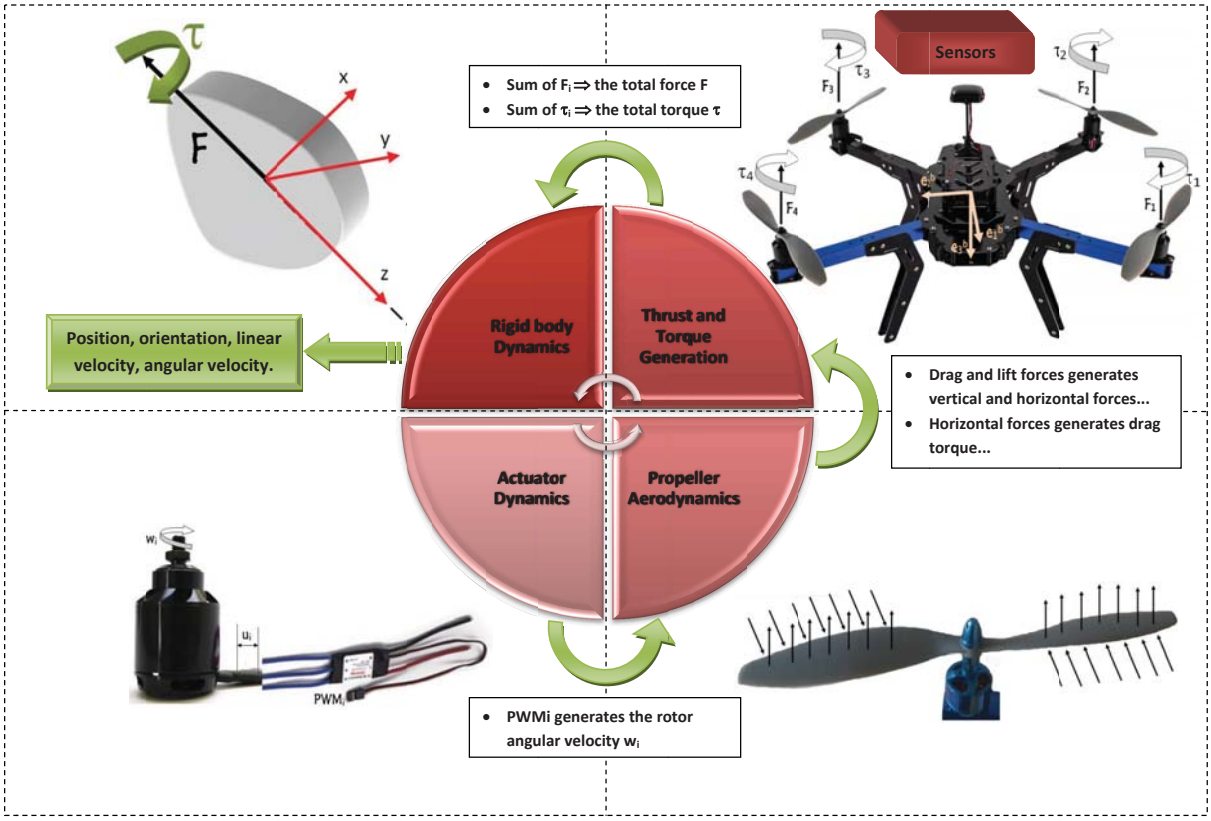

Figure 1.5.1: Quadrotor modeling levels

his COM is in the inverse direction of e_3^b (see Figure 1.3.1). Therefore,

$$F_T = -TRe_3^i$$

is the total thrust expressed in $\{\mathscr{I}\}$, where R is the rotation matrix defined by (1.3.1) and T is the magnitude of the total thrust.

Using the fundamental principle of dynamics, one can get

$$m\dot{v}(t) = -T(t)R(t)e_3^i + mge_3^i + f_{ext}(t), \tag{1.5.1}$$

where $f_{ext}(t)$ are the sum of all external forces acting on the rigid body and m denotes it's mass.

Finally, neglecting all external forces and all external torques and using (1.4.5), (1.4.16) and (1.5.1), the general simplified model of quadrotor [62] considered as rigid body is given by

$$\begin{cases} \dot{\xi}(t) & = v(t), \\ m\dot{v}(t) & = -T(t)R(t)e_3^i + mge_3^i, \\ \dot{R}(t) & = R(t)S(\omega(t)), \\ J\dot{\omega}(t) & = -S(\omega(t))J\omega(t) + \tau(t) \end{cases} \tag{1.5.2}$$

1.5.2 Thrust and Torque generation, Propeller aerodynamics and Actuator dynamics modeling levels

Consider a quadrotor equipped with four actuator with propellers, each propeller generates a Thrust T_i and a torque τ_i, and rotates at an angular velocity ω_i. Propellers attached to actuators M_1 and M_2 are rotating in Counter Clockwise direction (CCW), while those attached to actuators M_3 and M_4 are rotating in Clockwise direction (CW). The mobile reference attached to the quadrotor is chosen to be in "X" configuration as depicted in Figure 1.5.2. The total thrust $T(t)$ is the sum of all thrusts generated by each propeller [62] and given by

$$T(t) = |T_1(t)| + |T_2(t)| + |T_3(t)| + |T_4(t)| = c_T \sum_{i=1}^{4} \omega_i^2(t), \tag{1.5.3}$$

where $c_T > 0$ is the thrust constant and the assumption of the proportionality of propeller thrust and the square of rotor angular velocity ω_i is considered. The reaction torque generated

by each propeller [62] can be modeled by

$$\tau_i(t) = c_\tau \omega_i^2(t), \tag{1.5.4}$$

where $c_\tau > 0$ is the torque constant. More details about propeller aerodynamics can be found in [50, 62]. Denote the distance

$$d = \frac{\sqrt{2}}{2} l, \tag{1.5.5}$$

which represents the vertical distance from the principal axis e_1^b to the point of application of thrusts T_i, where l is the length of the quadrotor legs. Using (1.5.3), (1.5.4) and (1.5.5), one can write the total thrust $T(t)$ and torque $\tau(t) = \begin{bmatrix} \tau_x & \tau_y & \tau_z \end{bmatrix}^T$ as

$$\begin{bmatrix} T(t) \\ \tau_x(t) \\ \tau_y(t) \\ \tau_z(t) \end{bmatrix} = \overbrace{\begin{bmatrix} c_T & c_T & c_T & c_T \\ -dc_T & dc_T & dc_T & -dc_T \\ dc_T & -dc_T & dc_T & -dc_T \\ -c_\tau & -c_\tau & c_\tau & c_\tau \end{bmatrix}}^{\mathscr{P}} \begin{bmatrix} \omega_1^2(t) \\ \omega_2^2(t) \\ \omega_3^2(t) \\ \omega_4^2(t) \end{bmatrix},$$

where the constant matrix $\mathscr{P}$ can be determined experimentally, as detailed in [26].

Usually, autopilot of quadrotor generates $PWM_i(t)$ signals to drive the motor Electronic System Control "ESC" which it self generates the desired voltage u_i to drive the motor, depending on the duty cycle of the $PWM_i(t)$ signals, see Figure 1.5.1. The relation between $u_i(t)$ and $PWM_i(t)$ can be given by [50]

$$u_i(t) = k\sqrt{PWM_i(t)},$$

where $k \in \mathbb{R}^+$.

1.5.3 Sensors modeling level

A large set of sensors are used in aerial robots, Figure 1.5.3 illustrates an existing various sensors type. Depending on the application, the selection of required sensors is crucial. Some of them are exclusively used for outdoor application such as GPS. In our case, we used an Inertial Measurements Unit "IMU" (generally composed of three accelerometers, three rate gyros and three magnetometers).

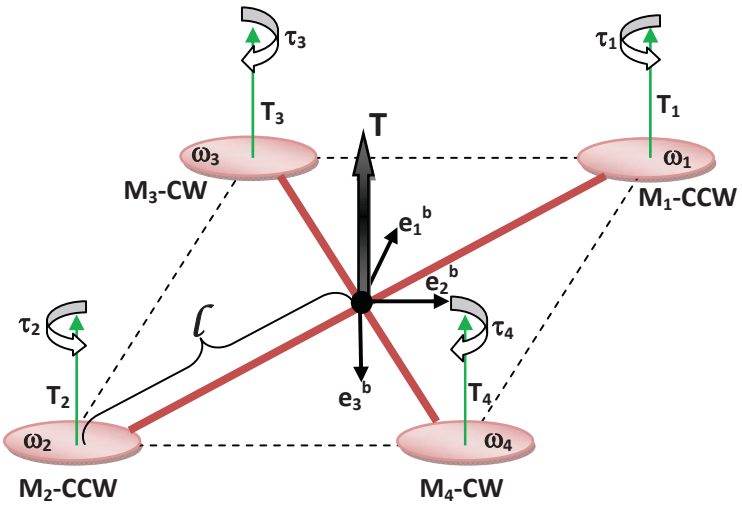

Figure 1.5.2: Thrust and Torque generation modeling level

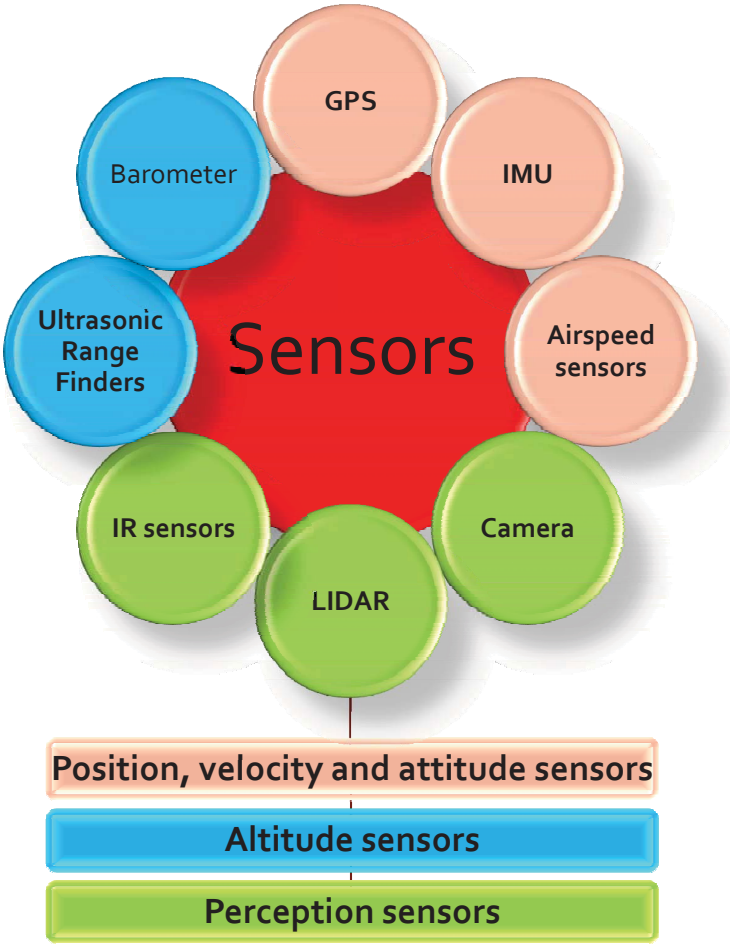

Figure 1.5.3: Various sensor types

Accelerometers

The accelerometer is a sensor which measures the force F which is the result of the action of acceleration to a mass m. The measured acceleration is the result of all the accelerations to which is subjected the mass m in the direction of given axis in $\{\mathscr{B}\}$. This takes into account the dynamic acceleration (motion) or static (gravity earth field). The accelerometer measures the following accelerations :

1. *The gravitational acceleration*: the gravitational force is always directed downward, and the projection of this force in the mobile frame $\{\mathscr{B}\}$ is written $a_g(t) = R^T(t)ge_3^i$, where $g = 9.81\,(m/s^2)$.

2. *The centripetal acceleration*: it is called centripetal force, any force perpendicular to the trajectory, which changes the rate only in direction. This force causes centripetal acceleration given by the following equation $a_c(t) = S(\omega(t))R^T(t)v(t)$.

3. *The linear acceleration*: by definition, it is the first derivative of the linear velocity of a mobile vehicle, expressed in $\{\mathscr{B}\}$ as $R^T(t)a(t) = R^T(t)\dot{v}(t)$.

Finally, if we denote the measured acceleration by $a_{\mathscr{B}}(t)$, then

$$a_{\mathscr{B}}(t) = R^T\left(\dot{v}(t) + S(\omega(t))v(t) - ge_3^i\right) + \eta_a + n_a(t), \tag{1.5.6}$$

where η_a denote the offset and $n_a(t)$ denote the additive measurements noise. In the case of micro aerial robots the centripetal acceleration can be neglected compared to the gravitational acceleration, therefore two models are considered in literature :

- **The case of accelerated motion**: In this case, the linear acceleration is non negligible compared to the gravitational acceleration. Without tacking into consideration the bias and noise (1.5.6) becomes

$$a_{\mathscr{B}}(t) \approx R^T\left(\dot{v}(t) - ge_3^i\right), \tag{1.5.7}$$

  and

$$a_{\mathscr{I}}(t) = R(t)a_{\mathscr{B}}(t), \tag{1.5.8}$$

  where $a_{\mathscr{I}}(t)$ denotes the apparent acceleration expressed in $\{\mathscr{I}\}$.

- **The case of non accelerated motion**: In this case, the linear acceleration is negligible compared to the gravitational acceleration. Thus, from (1.5.7), one can get

$$a_{\mathscr{B}}(t) \approx -R^T ge_3^i \tag{1.5.9}$$

Rate Gyros

The gyros allow the measurement of the angular velocity about a given axis. Generally, they are based on Coriolis forces effect measurements. The measured angular velocity of $\{\mathscr{B}\}$ relative to $\{\mathscr{I}\}$ expressed in $\{\mathscr{B}\}$ is modeled by

$$\omega_m(t) = \omega(t) + \eta_\omega + n_\omega(t), \tag{1.5.10}$$

where $\omega(t)$ is the true angular velocity, η_ω denotes the rate gyro bias and $n_\omega(t)$ an additive measurements noise.

Magnetometers

With three magnetometers forming a triad, the vector of the earth magnetic field in the mobile reference frame$\{\mathscr{B}\}$ is given by

$$m_{\mathscr{B}}(t) = R^T(t) m_{\mathscr{I}} + \eta_m(t) + n_m(t), \tag{1.5.11}$$

where $\eta_m(t)$ all magnetometers disturbances, composed of local hard and soft disturbances and $n_m(t)$ denotes the measurements noise. A special care for the placement of magnetometer should be taken into consideration because magnetometers disturbances can be very significant. The value of $m_{\mathscr{I}}$ depends on the geographic location. In Vélizy - FRANCE, the vector $m_{\mathscr{I}}$ is given by

$$m_{\mathscr{I}} = \begin{bmatrix} 0.2086 \\ 0.0004 \\ 0.4320 \end{bmatrix} (Gauss)$$

Usually, the normalized measurements of $m_{\mathscr{B}}(t)$ are used.

1.6 Assumptions

The following assumptions are made and will be used

Assumption 1. *We assume that m inertial vector-valued functions of time $b_i(t)$ are measured. Moreover, note that the b_i's actually depend on the rotation R and one could also write them as $b_i(R(t))$ or $b_i(Q(t))$ if we choose quaternions instead of rotations. In the sequel, we will write either $b_i(t)$ or $b_i(Q(t))$ or just b_i.*

Assumption 2. *We assume that, if we have m measured inertial vectors $b_i(t), i = 1,...,m$ expressed in $\{\mathscr{B}\}$, corresponding to m inertial constant vectors $r_i, i = 1,...,m$ expressed in $\{\mathscr{I}\}$, then at least two of them are non-collinear.*

Assumption 3. *We assume that the real unknown gyro-bias η_ω is bounded and constant (or slowly varying), such that $\dot{\eta}_\omega = 0$. Moreover, we assume that we are dealing with bounded measured angular velocities $\omega_m(t)$, in the case of attitude estimation, implying that the real angular velocity $\omega(t)$ is bounded as well.*

Assumption 4. *For attitude stabilization, the desired rigid body attitude is defined by the constant rotation matrix R_d, relates an inertial constant vector r_i to its corresponding vector in the desired frame, i.e., $b_i^d = R_d^T r_i$, with $\dot{b}_i^d = 0$. An equivalent constant desired unit-quaternion Q_d is defined as $R_d = \mathscr{R}(Q_d)$.*

Assumption 5. *We assume that the angular velocity vector $\omega(t)$ is unavailable in the case of velocity free attitude controller.*

1.7 Conclusion

With the aim to develop a model of the quadrotor, mathematical attitude parametrization was detailed after the presentation of the different reference frames. A fine quadrotor modeling can be complicated, therefore only a simplified model has been selected. Several modeling levels were considered. Each level provided an output used by the next level until arrival at the rigid body modeling level, which provided position, linear velocity, orientation, angular velocity. The simple rigid body model was based on the elaboration of translational and rotational kinematics and dynamics.

As it is well known, the attitude is not measurable. Therefore, a set of sensors combined with observers are needed to estimate attitude. A sensor level modeling was presented, in which all sensors needed and used in this work was presented. Sensor selection depend essentially on the chosen application, but some sensors are needed in all aerial robots such as IMU. IMUs are the most used sensor to estimate the attitude, which is the aim of the next chapter.

Chapter 2

Attitude Estimation Using Linear-Like Complementary Filters

2.1 Introduction

Attitude determination remains until today an interesting research topic. Indeed, the attitude is not a measurable quantity, its determination is based on measurements provided by appropriate sensors. Many sensors are used, depending generally on the application, such that IMU, star trackers and others, see Figure 2.1.1 for examples of the used sensors to estimate the attitude.

Generally, the problem of attitude estimation involves two process, estimation of the attitude and filtering as mentioned in the survey paper [24]. The widely used techniques are based on Kalman filter (KF) or Extended Kalman filter (EKF) (see, for instance, [24, 25, 49, 88]) and its variants (see, for instance, [37, 46, 52, 80, 83, 84, 90, 115]). Other techniques developed like a nonlinear observer [30], or based on unscented filter [23] or particle filter [24, 109]. Most of these methods are computationally demanding and some of them, depending on used attitude representation [85], suffer from topological limitations, double covering or singularities. Another class of techniques are based on complementary filters (see, for instance, [31, 106, 107]) which are not so computationally demanding, see [39] for comparison between complementary and Kalman filtering.

Due to their simplicity and efficiency, the use of complementary filters to reconstruct the attitude continues to attract many researchers. A lot of them focus on low-cost IMU and attitude heading reference system AHRS [65]. Nonlinear complementary filters designed on Special Orthogonal Group $SO(3)$ [61] and on the unit 3-sphere $\mathbb{S}^3$ [94] were used successfully to estimate the attitude, but not always achieving global stability. Modified complementary filters using only accelerometer and gyroscope measurements to estimate the orientation was

presented in [54]. Another recent work has used the inverse sensor models and complementary filters to develop a high-fidelity attitude estimator [66]. As mentioned in [6], traditional attitude solutions use directly raw vector measurements to compute the attitude data after that the filter is used to obtain the filtered attitude. Batista *et al.* [6] proposed a reverse strategy by combining a vector-based filter with an optimal attitude determination algorithm. A new interesting class of globally asymptotically stable filters for attitude estimation are obtained. The vector-based filter was designed as a Kalman filter using Linear Time Variant (LTV) representation of the nonlinear kinematic equation. Even if experimental results presented in [6] are very good, the theoretical drawback is the fact that the observability analysis were done on the LTV reformulation of the original nonlinear system and not explicitly on the non linear system.

Inspired by approach given in [6], this chapter presents firstly a globally asymptotically stable filters for attitude estimation based on linear complementary filtering. It has the advantage to improve the quality of estimation by choosing the adequate order of the filter. The gyro-bias estimation is also considered. Two filter forms, termed *direct* and *passive,* are designed similarly as the work presented in [61]. The main difference between these two proposed forms lies in the direct use of the raw or filtered measurements in the nonlinear part of the filter. The passive form is less sensitive to noise as claimed in [61]. In fact, the attitude estimation proposed in [6] can be regarded as Kalman filter representation of the first order passive proposed form used to filter the vector measurements followed by an optimal method to calculate the attitude. Moreover, the approach proposed here is completely deterministic as it is based on linear complementary filters followed by TRIAD algorithm for the attitude estimation. As a matter of fact, the TRIAD is the deterministic attitude estimation algorithm *par excellence* as claimed by [86]. Although it was proved that TRIAD is less accurate than other optimal approaches [86], we show throughout this work that it is possible to obtain higher quality of the attitude estimation when this approach is used. The new proposed observers for attitude estimation can be qualified as linear-like complementary filters. By doing so, the distortion of noise characteristics is avoided [6] and a globally asymptotic convergence of the filter can be ensured.

This chapter is organized as follow. In Section 2.2, Complementary linear-like filter-based attitude estimation approach is detailed. The design of linear complementary filters for attitude estimation along with stability analysis of the direct and passive filters are given in Section 2.3. Depending on the placement of a compensation term, four filter variants are presented. A first validation of the proposed solutions by simulations are presented in Section 2.4. A second validation by experiments will be presented in Chapter 5. The Chapter is ended by conclusion in Section 2.5. Note that, partial results in this Chapter were published in [12].

(a) Horizon sensor (*www.love2fly.co.uk*)

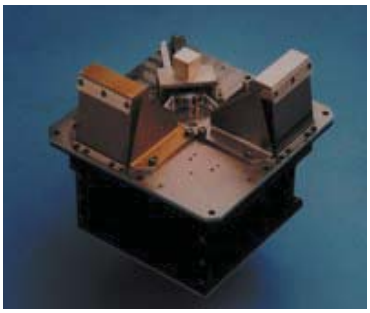

(b) Horizon sensor (*www.spinoff.nasa.gov*)

(c) Horizon sensor (*www.ssbv.com*)

(d) Solar sensor (*www.ssbv.com*)

(e) Star Tracker (*www.spacedaily.com*)

(f) Star Tracker (*www.ballaerospace.com*)

(g) AHRS (*www.xsens.com*)

(h) Zrazor (*www.sparkfun.com*)

Figure 2.1.1: Classical used sensors for attitude estimation

2.2 Complementary linear-like filter-based attitude estimation approach

The sensor-based attitude estimation approach, mentioned in [6], is consisting of two process: i) filter sensor measurements, and ii) determine attitude. Inspired by this approach, we propose a structure based on complementary linear filter rather than sensor-based filter method. Indeed, complementary filters give us a mean to fuse multiple heterogeneous independent noisy measurements of the same signal that have complementary spectral characteristics [61]. Taking care of developing a high-fidelity and simple algorithm for attitude estimation, the proposed structure must allow the possibility of using high order filter which leads to better performance.

Note that, in all what follows the indices $i = 1, ..., m$ denote the number of the used vectors.

Using the reduced attitude kinematics (1.4.8), the complementary filter model for fusing the measured inertial vector $b_i(t)$, $i = 1, ..., m$ and angular velocity $\omega(t)$ in order to get estimate $\hat{b}_i(t)$, $i = 1, ..., m$ is shown in Figure 2.2.1, where the notion of complementary filter is achieved if the following condition is satisfied

$$H_{1i}(s) + sH_{2i}(s) = 1, \quad i = 1, \ldots, m, \tag{2.2.1}$$

where $H_{1i}(s)$ is a low-pass filter and $sH_{2i}(s)$ is a high-pass filter.

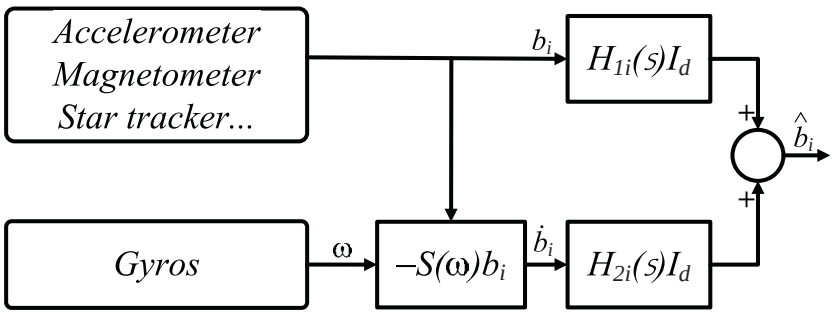

Figure 2.2.1: Classical form of complementary filter

From the structure of the complementary filter given in Figure 2.2.1, the estimate $\hat{b}_i$ of the state b_i by fusing measurements of ith inertial direction vector and gyro measurements can be written as

$$\hat{b}_i = H_{1i}(s)b_i + H_{2i}(s)\dot{b}_i, \quad i = 1, \cdots, m. \tag{2.2.2}$$

Now, for the determination of the attitude, the complementary filter can be followed by any algebraic algorithm such that TRIAD algorithm [87] as depicted in Figure 2.2.2 which can be considered as overall structure of the AHRS. Despite the fact that TRIAD is known less accurate than other statistical algorithms based on minimizing Wahba's loss function [86], we will show that we can obtain good results by using fused data. The choice of TRIAD algorithm is justified by the fact that statistical algorithms are usually much slower than deterministic algorithms [86, 87].

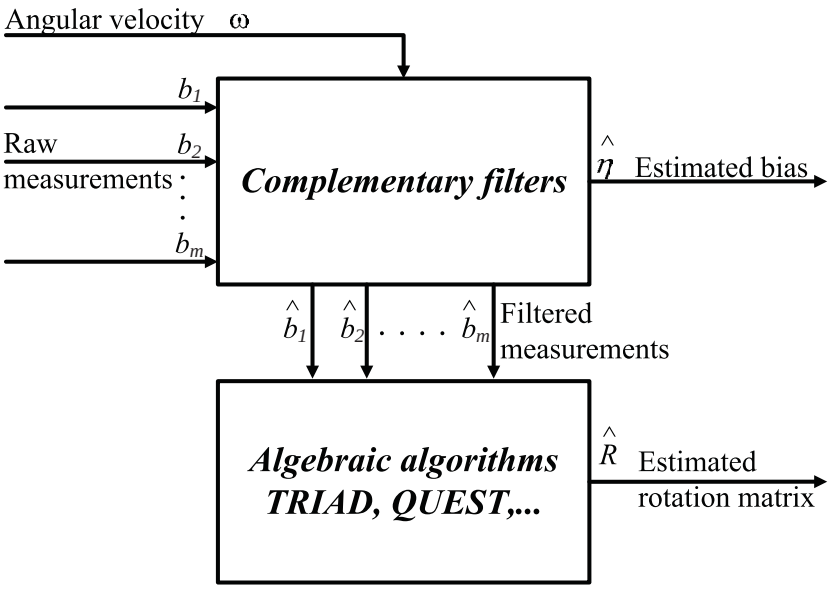

Figure 2.2.2: Proposed AHRS structure

For attitude estimation by TRIAD algorithm, we suppose that we are given two filtered measurements $\hat{b}_1, \hat{b}_2 \in \mathbb{R}^3$ expressed in $\{\mathscr{B}\}$ corresponding to their known inertial non-collinear vectors $r_1, r_2 \in \mathbb{R}^3$ expressed in $\{\mathscr{I}\}$, respectively. Then, we write $\hat{b}_1 = \hat{R}^T r_1$ and $\hat{b}_2 = \hat{R}^T r_2$. The determination of $\hat{R}$ is based on the use of the normalized filtered vector measurements $\hat{b}_1^u, \hat{b}_2^u$ rather than $\hat{b}_1, \hat{b}_2$ and their normalized known inertial vector r_1^u, r_2^u, which gives

$$\hat{R} = \sum_{\kappa=1}^{3} v_\kappa \hat{u}_\kappa^T \tag{2.2.3}$$

where

$$v_1 = r_1^u; \quad v_2 = \frac{r_1^u \times r_2^u}{\|r_1^u \times r_2^u\|}; \quad v_3 = v_1 \times v_2; \quad r_1^u = \frac{r_1}{\|r_1\|}; \quad r_2^u = \frac{r_2}{\|r_2\|};$$
$$\hat{u}_1 = \hat{b}_1^u; \quad \hat{u}_2 = \frac{\hat{b}_1^u \times \hat{b}_2^u}{\|\hat{b}_1^u \times \hat{b}_2^u\|}; \quad \hat{u}_3 = \hat{u}_1 \times \hat{u}_2; \quad \hat{b}_1^u = \frac{\hat{b}_1}{\|\hat{b}_1\|}; \quad \hat{b}_2^u = \frac{\hat{b}_2}{\|\hat{b}_2\|}$$

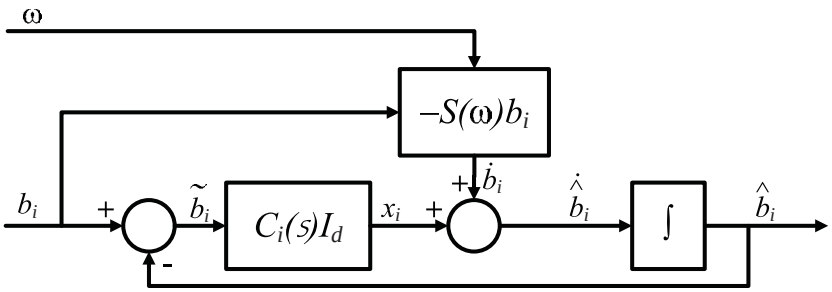

Figure 2.3.1: Direct linear-like complementary filter

2.3 Design of High Order Direct and Passive Filters

The principle of the *"classical form"* of complementary filters is based on the data fusion of measurements of inertial direction vectors and gyro measurements as depicted by the scheme in Figure 2.2.1. This scheme can be reformulated in *"feedback form"* as shown in Figure 2.3.1. Furthermore, according to the manner of offsetting the nonlinear term, we can obtain two structures of the complementary filter. The first one is termed *"direct linear-like complementary filter"* and the second one termed *"passive linear-like complementary filter"*. Indeed, in the first one, the offsetting of nonlinear term uses direct raw measurements as shown in Figure 2.3.1, while in the second one, the filtered measurements are used as depicted in block diagram given in Figure 2.3.2.

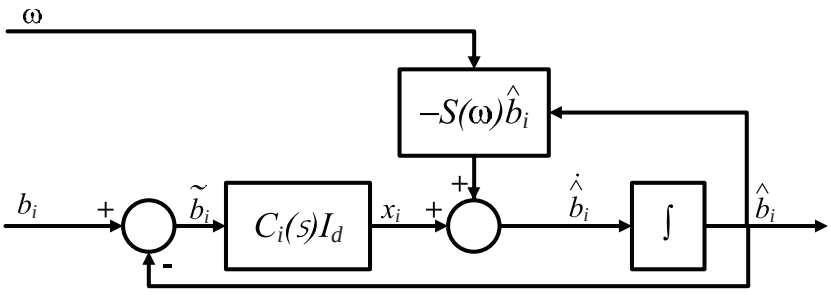

Figure 2.3.2: Passive linear-like complementary filter

From the equivalence between the *"classical form"* and the *"feedback form"*, one can get

$$H_{1i}(s) = \frac{C_i(s)}{s + C_i(s)}, \; H_{2i}(s) = \frac{1}{s + C_i(s)} \tag{2.3.1}$$

where $C_i(s)$ represents the compensator term in the feedback form, s is Laplace variable and $i = 1,...,m$. From (2.3.1), we can write the compensator term as

$$C_i(s) = \frac{sH_{1i}(s)}{1 - H_{1i}(s)}, i = 1,...,m \tag{2.3.2}$$

The design of the compensator $C_i(s)$ can be achieved by choosing the adequate order of the filter for improving the quality of the estimation. Now, we need to prove that for some selected low pass filter $H_{1i}(s)$ with Hurwitz polynomial denominator, $C_i(s)$ has also Hurwitz polynomial denominator.

First, if n is a positive integer, set $e_n = (0,\cdots,0,1)^T$ and for every $\Upsilon_i = (\gamma_{i1},\ldots,\gamma_{in}) \in \mathbb{R}^n$, we associate the polynomial

$$P_{\Upsilon_i}(s) = s^n + \sum_{k=1}^{n} \gamma_{ik} s^{n-k}, \tag{2.3.3}$$

and define the companion matrix A_{Υ_i}

$$A_{\Upsilon_i} = \begin{pmatrix} 0 & 1 & 0 & \cdots & \cdots & 0 \\ 0 & 0 & 1 & \ddots & \vdots & \vdots \\ \vdots & 0 & 0 & \ddots & \ddots & \vdots \\ \vdots & \vdots & \ddots & \ddots & 1 & 0 \\ 0 & 0 & \cdots & 0 & 0 & 1 \\ -\gamma_{in} & -\gamma_{i(n-1)} & \cdots & & -\gamma_{i2} & -\gamma_{i1} \end{pmatrix}, \tag{2.3.4}$$

whose characteristic polynomial is P_{Υ_i}. Use $\pi : \mathbb{R}^n \to \mathbb{R}^{n-1}$ to denote the projection onto $\mathbb{R}^{n-1}$ i.e., $\pi(\Upsilon_i) = (\gamma_{i1},\cdots,\gamma_{i(n-1)})$. Define the following subsets of $\mathbb{R}^n$,

$$\mathscr{H}_n = \{\Upsilon_i \in \mathbb{R}^n \mid P_{\Upsilon_i}\, Hurwitz\}, \quad \overline{\mathscr{H}}_n = \{\Upsilon_i \in \mathscr{H}_n \mid \pi(\Upsilon_i) \in \mathscr{H}_{n-1}\}.$$

Now, consider the general $n-order$ transfer function $H_{1i}(s)$ as

$$H_{1i}(s) = \frac{\gamma_{in}}{P_{\Upsilon_i}(s)}, \tag{2.3.5}$$

where $P_{\Upsilon_i}(s)$ and γ_{in} is a component of $\Upsilon_i \in \mathscr{H}_n$, then using (2.3.2) one can get

$$C_i(s) = \frac{\gamma_{in}}{P_{\pi(\Upsilon_i)}(s)}, \tag{2.3.6}$$

To find at least one $P_{\pi(\Upsilon_i)}(s)$ Hurwitz, it suffices to prove that $\overline{\mathscr{H}}_n$ is not empty.

Lemma 2.1. *If n is a positive integer, then $\overline{\mathscr{H}}_n$ is not empty.*

Proof. Showing the thesis amounts to exhibit an example. For that purpose, consider $\gamma = (C_n^l \alpha^l)_{1\leq l\leq n} \in \mathbb{R}^n$, where n is a positive integer, α a positive real number and the C_n^l are the binomial coefficients. Then $P_{\Upsilon_i}(s) = (s+\alpha)^n$ implying that $\Upsilon_i \in \mathscr{H}_n$. It remains to show that $\Upsilon_i \in \overline{\mathscr{H}}_n$. One clearly has that $P_{\pi(\Upsilon_i)} = \frac{P_{\Upsilon_i}(s) - P_{\Upsilon_i}(0)}{s}$ and thus the roots of $P_{\pi(\Upsilon_i)}$ are the non zero roots of $(s+\alpha)^n - \alpha^n$. Every root z of the previous polynomial verifies that $(\frac{z}{\alpha}+1)^n = 1$ and then $\frac{z}{\alpha}+1 = e^{j(2k\pi/n)}$, where $j^2 = -1$ and $k = 0,\ldots,n-1$. It yields that $Re(z) = \alpha(\cos(\frac{2k\pi}{n}) - 1)$, which is negative only if $k \neq 0$ and in the latter case $z = 0$. One deduces that all the roots of $P_{\pi(\Upsilon_i)}$ have negative real part, i.e., $P_{\pi(\Upsilon_i)}$ is Hurwitz and thus $\Upsilon_i \in \overline{\mathscr{H}}_n$. □

Remark 2.1. Let $A_{\gamma_i} \in \mathbb{R}^{(n\times n)}$ and $\sigma(A_{\gamma_i}) = \{\lambda_1,\ldots,\lambda_n\}$ its spectrum, where λ_l, $l = 1,\ldots,n$ are the eigenvalues of A_{γ_i}. Let $I_k \in \mathbb{R}^{(k\times k)}$, k integer, be the identity matrix. Then, the spectrum of the Kronecker product of A_{γ_i} by I_k, $A_{\gamma_i} \otimes I_k \in \mathbb{R}^{(kn\times kn)}$, is equal to $\sigma(A_{\gamma_i})$ according to Theorem in page 245 of '[40]'. In particular, $A_{\gamma_i} \otimes I_k$ is Hurwitz if and only A_{γ_i} is.

2.3.1 High-Order Direct Linear Complementary Filters : First form

Using the reduced attitude kinematics (1.4.8) and the model of the rate-gyro (1.5.10), under Assumption 3, one can write the following system

$$\left\{\begin{array}{lcl} \dot{b}_i &=& -S(\omega_m - \eta)b_i \\ \dot{\eta} &=& \mathbf{0} \end{array}\right. , \tag{2.3.7}$$

where $i = 1,\ldots,m$ and the rate gyro model is considered without noise.

Consider System (2.3.7) and the block diagram of the direct form in Figure 2.3.1 with the compensator $C_i(s)$ given by (2.3.6) for $i = 1,\ldots,m$. Then, the new *n-order direct filter of the first form* with gyro bias estimation is given as

$$\left\{\begin{array}{lcl} x_i^{(n-1)} &=& -\sum_{k=1}^{n-1} \gamma_{ik} x_i^{(n-k-1)} + \gamma_{in}(b_i - \hat{b}_i), \\ \dot{\hat{b}}_i &=& -S(\omega_m - \hat{\eta})b_i + x_i, \\ \dot{\hat{\eta}} &=& \Gamma_{d1} \sum_{i=1}^{m} S(b_i)\upsilon_i \end{array}\right. , \tag{2.3.8}$$

where $i = 1,\ldots,m$, $x_i^{(j)}$ is the $j-$th derivative of x_i with $x_i^{(0)} = x_i$, γ_{ik}, $i = 1,\ldots,m$, $k = 1,\ldots,n$ are components of $\Upsilon_i \in \mathscr{H}_n$, Γ_{d1} is a real positive definite diagonal matrix gain and υ_i is a

vector to be defined later. First, define the observation errors

$$\widetilde{b}_i = b_i - \hat{b}_i, i = 1, ..., m, \tag{2.3.9}$$

$$\widetilde{\eta} = \eta - \hat{\eta} \tag{2.3.10}$$

Then using (2.3.7), (2.3.8), (2.3.9) and (2.3.10) yield the following error dynamics,

$$\begin{cases} x_i^{(n-1)} = -\sum_{k=1}^{n-1} \gamma_{ik} x_i^{(n-k-1)} + \gamma_{in} \tilde{b}_i, \\ \dot{\widetilde{b}}_i = -S(b_i)\widetilde{\eta} - x_i, \\ \dot{\widetilde{\eta}} = -\Gamma_{d1} \sum_{i=1}^{m} S(b_i)\upsilon_i. \end{cases} \tag{2.3.11}$$

By evaluation of the time derivative of the first equation of (2.3.11), one can rewrite (2.3.11) as

$$\begin{cases} x_i^{(n)} = -\sum_{k=1}^{n} \gamma_{ik} x_i^{(n-k)} - \gamma_{in} S(b_i)\widetilde{\eta} \\ \dot{\widetilde{\eta}} = -\Gamma_{d1} \sum_{i=1}^{m} S(b_i)\upsilon_i \end{cases} \tag{2.3.12}$$

Now, consider the new state vector $z_i \in \mathbb{R}^{3n}$, $i = 1, ..., m$ such as $z_i^T = \left[x_i^T, \dot{x}_i^T, \cdots, x_i^{(n-1)T}\right]$ and define the vectors υ_i to be

$$\upsilon_i = B_{d1i}^T P_{d1i} z_i, i = 1, ..., m. \tag{2.3.13}$$

One can rewrite (2.3.12) as

$$\begin{cases} \dot{z}_i(t) = A_{d1i} z_i(t) + B_{d1i} S(\widetilde{\eta}) b_i, \\ \dot{\widetilde{\eta}} = -\Gamma_{d1} \sum_{i=1}^{m} S(b_i) B_{d1i}^T P_{d1i} z_i, \end{cases} \tag{2.3.14}$$

where $i = 1, ..., m$, the Hurwitz matrices $A_{d1i} = A_{\Upsilon_i} \otimes I_d \in \mathbb{R}^{(3n \times 3n)}$ (A_{Υ_i} is defined by (2.3.4)), $B_{d1i} = \gamma_{in} e_n \otimes I_3 \in \mathbb{R}^{3n \times 3}$ and the matrices $P_{d1i} \in \mathbb{R}^{(3n \times 3n)}$, $i = 1, ..., m$, are real symmetric positive definite solutions of the following Lyapunov equations for given symmetric positive definite matrices Q_{d1i} :

$$A_{d1i}^T P_{d1i} + P_{d1i} A_{d1i} = -Q_{d1i}, i = 1, ..., m \tag{2.3.15}$$

Now, the first result can be stated

Proposition 2.1. *Consider the filter (2.3.8) with (2.3.13), applied for m inertial measurable vectors b_i $(i = 1, \cdots, m)$ expressed in $\{\mathscr{B}\}$, under Assumption 2 in section 1.6, then the errors*

(2.3.9) and (2.3.10) converge globally asymptotically to zero.

Proof. Consider the following Lyapunov function candidate

$$V_1 = \sum_{i=1}^{m} z_i^T P_{d1i} z_i + \widetilde{\eta}^T \Gamma_{d1}^{-1} \widetilde{\eta} \tag{2.3.16}$$

where $P_{d1i} \in \mathbb{R}^{(3n\times 3n)}$, $i = 1,...,m$ is given by (2.3.15). The time derivative of (2.3.16) in view of (2.3.14) is given by

$$\begin{aligned} \dot{V}_1 &= \textstyle\sum_{i=1}^{m} \left(z_i^T P_{d1i} \dot{z}_i + \dot{z}_i^T P_{d1i} z_i \right) + 2\widetilde{\eta}^T \Gamma_{d1}^{-1} \dot{\widetilde{\eta}}, \\ &= \textstyle\sum_{i=1}^{m} \left(z_i^T \left(A_{d1i}^T P_{d1i} + P_{d1i} A_{d1i} \right) z_i + 2 z_i^T P_{d1i} B_{d1i} S(\widetilde{\eta}) b_i \right) - 2\widetilde{\eta}^T \textstyle\sum_{i=1}^{m} S(b_i) B_{d1i}^T P_{d1i} z_i, \end{aligned}$$

using (2.3.15) and the fact that $\widetilde{\eta}^T S(b_i) B_{d1i}^T P_{d1i} z_i = z_i^T P_{d1i} B_{d1i} S(\widetilde{\eta}) b_i$, then

$$\dot{V}_1 = -\sum_{i=1}^{m} z_i^T Q_{d1i} z_i \leqslant 0. \tag{2.3.17}$$

Therefore z_i and $\widetilde{\eta}_i$ are bounded and consequently by using (2.3.14), $\dot{z}_i$ and $\dot{\widetilde{\eta}}_i$ are bounded. The evaluation of the second derivative of (2.3.16) in view of (2.3.14) gives

$$\ddot{V}_1 = -\sum_{i=1}^{m} z_i^T \left(A_{d1i}^T Q_{d1i} + Q_{d1i} A_{d1i} \right) z_i + 2 z_i^T Q_{d1i} B_{d1i} S(b_i) \widetilde{\eta}, \tag{2.3.18}$$

which is clearly bounded. By Barbalat's lemma, $\lim_{t\to\infty} \dot{V}_1(t) = 0$ and consequently $\lim_{t\to\infty} z_i(t) = 0_{3n}$, which means that $\lim_{t\to\infty} x_i^{(j)}(t) = \mathbf{0}$, $i = 1,...,m$, $j = 0,...,(n-1)$. Then, according to the first equation of (2.3.11), one can obtain $\lim_{t\to\infty} \widetilde{b}_i(t) = \mathbf{0}$. The second time derivative of z_i is given by

$$\ddot{z}_i = A_{d1i} \left(A_{d1i} z_{d1i}(t) + B_{d1i} S(b_i) \widetilde{\eta} \right) + B_{d1i} S(S(b_i)\omega) \widetilde{\eta} + B_{d1i} S(b_i) \dot{\widetilde{\eta}}, \tag{2.3.19}$$

where all terms are bounded. Thus using Barbalat's lemma, $\lim_{t\to\infty} \dot{z}_i(t) = 0_{3n}$. Therefore, using (2.3.14) and $\lim_{t\to\infty} z_i(t) = 0_{3n}$, one can conclude that $B_{d1i} S(b_i) \widetilde{\eta}$ converges to zero and equivalently $\lim_{t\to\infty} S(b_i(t)) \widetilde{\eta}(t) = \mathbf{0}$, $i = 1,...,m$. Under Assumption 2, the unique solution of the last limit is $\lim_{t\to\infty} \widetilde{\eta}(t) = \mathbf{0}$, which ends the proof. □

2.3.2 High Order Direct Linear-like Filter : Second form

It is possible to propose a second form for the High order Direct filter. In this form, the vector u_i (the equivalent of υ_i vector in the first form) is used as a second term in the dynamic of $\tilde{b}_i$

rather than x_i. Then, a new *n-order direct filter second form* is proposed as follows

$$\left\{\begin{array}{lcl} x_i^{(n-1)} & = & -\sum_{k=1}^{n-1}\gamma_{ik}x_i^{(n-k-1)}+\gamma_{in}(b_i-\hat{b}_i) \\ \dot{\hat{b}}_i & = & -S(\omega_m-\hat{\eta})b_i+u_i \\ \dot{\hat{\eta}} & = & -\Gamma_{d2}\sum_{i=1}^{m}S(b_i)\hat{b}_i \end{array}\right. , \tag{2.3.20}$$

where $i=1...m$, $x_i^{(j)}$ is the jth order derivative of x_i with $x_i^{(0)}=x_i$, γ_{ik}, $i=1,...,m$, $k=1,...,n$ are components of $\Upsilon_i\in\overline{\mathscr{H}}_n$, Γ_{d2} is a real positive definite diagonal matrix gain and u_i is a vector to be defined later.

Using (2.3.7), (2.3.9), (2.3.10) and (2.3.20) leads to the following error dynamics,

$$\left\{\begin{array}{lcl} x_i^{(n-1)} & = & -\sum_{k=1}^{n-1}\gamma_{ik}x_i^{(n-k-1)}+\gamma_{in}\tilde{b}_i, \\ \dot{\tilde{b}}_i & = & -S(b_i)\tilde{\eta}-u_i, \\ \dot{\tilde{\eta}} & = & -\Gamma_{d2}\sum_{i=1}^{m}S(b_i)\tilde{b}_i. \end{array}\right. \tag{2.3.21}$$

Now, consider the new state variable $X_{d2i}\in\mathbb{R}^{3(n-1)}$, $i=1...m$ such as $X_{d2i}^T=\left[x^T,\dot{x}^T,\cdots,x^{(n-2)T}\right]$ and the vector

$$u_i=\beta_i B_{d2i}^T P_{d2i}X_{d2i} \tag{2.3.22}$$

such that $\beta_i\in\mathbb{R}_+^*$, $P_{d2i}\in\mathbb{R}^{(3(n-1)\times 3(n-1))}$ will be defined later and $i=1,...,m$

With the notation above, one can rewrite (2.3.21) as

$$\left\{\begin{array}{lcl} \dot{X}_{d2i}(t) & = & A_{d2i}X_{d2i}(t)+B_{d2i}\tilde{b}_i, \\ \dot{\tilde{b}}_i & = & -S(b_i)\tilde{\eta}-\beta_i B_{d2i}^T P_{d2i}X_{d2i}, \\ \dot{\tilde{\eta}} & = & -\Gamma_{d2}\sum_{i=1}^{m}S(b_i)\tilde{b}_i, \end{array}\right. \tag{2.3.23}$$

where the Hurwitz matrices $A_{d2i}=A_{\pi(\Upsilon_i)}\otimes I_d\in\mathbb{R}^{(3(n-1)\times 3(n-1))}$ ($A_{\pi(\Upsilon_i)}$ is defined by (2.3.4), see Note 2.1 for A_{d2i} Hurwitz) and the matrices $B_{d2i}=\gamma_{in}e_{(n-1)}\otimes I_d\in\mathbb{R}^{3(n-1)\times 3}$ and the matrices $P_{d2i}\in\mathbb{R}^{(3(n-1)\times 3(n-1))}$, $i=1,...,m$, are real symmetric positive definite solutions of the following Lyapunov equations for given symmetric positive definite matrices Q_{d2i}

$$A_{d2i}^T P_{d2i}+P_{d2i}A_{d2i}=-Q_{d2i}, \tag{2.3.24}$$

Now, the second result can be stated

Proposition 2.2. *Consider the filter (2.3.20) with (2.3.22), applied for m inertial measurable vectors b_i $(i=1,\cdots,m)$ expressed in $\{\mathscr{B}\}$, under Assumptions 2 and 3 in section 1.6, then the errors (2.3.9) and (2.3.10) converge globally asymptotically to zero.*

Proof. The proof is identical to the proof of the proposition 2.1 by using the following Lyapunov function

$$V_2 = \sum_{i=1}^{m} \beta_i X_{d2i}^T P_{d2i} X_{d2i} + \sum_{i=1}^{m} \tilde{b}_i^T \tilde{b}_i + \tilde{\eta}^T \Gamma_{d2}^{-1} \tilde{\eta}$$

. □

2.3.3 High-Order Passive Linear-like Filters : First form

In the passive form, the design of the complementary filter is performed by injecting the filtered measurements for offsetting nonlinear term as shown in block diagram of Figure 2.3.2 with a compensator $C_i(s)$, $i = 1, \cdots, m$, defined by (2.3.6). Then, a new *n-order passive filter of the first form* is proposed as follows

$$\left\{ \begin{array}{lcl} x_i^{(n-1)} & = & -\sum_{k=1}^{n-1} \gamma_{ik} x_i^{(n-k-1)} + \gamma_{in}(b_i - \hat{b}_i), \\ \dot{\hat{b}}_i & = & -S(\omega_m - \hat{\eta})\hat{b}_i + w_i, \\ \dot{\hat{\eta}} & = & -\Gamma_{p1} \sum_{i=1}^{m} S(b_i)\hat{b}_i, \end{array} \right. , \tag{2.3.25}$$

where $i = 1, ..., m$, $x_i^{(j)}$ is the jth order derivative of x_i with $x_i^{(0)} = x_i$, γ_{ik}, $i = 1, ..., m$, $k = 1, ..., n$ are components of $\Upsilon_i \in \overline{\mathscr{H}}_n$, Γ_{p1} is a real positive definite diagonal matrix gain and w_i are given by

$$w_i = \delta_i B_{p1i}^T P_{p1i} X_{p1i}, \tag{2.3.26}$$

with $\delta_i \in \mathbb{R}_+^*$, $X_{p1i} \in \mathbb{R}^{3(n-1)}$, $i = 1, ..., m$ such as $X_{p1i}^T = \left[x_i^T, \dot{x}_i^T, \cdots, x_i^{(n-2)T} \right]$, allowing to rewrite (2.3.25) as

$$\left\{ \begin{array}{lcl} \dot{X}_{p1i}(t) & = & A_{p1i} X_{p1i}(t) + B_{p1i}(b_i - \hat{b}_i), \\ \dot{\hat{b}}_i & = & -S(\omega_m - \hat{\eta})\hat{b}_i + B_{p1i}^T P_{p1i} X_{p1i}, \\ \dot{\hat{\eta}} & = & -\Gamma_{p1} \sum_{i=1}^{m} S(b_i)\hat{b}_i, \end{array} \right. \tag{2.3.27}$$

where the Hurwitz matrices $A_{p1i} = A_{\pi(\Upsilon_i)} \otimes I_d \in \mathbb{R}^{(3(n-1)\times 3(n-1))}$ ($A_{\pi(\Upsilon_i)}$ is defined by (2.3.4), see Note 2.1 for A_{p1i} Hurwitz) and the matrices $B_{p1i} = \gamma_{in} e_{(n-1)} \otimes I_d \in \mathbb{R}^{3(n-1)\times 3}$ and the matrices $P_{p1i} \in \mathbb{R}^{(3(n-1)\times 3(n-1))}$, $i = 1, ..., m$, are real symmetric positive definite solutions of the following Lyapunov equations for given symmetric positive definite matrices Q_{p1i} :

$$A_{p1i}^T P_{p1i} + P_{p1i} A_{p1i} = -Q_{p1i}, \tag{2.3.28}$$

Now, the third result can be stated

Proposition 2.3. *Consider the filter (2.3.25) with (2.3.26), applied for m inertial measurable vectors b_i $(i = 1, \cdots, m)$ expressed in $\{\mathscr{B}\}$, under Assumptions 2 and 3 in section 1.6, then the errors (2.3.9) and (2.3.10) converge globally asymptotically to zero.*

Proof. The error dynamics of (2.3.27) can be evaluated by using (2.3.7), (2.3.9) and (2.3.10), as follow

$$\left\{\begin{array}{lcl} \dot{X}_{p1i}(t) & = & A_{p1i}X_{p1i}(t) + B_{p1i}\tilde{b}_i, \\ \dot{\tilde{b}}_i & = & -S(b_i)\widetilde{\eta} + S(\tilde{b}_i)(\omega + \widetilde{\eta}) - \delta_i B_{p1i}^T P_{p1i} X_{p1i}, \\ \dot{\widetilde{\eta}} & = & -\Gamma_{p1}\sum_{i=1}^{m} S(b_i)\tilde{b}_i, \end{array}\right. \tag{2.3.29}$$

Consider now, the following Lyapunov function

$$V_3 = \sum_{i=1}^{m} \delta_i X_{p1i}^T P_{p1i} X_{p1i} + \sum_{i=1}^{m} \tilde{b}_i^T \tilde{b}_i + \widetilde{\eta}^T \Gamma_{p1}^{-1} \widetilde{\eta}, \tag{2.3.30}$$

the time derivative of (2.3.30) in view of (2.3.29) is given by

$$\dot{V}_3 = \sum_{i=1}^{m} \delta_i \left(X_{p1i}^T \left(A_{p1i}^T P_{p1i} + P_{p1i} A_{p1i} \right) X_{p1i} \right),$$

since A_{p1i}, $i = 1, \ldots, m$ is Hurwitz, then the Lyapunov equation (2.3.28) holds. Therefore, one can obtain

$$\dot{V}_3 = -\sum_{i=1}^{m} \delta_i X_{p1i}^T Q_{p1i} X_{p1i} \leqslant 0. \tag{2.3.31}$$

Therefore, X_{p1i}, $\tilde{b}_i$ and $\widetilde{\eta}_i$ are bounded and consequently from (2.3.29) and Assumption 3 in section 1.6, $\dot{X}_{p1i}$, $\dot{\tilde{b}}_i$ and $\dot{\widetilde{\eta}}_i$ are also bounded. The rest of the proof is similar to the proof of Proposition 2.1. It is easy to verify that $\ddot{V}_3$ is bounded. Thus using Barbalat's lemma, $\lim_{t\to\infty} \dot{V}_3(t) = 0$ and consequently $\lim_{t\to\infty} X_{p1i}(t) = 0_{3(n-1)}$. In addition, $\ddot{X}_{p1i}$ are bounded, then $\lim_{t\to\infty} \dot{X}_{p1i}(t) = 0_{3(n-1)}$ and using (2.3.29), $\lim_{t\to\infty} \widetilde{b}_i(t) = \mathbf{0}$. By a standard reasoning by contradiction, one gets that $\lim_{t\to\infty} \dot{\tilde{b}}_i(t) = \mathbf{0}$. Using this fact and (2.3.29), therefore $\lim_{t\to\infty} S(b_i)\widetilde{\eta} = \mathbf{0}$. Under Assumption 2, one can conclude that $\lim_{t\to\infty} \widetilde{\eta}(t) = \mathbf{0}$. □

2.3.4 High-Order Passive Linear-like Filters : Second form

Similar to the case of direct filter, it is possible to propose a second form high order passive filter. Then, a new *n-order passive filter second form* is proposed as follows

$$\begin{cases} x_i^{(n-1)} &= -\sum_{k=1}^{n-1} \gamma_{ik} x_i^{(n-k-1)} + \gamma_{in}(b_i - \hat{b}_i) \\ \dot{\hat{b}}_i &= -S(\omega_m - \hat{\eta})\hat{b}_i + x_i \\ \dot{\hat{\eta}} &= \Gamma_{p2} \sum_{i=1}^{m} S(\hat{b}_i) y_i \end{cases} \tag{2.3.32}$$

where $i = 1...m$, $x_i^{(j)}$ is the jth order derivative of x_i with $x_i^{(0)} = x_i$, Γ_{p2} is a real positive definite diagonal matrix gain. There are many possibilities to reformulate (2.3.32) and give a definition to the vector y_i. My best is to obtain some condition on the selection of γ_{ik} depending on the norm of the angular velocity. *The stability analysis of this filter for order higher than three remain an open problem.*

In this case, it is possible to write the first and the second order passive filters of the second form similar to those of the first form. Thus it is possible to state about the stability of these two cases.

2.4 Simulations

To show the effectiveness and performance of the proposed filters, many simulations were done. Three cases were selected, depending on the order of the filters. Table 2.4.1 and 2.4.2 gives an overview of the first, second and third order filters in all forms, with the corresponding chosen gains and matrices. The selected transfer functions are

$$H_{1i}(s) = \frac{\gamma_{in}}{P_{\Upsilon_i}(s)} = \frac{\alpha^n}{(s+\alpha)^n}, i = 1,2, n = 1,2,3,$$

therefore

$$C_i(s) = \frac{\gamma_{in}}{P_{\pi(\Upsilon_i)}(s)} = \frac{s\alpha^n}{(s+\alpha)^n - \alpha^n}, i = 1,2, n = 1,2,3,$$

An additive zero-mean white noise were taken for measurements with standard deviation $0.01\,(normalized)$ for accelerometer and magnetometer, $1\,(^\circ/s)$ for rate gyros. The measurements from gyroscope are also corrupted by a constant bias $\eta = [2, -3, 1]\,(^\circ/s)$. The used integration method is "ode5" with $0.01s$ as sample time, all gains are presented in Table 2.4.1 and 2.4.2.

Figures 2.4.1-(a), (b) and (c) illustrate Euler angles evolution of the two first order direct forms and first order passive form 1 filters, denoted D1F1, D1F2 and P1F1, respectively. The

same results are presented in Figures 2.4.1-(d), (e) and (f) for the second order (denoted D2F1, D2F2 and P2F1) and in Figures 2.4.1-(g), (h) and (i) for the third order (denoted D3F1, D3F2 and P3F1). Figure 2.4.2 illustrates gyro rate bias estimation in all selected filters and Figure 2.4.3 illustrates an example of the inertial vectors measurements with their form1 first order passive estimates and rate gyro measurements.

The difference between all these filters can be showed by the evaluation of the standard deviation of Euler angles in each case, Table 2.4.3 illustrates this evaluation, from which some conclusion remarks should be stated :

1. With selected gains, the first order direct form1 and form2 are equivalent;

2. It is possible to find Q_{d1i} such that the second order direct form1 and form2 will be equivalent, gains presented in Table 2.4.1 are an arbitrary selection to show the difference;

3. For the same order, as expected, the passive form is less sensitive to noise;

4. For the same form, the second order is slightly better than the first order. This fact is expected since in the case of second order filters, the second term in the expression of $\dot{\hat{b}}_i$ are function of x_i itself filtered by a first order filter. While in the first order filter, this second term is formed by $\tilde{b}_i$ which is more sensitive to noise than x_i;

5. With selected gains, the third order in all cases seems to exhibit poor performances compared to the first and second order. In the case of direct first form, the vector υ_i introduce disturbance on the bias estimation, which affect $\hat{b}_i$ dynamics. One possible solution is to review the gain tuning method and an optimal method will be better. The drawback of the direct second form is that the complementarity aspect will be lost starting from the third order. Similar remark in the case of passive third order filter.

Finally, the most interesting filters are the first and second order filters in all forms.

order	Direct first form	Direct second form	Passive first form
n	$x_i^{(n-1)} = -\sum_{k=1}^{n-1} \gamma_{ik} x_i^{(n-k-1)} + \gamma_{in}\tilde{b}_i$ $\dot{\hat{b}}_i = -S(\omega_m - \hat{\eta})b_i + x_i$ $\dot{\hat{\eta}} = \Gamma_{d1}\sum_{i=1}^{m} S(b_i)\upsilon_i$ $\upsilon_i = B_{di}^T P_{di} z_i$ $z_i^T = \left[x^T, \dot{x}^T, \cdots, x^{(n-1)T}\right]$ $B_{d1i} = \gamma_{in} e_n \otimes I_d \in \mathbb{R}^{3n\times 3}$ $A_{d1i} = A_{\gamma_i} \otimes I_d \in \mathbb{R}^{(3n\times 3n)}$ $P_{d1i} \in \mathbb{R}^{(3n\times 3n)}$ $A_{d1i}^T P_{d1i} + P_{d1i} A_{d1i} = -Q_{d1i}$	$x_i^{(n-1)} = -\sum_{k=1}^{n-1} \gamma_{ik} x_i^{(n-k-1)} + \gamma_{in}\tilde{b}_i$ $\dot{\hat{b}}_i = -S(\omega_m - \hat{\eta})b_i + u_i$ $\dot{\hat{\eta}} = -\Gamma_{d2}\sum_{i=1}^{m} S(b_i)\hat{b}_i$ $u_i = \beta_i B_{d2i}^T P_{d2i} X_{d2i}$ $X_{d2i}^T = \left[x^T, \dot{x}^T, \cdots, x^{(n-2)T}\right]$ $B_{d2i} = \gamma_{in} e_{(n-1)} \otimes I_d \in \mathbb{R}^{3(n-1)\times 3}$ $A_{d2i} = A_{\pi(\gamma_i)} \otimes I_d \in \mathbb{R}^{(3(n-1)\times 3(n-1))}$ $P_{d2i} \in \mathbb{R}^{(3(n-1)\times 3(n-1))}$ $A_{d2i}^T P_{d2i} + P_{d2i} A_{d2i} = -Q_{d2i}$	$x_i^{(n-1)} = -\sum_{k=1}^{n-1} \gamma_{ik} x_i^{(n-k-1)} + \gamma_{in}\tilde{b}_i$ $\dot{\hat{b}}_i = -S(\omega_m - \hat{\eta})\hat{b}_i + w_i$ $\dot{\hat{\eta}} = -\Gamma_p\sum_{i=1}^{m} S(b_i)\hat{b}_i$ $w_i = \delta_i B_{p1i}^T P_{p1i} X_{p1i}$ $X_{p1i}^T = \left[x^T, \dot{x}^T, \cdots, x^{(n-2)T}\right]$ $B_{p1i} = \gamma_{in} e_{(n-1)} \otimes I_d \in \mathbb{R}^{3(n-1)\times 3}$ $A_{p1i} = A_{\pi(\gamma_i)} \otimes I_d \in \mathbb{R}^{(3(n-1)\times 3(n-1))}$ $P_{p1i} \in \mathbb{R}^{(3(n-1)\times 3(n-1))}$ $A_{p1i}^T P_{p1i} + P_{p1i} A_{p1i} = -Q_{p1i}$
1	**Direct_D1_F1**	**Direct_D1_F2**	**Passive_P1_F1**
	$\dot{\hat{b}}_i = -S(\omega_m - \hat{\eta})b_i + \gamma_{i1}\tilde{b}_i$ $\dot{\hat{\eta}} = -\gamma_{i1}^2\Gamma_{d1}\sum_{i=1}^{2} S(b_i)\hat{b}_i$	$\dot{\hat{b}}_i = -S(\omega_m - \hat{\eta})b_i + \beta_i\gamma_{i1}^2\tilde{b}_i$ $\dot{\hat{\eta}} = -\Gamma_{d2}\sum_{i=1}^{2} S(b_i)\hat{b}_i$	$\dot{\hat{b}}_i = -S(\omega_m - \hat{\eta})\hat{b}_i + \delta_i\gamma_{i1}^2\tilde{b}_i$ $\dot{\hat{\eta}} = -\Gamma_{p1}\sum_{i=1}^{2} S(b_i)\hat{b}_i$
	$\gamma_{i1} = 1, \gamma_{i2} = 1, \Gamma_{d1} = 0.1 I_d$	$\gamma_{i1} = 1, \gamma_{i2} = 1, \Gamma_{d2} = 0.1 I_d, \beta_i = 1$	$\gamma_{i1} = 1, \gamma_{i2} = 1, \Gamma_{p1} = 0.1 I_d, \delta_i = 1$
2	**Direct_D2_F1**	**Direct_D2_F2**	**Passive_P2_F1**
	$\dot{x}_i = -\gamma_{i1} x_i + \gamma_{i2}\tilde{b}_i$ $\dot{\hat{b}}_i = -S(\omega_m - \hat{\eta})b_i + x_i$ $\dot{\hat{\eta}} = \Gamma_{d1}\sum_{i=1}^{2} S(b_i)\upsilon_i$	$\dot{x}_i = -\gamma_{i1} x_i + \gamma_{i2}\tilde{b}_i$ $\dot{\hat{b}}_i = -S(\omega_m - \hat{\eta})b_i + u_i$ $\dot{\hat{\eta}} = -\Gamma_{d2}\sum_{i=1}^{2} S(b_i)\hat{b}_i$	$\dot{x}_i = -\gamma_{i1} x_i + \gamma_{i2}\tilde{b}_i$ $\dot{\hat{b}}_i = -S(\omega_m - \hat{\eta})\hat{b}_i + w_i$ $\dot{\hat{\eta}} = -\Gamma_{p1}\sum_{i=1}^{m} S(b_i)\hat{b}_i$
	$z_i = \begin{bmatrix} x_i & \dot{x}_i \end{bmatrix}, \upsilon_i = B_{di}^T P_{di} z_i$	$X_{d2i} = x_i, u_i = \beta_i\gamma_{i2} x_i$	$X_{p1i} = x_i, w_i = \delta_i\gamma_{i2} x_i$
	$\gamma_{i1} = 2\alpha = 2, \gamma_{i2} = \alpha^2 = 1$	$\gamma_{i1} = 2\alpha = 2, \gamma_{i2} = \alpha^2 = 1, \beta_i = 2$	$\gamma_{i1} = 2\alpha = 2, \gamma_{i2} = \alpha^2 = 1, \delta_i = 2$
	$A_{d1i} = \begin{bmatrix} 0 & I_d \\ -\gamma_2 I_d & -\gamma_1 I_d \end{bmatrix}, \Gamma_{d1} = 0.1 I_d$	$A_{d2i} = 0, \Gamma_{d2} = 0.1 I_d$	$A_{p1i} = 0, \Gamma_{p1} = 0.1 I_d$
	$B_{d1i} = \begin{bmatrix} 0 \\ \gamma_2 I_d \end{bmatrix}, P_{d1i} = \begin{bmatrix} 1.5 I_d & 0.5 I_d \\ 0.5 I_d & 0.5 I_d \end{bmatrix}$	$B_{d2i} = \gamma_2 I_d$	$B_{p1i} = \gamma_2 I_d$
	$A_{d1i}^T P_{d1i} + P_{d1i} A_{d1i} = -Q_{d1i} = -I_{6\times 6}$	$P_{d2i} = I_d$	$P_{p1i} = I_d$

Table 2.4.1: Overview of the 1st, 2nd order filters in all forms with selected gains

order	Direct first form	Direct second form	Passive first form
3	**Direct_D3_F1**	**Direct_D3_F2**	**Passive_P3_F1**
	$\ddot{x}_i = -\gamma_{i1}\dot{x}_i - \gamma_{i2}x_i + \gamma_{i3}\tilde{b}_i$ $\dot{\hat{b}}_i = -S(\omega_m - \hat{\eta})b_i + x_i$ $\dot{\hat{\eta}} = \Gamma_{d1}\sum_{i=1}^{m} S(b_i)\upsilon_i$	$\ddot{x}_i = -\gamma_{i1}\dot{x}_i - \gamma_{i2}x_i + \gamma_{i3}\tilde{b}_i$ $\dot{\hat{b}}_i = -S(\omega_m - \hat{\eta})b_i + u_i$ $\dot{\hat{\eta}} = -\Gamma_{d2}\sum_{i=1}^{m} S(b_i)\hat{b}_i$	$\ddot{x}_i = -\gamma_{i1}\dot{x}_i - \gamma_{i2}x_i + \gamma_{i3}\tilde{b}_i$ $\dot{\hat{b}}_i = -S(\omega_m - \hat{\eta})\hat{b}_i + w_i$ $\dot{\hat{\eta}} = -\Gamma_{p1}\sum_{i=1}^{m} S(b_i)\hat{b}_i$
	$\upsilon_i = B_{d1i}^T P_{d1i} z_i$	$u_i = \beta_i B_{d2i}^T P_{d2i} X_{di}$	$w_i = \delta_i B_{p1i}^T P_{p1i} X_{p1i}$
	$\gamma_{i1} = 3\alpha,\ \gamma_{i2} = 3\alpha^2,\ \gamma_{i3} = \alpha^3$	$\gamma_{i1} = 3\alpha,\ \gamma_{i2} = 3\alpha^2,\ \gamma_{i3} = \alpha^3$	$\gamma_{i1} = 3\alpha,\ \gamma_{i2} = 3\alpha^2,\ \gamma_{i3} = \alpha^3$
	$A_{d1i} = \begin{bmatrix} 0 & I_d & 0 \\ 0 & 0 & I_d \\ -\gamma_3 I_d & -\gamma_2 I_d & -\gamma_1 I_d \end{bmatrix}$	$A_{d2i} = \begin{bmatrix} 0 & I_d \\ -\gamma_2 I_d & -\gamma_1 I_d \end{bmatrix}$	$A_{p1i} = \begin{bmatrix} 0 & I_d \\ -\gamma_2 I_d & -\gamma_1 I_d \end{bmatrix}$
	$A_{d1i}^T P_{d1i} + P_{d1i} A_{d1i} = -Q_{d1i} = -I_{9\times 9}$	$A_{d2i}^T P_{d2i} + P_{d2i} A_{d2i} = -Q_{d2i}$	$A_{p1i}^T P_{p1i} + P_{p1i} A_{p1i} = -Q_{p1i}$
	$B_{d1i} = \begin{bmatrix} 0 \\ 0 \\ \gamma_3 I_d \end{bmatrix},\ \Gamma_{d1} = 0.1 I_d$ $P_{d1i} = \begin{bmatrix} 2.31 I_d & 1.94 I_d & 0.5 I_d \\ 1.94 I_d & 3.25 I_d & 0.81 I_d \\ 0.5 I_d & 0.81 I_d & 0.44 I_d \end{bmatrix}$	$B_{d2i} = \begin{bmatrix} 0 \\ \gamma_2 I_d \end{bmatrix},\ \Gamma_{d2} = 0.1 I_d$ $P_{d2i} = \begin{bmatrix} 1.17 I_d & 0.17 I_d \\ 0.17 I_d & 0.22 I_d \end{bmatrix}$	$B_{p1i} = \begin{bmatrix} 0 \\ \gamma_2 I_d \end{bmatrix},\ \Gamma_{p1} = 0.1 I_d$ $P_{p1i} = \begin{bmatrix} 1.17 I_d & 0.17 I_d \\ 0.17 I_d & 0.22 I_d \end{bmatrix}$
	$z_i = \begin{bmatrix} x_i^T & \dot{x}_i^T & \ddot{x}_i^T \end{bmatrix}^T$	$X_{d2i} = \begin{bmatrix} x_i^T & \dot{x}_i^T \end{bmatrix}^T$	$X_{p1i} = \begin{bmatrix} x_i^T & \dot{x}_i^T \end{bmatrix}^T$

Table 2.4.2: Overview of the 3rd order filters in all forms with selected gains

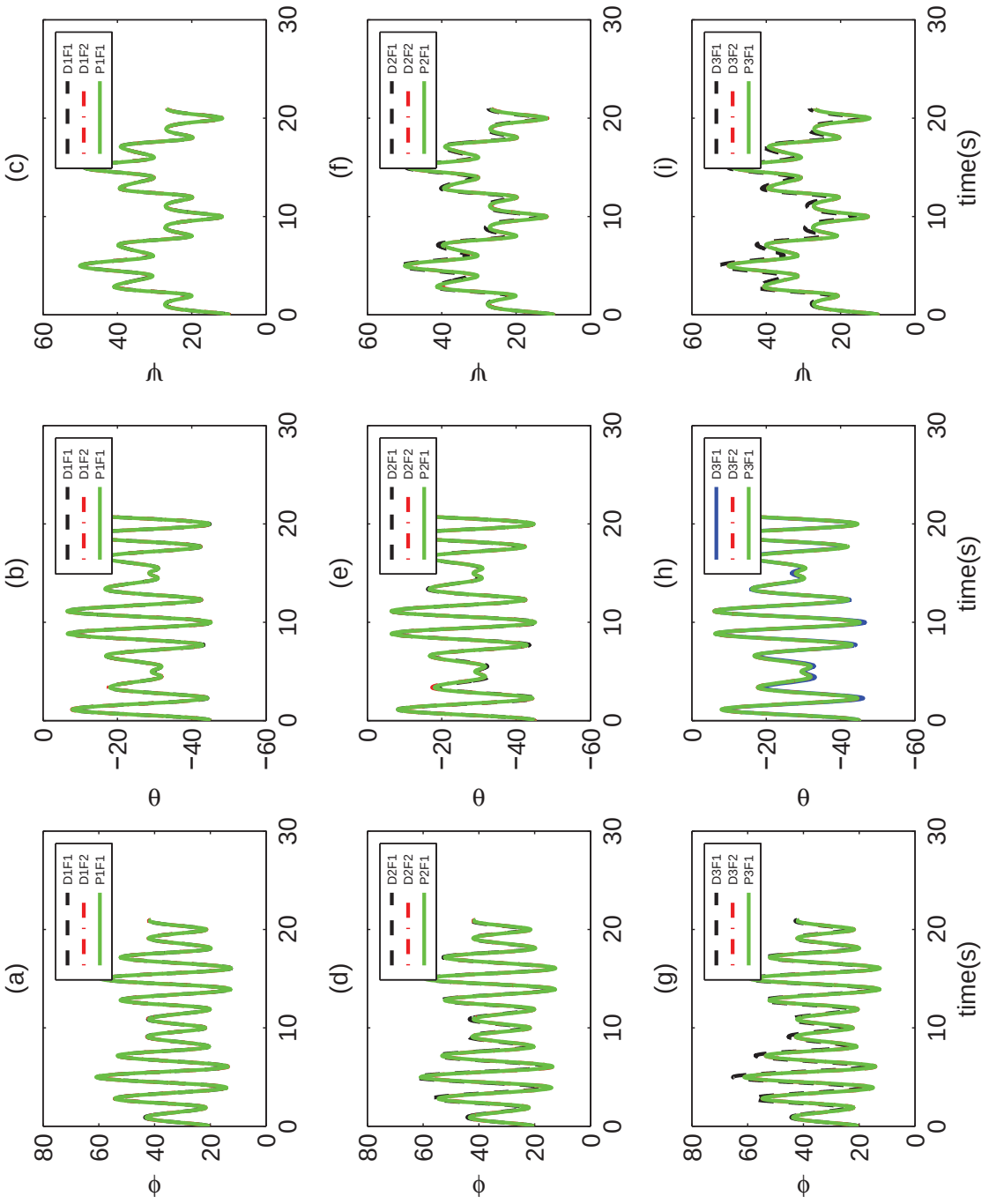

Figure 2.4.1: Euler angles results in ()

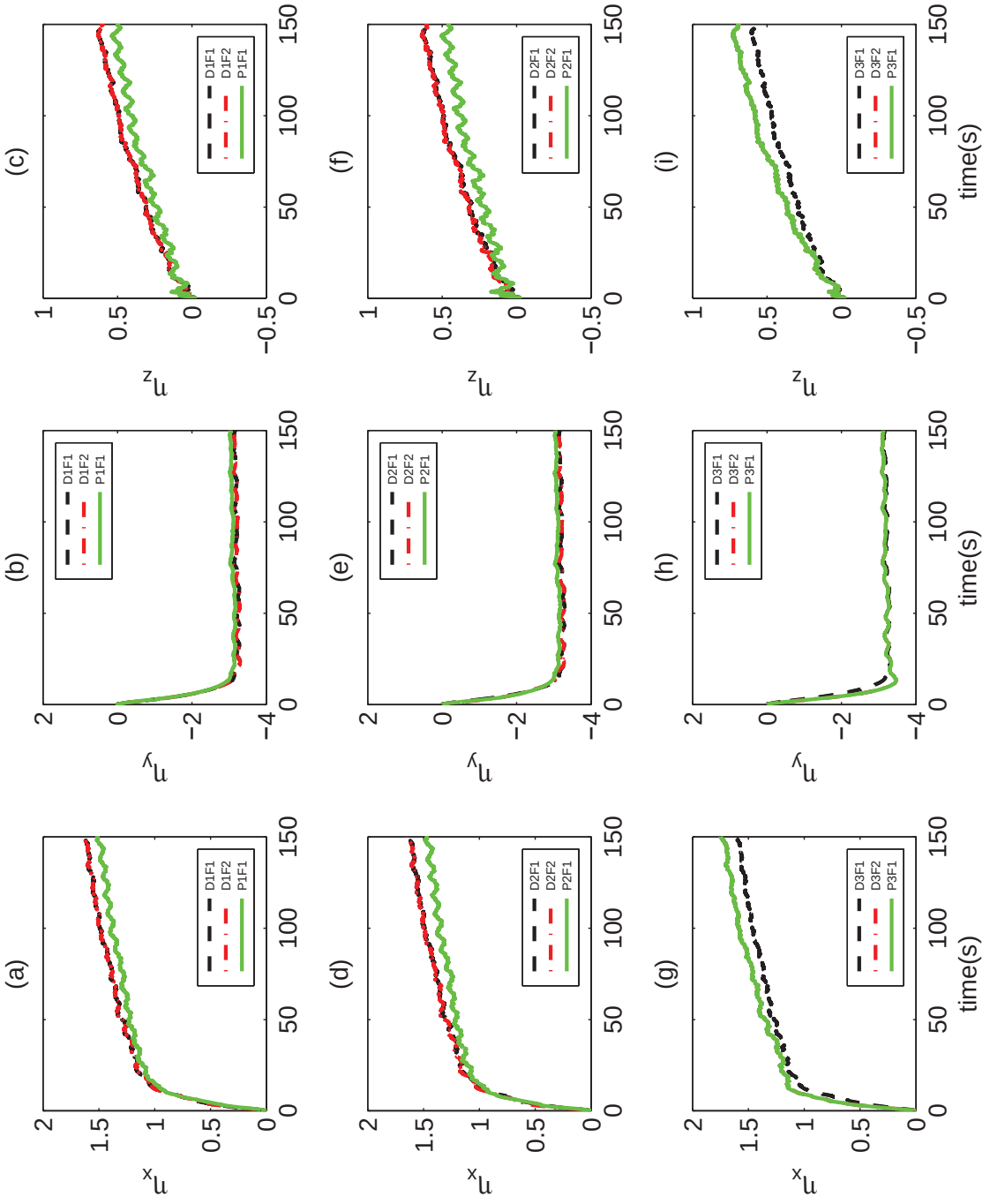

Figure 2.4.2: Rate gyro bias estimates for all filters in (/s)

order	Direct first form			Direct second form			Passive first form		
	σ_x	σ_y	σ_z	σ_x	σ_y	σ_z	σ_x	σ_y	σ_z
1	**Direct_D1_F1**			**Direct_D1_F2**			**Passive_P1_F1**		
	0.4841	0.3437	0.3707	0.4841	0.3437	0.3707	0.4741	0.3367	0.3553
2	**Direct_D2_F1**			**Direct_D2_F2**			**Passive_P2_F1**		
	0.4781	0.3372	0.3625	0.4776	0.3416	0.3689	0.4638	0.3360	0.3530
3	**Direct_D3_F1**			**Direct_D3_F2**			**Passive_P3_F1**		
	1.0158	0.8759	0.9572	0.6090	0.4521	0.5202	0.5990	0.4403	0.5117

Table 2.4.3: Standard deviation of Euler angles errors of all filters

2.5 Conclusions

Due to its importance and despite the considerable number of solutions, the problem of attitude estimation is still relevant. This chapter presented complementary linear-like filter-based attitude estimation approach. In which, three kind of filters that ensure global asymptotic convergence of the estimation errors have been presented. The proposed solutions allow the choice between different possible combinations obtained by the selection of the form (direct, passive) and the filter order. Thus, the non-sensitivity to noise and the quality of filtering can be examined. These solutions includes the bias gyro-rate estimation as well.

The direct first form proposed filters preserve the structure of complementary filters without any dependence on the selected filter order. Contrary to direct second form and passive filters, where complementary aspect is lost starting from the third order. Nevertheless, it is possible to preserve the structure of the passive complementary filters similar to the direct high-order filter ensuring global convergence to the detriment of the choice of the cutoff frequency depending on bound of the measured angular velocity. Another important conclusion is the fact that the passive second order filter can be of great help. Indeed, in future work, this filter will be used to enhance the low sampling frequency of magnetometer measurements compared to that of accelerometer.

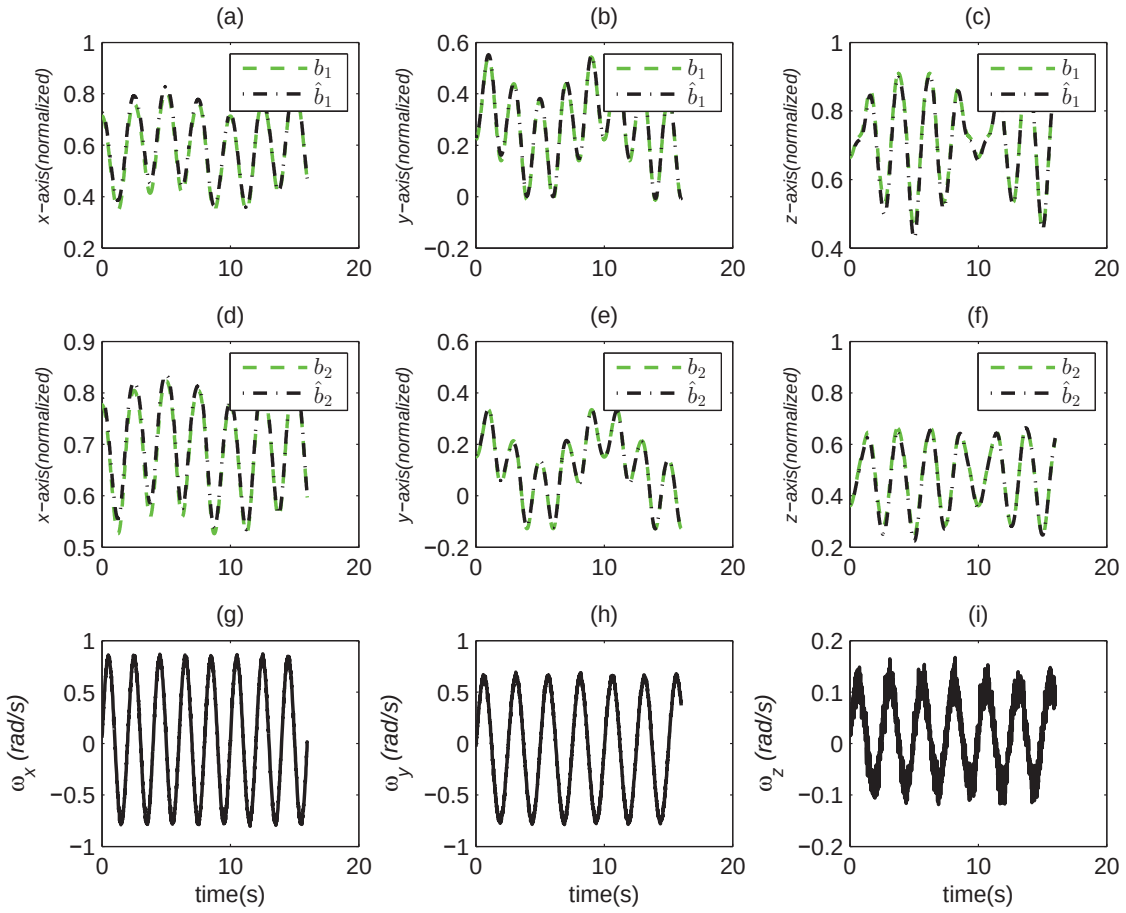

Figure 2.4.3: Inertial vectors with their 1st form 1st order passive estimates and rate gyro

Chapter 3

Attitude Tracking using Linear-Like Complementary Filters and without "Attitude measurements"

3.1 Introduction

The problem of attitude control was treated using several type of parametrization of the attitude (see, for instance, [85]). Review of attitude control problem can be found in [20, 110]. Classical solutions to this problem have been proposed using local-minimal parametrization which lies in $\mathbb{R}^3$, such as Euler angles or modified Rodriguez parameters (see, for instance, [19, 73, 110, 117]). The global-unique representation, which is the natural parametrization of the attitude is the direction cosine rotation matrix that lies in the special orthogonal group $SO(3)$. As a consequence, many recent solutions use this parametrization (see, for instance, [7, 20, 56, 61]). However, for simplicity of analysis and numerical implementation reasons, a considerable number of solutions to the problem of rigid body attitude control use rather quaternion parametrization as global representation which lies in the unit sphere $\mathbb{S}^3$ (see, for instance, [33, 48, 68, 98, 116]).

Numerous advanced control techniques have been proposed for the UAV control for which accurate attitude tracking requires precise knowledge of its dynamic state (see, for instance, [8, 17, 20, 56, 73, 95]). Most of traditional attitude control approaches are based on feedback scheme using attitude estimation (see, for instance, [8, 48, 56, 97, 102]). Recently, some authors propose to use directly raw vector measurements to perform attitude control (see, for instance, [10, 95, 100]). In fact, the explicit use of the attitude in the control law involves the determination of attitude from measurements provided by appropriate sensors. Many at-

titude control applications use measurement data from an embedded "IMU" with three-axis accelerometers, magnetometers and gyroscopes. The capability of the UAV to track desired trajectories depends on the reliability of these sensors and the quality of measurements related to sensitivity to noise, bias, etc.

The advantage of the method presented in this Chapter is the use of the data fusion to improve the attitude tracking, where only inertial measurements and rate gyro measurements are used to track the desired trajectories. In fact, some proposed control laws used to generate the torque to be applied to the system, are mainly based on an error term between the desired inertial vectors and the raw measurements inertial vectors. The new proposed control is based on the use of an error term between the desired inertial vectors and the filtered measurements inertial vectors. It should be noted that the quality of IMU measurements is much degraded by the phenomenon of vibrations of real system since it influences their measurements. Frequently, the implementation of some attitude control using directly raw vector measurements are confronted with this phenomenon. The stability analysis of the tracking error dynamics based on Lyapunov method and Invariance LaSalle's theorem show that almost all trajectories converge asymptotically to the equilibrium point. Although unit quaternion are used in stability analysis, the proposed control law take into consideration the projection of the closed-loop vector field from $\mathbb{R}^{3m} \times \mathbb{S}^3 \times \mathbb{R}^3$ onto $\mathbb{R}^{3m} \times SO(3) \times \mathbb{R}^3$. Thus, the unwinding phenomenon is avoided. Moreover and contrarily to what is stated in [7, 95], it is showed that the set of control gains leading to a continuum of equilibria of the closed loop system is an algebraic variety of positive co-dimension, independently on the choice of the observed vectors.

This Chapter is organized as follow. In Section 3.2, the notion of attitude tracking using complementary filters principle is presented. The design of the new controller coupled with a new linear-like complementary filter is detailed. After, stability analysis based on Lyapunov theory and LaSalle's theorem is presented. A more simplified control law for stabilization case, where the desired trajectories are time invariant, is derived in Section 3.3. Section 3.4 illustrates the effectiveness of the proposed solution using simulations, a second validation using experiment will be presented in Chapter 5. Finally, some concluding remarks are presented in Section 3.5. Partial results in this Chapter were presented in [12].

3.2 Attitude tracking using complementary filter principle

A novel attitude control law that use only filtered inertial vectors and rate gyro measurements to track the desired trajectories, without using "attitude measurements" is presented. The filtered inertial vectors are obtained using a new version of the filter based on first order direct linear-like complementary filter already presented in Chapter 2.

3.2.1 Controller Design

Let us first define the tracking orientation error by

$$\bar{R}(t) = R(t)R_d^T(t),$$

which corresponds to the quaternion error $\bar{Q}(t)$ such that $\mathscr{R}(\bar{Q}(t)) = \bar{R}(t)$ (The mapping $\mathscr{R}$ is defined by (1.3.39)) and

$$\bar{Q}(t) = Q(t) \odot Q_d^{-1}(t) \equiv \begin{bmatrix} \bar{q}_0(t) \\ \bar{q}(t) \end{bmatrix} \in \mathbb{S}^3,$$

whose dynamics are governed by

$$\begin{bmatrix} \dot{\bar{q}}_0(t) \\ \dot{\bar{q}}(t) \end{bmatrix} = \begin{bmatrix} -\frac{1}{2}\bar{q}^T(t)R_d(t)(\omega(t) - \omega_d(t)) \\ \frac{1}{2}(\bar{q}_0(t)I_d + S(\bar{q}(t)))R_d(t)(\omega(t) - \omega_d(t)) \end{bmatrix}, \tag{3.2.1}$$

where $\omega(t)$ is the angular velocity of the rigid body expressed in $\{\mathscr{B}\}$, $\omega_d(t)$ is the desired angular velocity and $R_d(t)$ is a time-varying desired rotation matrix with its equivalent unit-quaternion $Q_d(t)$ such that $\mathscr{R}(Q_d(t)) = R_d(t)$.

Now, the following new filter for attitude control problem with new control law is proposed as

$$\begin{aligned} \dot{\hat{b}}_i(t) &= \alpha_i(b_i(t) - \hat{b}_i(t)) + S(\omega_d)(b_i(t) - \hat{b}_i(t)) \\ &\quad -S(\omega)b_i + \delta_i S(b_i^d(t))(\omega(t) - \omega_d(t)), \qquad (3.2.2) \\ \tau(t) &= S(\omega(t))J\omega(t) - JS(\omega_d(t))\omega(t) + J\dot{\omega}_d(t) \\ &\quad +J\sum_{i=1}^{m}\rho_i S(b_i^d(t))\hat{b}_i(t) - kJ(\omega(t) - \omega_d(t)), \qquad (3.2.3) \end{aligned}$$

where $\alpha_i > 0$, $\delta_i > 0$, $\rho_i > 0$ $(i = 1, ..., m)$ and b_i, $i = 1, \ldots, m$ are the inertial measurements.

Define the following tracking errors

$$\begin{aligned} \bar{\omega}(t) &= R_d(t)(\omega(t) - \omega_d(t)), \qquad (3.2.4) \\ \bar{b}_i(t) &= R_d(t)(b_i(t) - \hat{b}_i(t)) \qquad (3.2.5) \end{aligned}$$

Then, using the fact that $b_i^d(t) = R_d^T(t)r_i$ and properties (1.3.13), (1.3.18), one can obtain the error dynamics as

$$\dot{\bar{\omega}}(t) = R_d(t)S(\omega_d(t))\omega(t) + R_d(t)(\dot{\omega}(t) - \dot{\omega}_d(t)), \tag{3.2.6}$$
$$\dot{\bar{b}}_i(t) = -\alpha_i \bar{b}_i(t) - \delta_i S(r_i)\bar{\omega}(t), \tag{3.2.7}$$

then the torque $\tau(t)$ can be rewritten as

$$\begin{aligned}\tau(t) &= S(\omega(t))J\omega(t) - JS(\omega_d(t))\omega(t) + J\dot{\omega}_d(t) - kJR_d^T\bar{\omega}(t) \\ &\quad + J\sum_{i=1}^{m}\rho_i S(b_i^d(t))b_i(t) - JR_d^T\sum_{i=1}^{m}\rho_i S(r_i)\bar{b}_i(t), \\ &= S(\omega(t))J\omega(t) - JS(\omega_d(t))\omega(t) + J\dot{\omega}_d(t) - kJR_d^T\bar{\omega}(t) \\ &\quad -2JR_d^T\left(\bar{q}_0(t)I_d - S(\bar{q}(t))\right)W_\rho\bar{q}(t) - JR_d^T\sum_{i=1}^{m}\rho_i S(r_i)\bar{b}_i(t),\end{aligned} \tag{3.2.8}$$

where Lemma 1 of [95] are used to rewrite the term

$$\sum_{i=1}^{m}\rho_i S(b_i^d(t))b_i(t) = -2R_d^T\left(\bar{q}_0(t)I_d - S(\bar{q}(t))\right)W\bar{q}(t), \tag{3.2.9}$$

with

$$W_\rho = -\sum_{i=1}^{m}\rho_i S(r_i)^2, \tag{3.2.10}$$

is a positive define matrix (see Lemma 2 [95]).

Finally, using (1.4.16), (3.2.1), (3.2.4), (3.2.5), (3.2.6), (3.2.7), (3.2.8) and (3.2.9), one can get the following closed loop dynamics

$$\begin{cases}\dot{\bar{b}}_i(t) = -\alpha_i\bar{b}_i(t) - \delta_i S(r_i)\bar{\omega}(t) \\ \dot{\bar{q}}_0(t) = -\frac{1}{2}\bar{q}^T(t)\bar{\omega}(t) \\ \dot{\bar{q}}(t) = \frac{1}{2}\left(\bar{q}_0(t)I_d + S\left(\bar{q}(t)\right)\right)\bar{\omega}(t) \\ \dot{\bar{\omega}}(t) = -2\left(\bar{q}_0(t)I_d - S(\bar{q}(t))\right)W_\rho\bar{q}(t) - \sum_{i=1}^{m}\rho_i S(r_i)\bar{b}_i(t) - k\bar{\omega}(t)\end{cases} \tag{3.2.11}$$

3.2.2 Stability analysis

Before stating our results, it is necessary to extend the results presented in [95], where the authors take in consideration the case of continuum of equilibria due to the properties of the matrix W_ρ. In this work, it is shown that the set of control gains $\rho_i, i = 1,\ldots,m$ leading to a continuum of equilibria of the closed loop system (3.2.11) is an algebraic variety of

positive co-dimension, independently on the choice of the observed vectors $r_i, i = 1,\ldots,m$. The following important Lemma is stated and will be used.

Lemma 3.1. *With the notations above, one gets that the matrix W_ρ defined in (3.2.10) has simple eigenvalues generically with respect to $\rho = (\rho_1,\cdots,\rho_n) \in (\mathbb{R}_+^*)^n$, which mean that the set of gains ρ leading to simple eigenvalues of W_ρ is dense and open in $(\mathbb{R}_+^*)^n$.*

Proof. For $\rho \in (\mathbb{R}_+^*)^n$, let $P_\rho(t)$ be the characteristic polynomial of W_ρ and $\Lambda(\rho)$ its discriminant [89]. From (3.2.10), one can express $P_\rho(t)$ as

$$\begin{aligned}
P_\rho(t) &= det\left(tI_d - \sum_{i=1}^{m}\begin{bmatrix}\rho_i w_{11} & \rho_i w_{12} & \rho_i w_{13}\\ \rho_i w_{12} & \rho_i w_{22} & \rho_i w_{21}\\ \rho_i w_{13} & \rho_i w_{21} & \rho_i w_{33}\end{bmatrix}\right)\\
&= det\left(\begin{bmatrix}(t-\sum_{i=1}^m \rho_i w_{11}) & \sum_{i=1}^m \rho_i w_{12} & \sum_{i=1}^m \rho_i w_{13}\\ \sum_{i=1}^m \rho_i w_{12} & (t-\sum_{i=1}^m \rho_i w_{22}) & \sum_{i=1}^m \rho_i w_{21}\\ \sum_{i=1}^m \rho_i w_{13} & \sum_{i=1}^m \rho_i w_{21} & (t-\sum_{i=1}^m \rho_i w_{33})\end{bmatrix}\right)\\
&= \left(t-\sum_{i=1}^{m}\rho_i w_{11}\right)\left(t-\sum_{i=1}^{m}\rho_i w_{22}\right)\left(t-\sum_{i=1}^{m}\rho_i w_{33}\right)\\
&\quad +2\left(\sum_{i=1}^{m}\rho_i w_{13}\right)\left(\sum_{i=1}^{m}\rho_i w_{12}\right)\left(\sum_{i=1}^{m}\rho_i w_{21}\right) - \left(\sum_{i=1}^{m}\rho_i w_{13}\right)^2\left(t-\sum_{i=1}^{m}\rho_i w_{22}\right)\\
&\quad -\left(\sum_{i=1}^{m}\rho_i w_{21}\right)^2\left(t-\sum_{i=1}^{m}\rho_i w_{11}\right) - \left(t-\sum_{i=1}^{m}\rho_i w_{33}\right)\left(\sum_{i=1}^{m}\rho_i w_{12}\right)^2\\
&= a_0 t^3 + a_1 t^2 + a_2 t + a_3,
\end{aligned}$$

where

$$a_0 = 1 \tag{3.2.12}$$
$$a_1 = f_1(\rho_i,\ldots) \tag{3.2.13}$$
$$a_2 = f_2(\rho_i^2,\ldots) \tag{3.2.14}$$
$$a_3 = f_3(\rho_i^3,\ldots) \tag{3.2.15}$$

with f_j, $j = 1,2,3$ are real functions. Since W_ρ is a 3 by 3 real symmetric positive definite matrix for every $\rho \in (\mathbb{R}_+^*)^n$ and using the discriminant formula (see page 102 of [105]) one can get that $\Lambda(\rho)$ is actually a homogeneous polynomial of degree four in coefficients of $P_\rho(t)$ such that

$$\Lambda(\rho) = a_1^2a_2^2 - 4a_0a_2^3 - 4a_1^3a_3 - 27a_0^2a_3^2 + 18a_0a_1a_2a_3, \tag{3.2.16}$$

therefore, one can use (3.2.12), (3.2.13), (3.2.14), (3.2.15) and (3.2.16) to deduce that $\Lambda(\rho)$ is homogeneous polynomial of degree six in ρ.

Recall that $\Lambda(\rho)=0$ if and only if $P_\rho(t)$ admits a multiple root. Since W_ρ is a 3 by 3 real symmetric positive definite matrix for every $\rho\in(\mathbb{R}_+^*)^n$. Thus the locus $\Lambda(\rho)=0$ defines an algebraic variety of co-dimension one in $(\mathbb{R}_+^*)^n$ and, on its complementary set $\mathscr{S}$ in $(\mathbb{R}_+^*)^n$, W_ρ has simple eigenvalues. □

This genericity result serves a justification to the following working hypothesis, which will hold for the rest of this work.

(**GEN**) *W_ρ has simple eigenvalues.*

Before stating the main result, let's defined the vector field $\Delta := \mathbb{R}^{3m}\times\mathbb{S}^3\times\mathbb{R}^3$ and given a state vector $\Theta\in\Delta$ such that $\Theta := (\bar{b}_1,...,\bar{b}_m,\bar{Q},\bar{\omega})$. Therefore, the closed loop dynamics (3.2.11) can be rewritten as

$$\dot{\Theta}=G(\Theta),$$

which means that the error dynamics are autonomous.

Define the following positive radially unbounded function : $V_1:\Delta\to\mathbb{R}$

$$V_1(\Theta)=\sum_{i=1}^{m}\frac{\rho_i}{\delta_i}\bar{b}_i^T(t)\bar{b}_i(t)+4\bar{q}(t)^TW_\rho\bar{q}(t)+\bar{\omega}(t)^T\bar{\omega}(t) \tag{3.2.17}$$

Now, the main result can be stated.

Theorem 3.1. *Consider System (1.4.9), (1.4.16) and the control law (3.2.3) with the filter given by (3.2.2). Under Assumptions 1 and 2 in Section 1.6 and if hypothesis of Lemma 3.1 holds, then*

(1) *The equilibria of the closed-loop system (3.2.11) are defined by*

$$\Theta_1^{\pm}=(\underbrace{\mathbf{0},...,\mathbf{0}}_{m},\begin{bmatrix}\pm1\\ \mathbf{0}\end{bmatrix},\mathbf{0}),\ \Theta_{2,3,4}^{\pm}=(\underbrace{\mathbf{0},...,\mathbf{0}}_{m},\begin{bmatrix}0\\ \pm v_j\end{bmatrix},\mathbf{0}),$$

where v_j , $j=1,2,3$ are the eigenvectors of W_ρ.

(2) *The equilibria $\Theta_1^{\pm}$ are asymptotically stable with a domain of attraction containing the set*

$$C_a^+ := \{\Theta\in\triangle \mid V_1(\Theta)<4\lambda_{min}(W) \text{ and } \bar{q}_0>0\},$$

for Θ_1^+ and

$$C_a^- := \{\Theta\in\triangle \mid V_1(\Theta)<4\lambda_{min}(W) \text{ and } \bar{q}_0<0\},$$

for Θ_1^-, where $\lambda_{min}(W_\rho)$ is the smallest eigenvalue of W_ρ.

(3) *The equilibria $\Theta_{2,3,4}^{\pm}$ are locally unstable and $\Theta_1^{\pm}$ are almost globally asymptotically stable.*

Proof. (1) To proof the first item one can solve $G(\Theta) = 0$, where G is the non linear function describing (3.2.11). For this, two cases can be considered.

The first one is when $\bar{q}_0 \neq 0$ and since $\bar{q}_0 I_d + S(\bar{q})$ and $\bar{q}_0 I_d - S(\bar{q})$ are non singular, therefore one can conclude, using the third equation of (3.2.11) that $\bar{\omega} = \mathbf{0}$ and thus, from the first equation of (3.2.11) $\bar{b}_i = \mathbf{0}$, $i = 1, \ldots, m$. Now, from the forth equation of (3.2.11) and since W_ρ is a positive definite matrix, then one can get $\bar{q} = \mathbf{0}$, which means that $\bar{q}_0 = \pm 1$. Finally, in this case, there are two equilibria

$$\Theta_1^+ = (\underbrace{\mathbf{0}, \ldots, \mathbf{0}}_{m}, \begin{bmatrix} 1 \\ \mathbf{0} \end{bmatrix}, \mathbf{0}),$$

and

$$\Theta_1^- = (\underbrace{\mathbf{0}, \ldots, \mathbf{0}}_{m}, \begin{bmatrix} -1 \\ \mathbf{0} \end{bmatrix}, \mathbf{0})$$

In the second case, assume that $\bar{q}_0 = 0$, then from the third equation of (3.2.11) $\bar{q}$ is collinear with $\bar{\omega}$. Using this fact together with the second equation of (3.2.11), one can conclude that $\bar{\omega} = \mathbf{0}$ and thus, from the first equation of (3.2.11) $\bar{b}_i = \mathbf{0}$, $i = 1, \ldots, m$. Now, using the forth equation of (3.2.11), one can get that $S(\bar{q}) W_\rho \bar{q} = \mathbf{0}$, which mean that $\bar{q}$ are collinear with $W_\rho \bar{q}$. Equivalently, $W_\rho \bar{q} = \lambda \bar{q}$ and therefore $\bar{q}$ is one of the eigenvectors of W_ρ. Finally, in this case, there are six equilibria

$$\Theta_{2,3,4}^{\pm} = (\underbrace{\mathbf{0}, \ldots, \mathbf{0}}_{m}, \begin{bmatrix} 0 \\ \pm v_j \end{bmatrix}, \mathbf{0}), \ , j = 1, 2, 3,$$

where v_j , $j = 1, 2, 3$ are the eigenvectors of W_ρ.

(2) It is clear that (3.2.11) are autonomous, therefore it is possible to use LaSalle's invariance theorem to proof the second item.

The time derivative of (3.2.17) in view of (3.2.11) can be evaluated as follows :

$$\begin{aligned} \dot{V}_1(\Theta) \quad = \quad & -2\sum_{i=1}^{m} \alpha_i \frac{\rho_i}{\delta_i} \bar{b}_i(t)^T \bar{b}_i(t) - 2\sum_{i=1}^{m} \rho_i \bar{b}_i^T(t) S(r_i(t)) \bar{\omega}(t) \\ & + 4\bar{q}(t)^T W_\rho \left(\bar{q}_0(t) I_d + S\left(\bar{q}(t)\right)\right) \bar{\omega}(t) - 4\bar{\omega}(t)^T \left(\bar{q}_0(t) I_d - S(\bar{q}(t))\right) W_\rho \bar{q}(t) \\ & - 2\bar{\omega}(t)^T \sum_{i=1}^{m} \rho_i S(r_i) \bar{b}_i(t) - 2k\bar{\omega}(t)^T \bar{\omega}(t), \end{aligned}$$

using the fact that

$$\bar{\omega}(t)^T \sum_{i=1}^{m} \rho_i S(r_i)\bar{b}_i(t) = -\sum_{i=1}^{m} \rho_i \bar{b}_i^T(t) S(r_i(t))\bar{\omega}(t),$$

and

$$\bar{\omega}(t)^T \left(\bar{q}_0(t) I_d - S(\bar{q}(t))\right) W_\rho \bar{q}(t) = \bar{q}(t)^T W_\rho \left(\bar{q}_0(t) I_d + S\left(\bar{q}(t)\right)\right) \bar{\omega}(t),$$

where property 1.3.19 was used, the time derivative $\dot{V}_1(\Theta)$ becomes

$$\dot{V}_1(\Theta) = -2k\bar{\omega}(t)^T \bar{\omega}(t) - 2\sum_{i=1}^{m} \alpha_i \frac{\rho_i}{\delta_i} \bar{b}_i(t)^T \bar{b}_i(t) \leq 0 \tag{3.2.18}$$

Therefore, all trajectories of (3.2.11) are bounded.

Since V_1 is positive radially unbounded function and (3.2.11) is autonomous, then using LaSalle's invariance theorem every trajectory converges to a trajectory along which $\dot{V}_1 \equiv 0$. Therefore, using (3.2.18) one can obtain that $\bar{\omega} = \mathbf{0}$ and $\bar{b}_i = \mathbf{0}$, $i = 1, \ldots, m$. Then, using the forth equation of (3.2.11), we get $\left(\bar{q}_0(t) I_d - S(\bar{q}(t))\right) W_\rho \bar{q}(t) = 0$ and similarly to first item, one can get that the largest invariant set characterized by $\dot{V}_1 \equiv 0$ are composed of $\Theta_1^{\pm}$ and $\Theta_{2,3,4}^{\pm}$.

Now, one can use quadratic property to obtain $V_1(\Theta) \geq 4\lambda_{min}(W_\rho) \|\bar{q}(t)\|^2$, which means that

$$\min_{\|\bar{q}(t)\|=1} \{V_1(\Theta)\} = 4min\left\{\lambda_{min}(W_\rho)\right\},$$

and since V_1 is decreasing, therefore for every $t \geq 0$ $\|\bar{q}(t)\| < 1$ and thus $\bar{q}_0(t)$ never cross the zero and keeps the same sign. Finally, since for every $t \geq 0$ $\bar{q}_0(t) \neq 0$ then $\Theta_{2,3,4}^{\pm}$ don't belong to the largest invariant set characterized by $\dot{V}_1 \equiv 0$. Moreover, if a trajectory starts inside C_a^+ or C_a^- then it remains there, which leads to the results of the second item.

(3) Now, let us proof that the equilibria $\Theta_{2,3,4}^{\pm}$ are unstable.

Since the only difference between these equilibria is the value of the eigenvector, the proof is given for $\Theta_2^+ \in \Delta$. The other cases will be similar. To do this, we consider $\Theta_2^* := (\bar{b}_1^*, ..., \bar{b}_m^*, \bar{Q}^*, \bar{\omega}^*)$ a neighborhood of Θ_2^+ (arbitrary close) and since the function V_1 is non-increasing, it suffices to prove that $V_1(\Theta_2^*) - V_1(\Theta_2^+) < 0$. Let us use the following change of variable

$$\bar{Q}^* = \begin{bmatrix} \bar{q}_0^* \\ \bar{q}^* \end{bmatrix} = \begin{bmatrix} 0 \\ v_1 \end{bmatrix} \odot \begin{bmatrix} x_0 \\ x \end{bmatrix} = \begin{bmatrix} -v_1^T x \\ x_0 v_1 + S(v_1)x \end{bmatrix} \tag{3.2.19}$$

Using (3.2.19) and the fact that $W_\rho v_1 = \lambda_1 v_1$ (where λ_1 is the eigenvalue associated to the

unit eigenvector v_1 of W_ρ), one can evaluate $D = V_1(\Theta_2^*) - V_1(\Theta_2^+)$ as follow

$$D = \sum_{i=1}^{m} \frac{\rho_i}{\delta_i} \bar{b}_i^{*T} \bar{b}_i^* + \bar{\omega}^{*T} \bar{\omega}^* + 4\lambda(x_0^2 - 1) - 4x^T S(v_1) W_\rho S(v_1) x, \tag{3.2.20}$$

If we take x close to v_1 such that $x = \varepsilon v_1$, where $\varepsilon > 0$ sufficiently small, the unit quaternion constraint gives $x_0^2 = 1 - \varepsilon^2$. In this case, one can get

$$D = \sum_{i=1}^{m} \frac{\rho_i}{\delta_i} \bar{b}_i^{*T} \bar{b}_i^* + \bar{\omega}^{*T} \bar{\omega}^* - 4\lambda_1 \varepsilon^2,$$

which means that if

$$\varepsilon^2 > \frac{1}{4\lambda_1} \left(\sum_{i=1}^{m} \frac{\rho_i}{\delta_i} \bar{b}_i^{*T} \bar{b}_i^* + \bar{\omega}^{*T} \bar{\omega}^* \right),$$

then $D < 0$.

As a result, there exist Θ_2^* arbitrary close to Θ_2^+ such that $V_1(\Theta_2^*) < V_1(\Theta_2^+)$ and since the function V_1 is non increasing, it is clear that Θ_2^+ is unstable. Similarly, all equilibria $\Theta_{3,4}^{\pm}$ are unstable.

Finally, in the state space Δ the set of unstable equilibria is Lebesgue measure zero. Therefore, almost all trajectories converge asymptotically to $\Theta_1^{\pm}$. □

3.3 The attitude stabilization case

In the case of attitude stabilization the desired angular velocity is equal to zero, then using (3.2.2) and (3.2.3), one can obtain

$$\dot{\hat{b}}_i(t) = \alpha_i(b_i(t) - \hat{b}_i(t)) - S(\omega) b_i + \delta_i S(b_i^d(t))\omega(t), \tag{3.3.1}$$

$$\tau(t) = S(\omega(t))J\omega(t) + J\sum_{i=1}^{m} \rho_i S(b_i^d(t))\hat{b}_i(t) - kJ\omega(t), \tag{3.3.2}$$

Rather than using (3.3.1) and (3.3.2) for stabilization case, we propose a more simple control law as follows

$$\dot{\hat{b}}_{si}(t) = \alpha_i(b_i(t) - \hat{b}_{si}(t)) - S(\omega(t)) b_i(t) + \delta_i S(b_i^d)\omega(t), \tag{3.3.3}$$

$$\tau_s(t) = \sum_{i=1}^{m} \rho_i S(b_i^d(t))\hat{b}_{si}(t) - k\omega(t), \tag{3.3.4}$$

In this case, it is also possible to get an almost global stability of the closed loop dynamics. Indeed, using the same steps as in the case of tracking, one can write the closed loop dynamics as

$$\left\{\begin{array}{lcl} \dot{\widetilde{b}}_i(t) & = & -\alpha_i\widetilde{b}_i(t) - \delta_i S(b_i^d)\omega(t) - S(\omega(t))\widetilde{b}_i(t), \\ \dot{\tilde{q}}_0(t) & = & -\frac{1}{2}\bar{q}^T(t)R_d\omega(t), \\ \dot{\bar{q}}(t) & = & \frac{1}{2}\left(\bar{q}_0(t)I_d + S\left(\bar{q}(t)\right)\right)R_d\omega(t), \\ J\dot{\omega}(t) & = & -S(\omega(t))J\omega(t) - 2R_d^T(\bar{q}_0(t)I_d - S(\bar{q}(t)))W_\rho\bar{q}(t) \\ & & -\sum_{i=1}^m \rho_i S(b_i^d)\widetilde{b}_i(t) - k\omega(t), \end{array}\right. , \tag{3.3.5}$$

where $\widetilde{b}_i(t) = b_i(t) - \hat{b}_{si}(t)$. Then, using

$$V_2 = \frac{1}{2}\sum_{i=1}^m \frac{\rho_i}{\delta_i}\widetilde{b}_i^T\widetilde{b}_i + 4\bar{q}^T W_\rho\bar{q} + \omega^T J\omega,$$

as a positive radially unbounded function, one can get the same stability results as in tracking case.

3.4 Simulations

In this section, full sets of simulations are presented to show the effectiveness of the proposed solution in two cases, stabilization and tracking. The desired trajectories are generated using the desired angular acceleration

$$\dot{\omega}_d = \begin{bmatrix} 0.4sin(0.4t) \\ 0.5sin(0.5t+0.1) \\ 0.3sin(t-0.2) \end{bmatrix} (rad/s^2)$$

Additive zero-mean white noises were taken for measurements with standard deviation of $0.9\,(m/s2)$, $0.1\,(Gauss)$ and $0.02\,(^\circ/s)$ for accelerometer, magnetometer and rate gyros respectively. The used fixed inertial vectors are

$$r_1 = \begin{bmatrix} 0 \\ 0 \\ 9.81 \end{bmatrix} (m/s^2),\ r_2 = \begin{bmatrix} 0.2086 \\ 0.0004 \\ 0.4320 \end{bmatrix} (Gauss)$$

The other used parameters are:

- The *ode*5 integration method with $0.01s$ as sample time;

- The chosen gains for the two cases are : $\alpha_1 = \alpha_2 = 1$, $\delta_1 = \delta_2 = 1$, $\rho_1 = \rho_2 = 8$ and $k = 5$;
- The initial value of vector measurements b_1, b_2 were taken as initial values for filtered ones $\hat{b}_1, \hat{b}_2$, where $b_1\,(m/s^2)$ represents the accelerometer measurements and $b_2\,(Gauss)$ represents the magnetometer measurements;
- The initial attitude in Euler angles were taken $(\varphi(0), \theta(0), \psi(0)) = (-30, 15, 5)$ and $(\varphi_d(0), \theta_d(0), \psi_d(0)) = (0, 0, 0)$ for rigid body and desired attitude, respectively.

Despite the fact that the chosen noise represents nearly 10% of the amplitude of the measured vectors, the proposed attitude controller stabilize and track the desired attitude successfully, as shown in Figures 3.4.1, 3.4.2, 3.4.3 and 3.4.4. Figures 3.4.1-(a), -(b), -(c) and 3.4.1-(d), -(e), -(f) illustrate the appearance of the raw measurements compared to the filtered ones in the case of stabilization. In Figures 3.4.2-(a), -(b), -(c) desired and attitude error in quaternion are presented, respectively.

To show the impact of using the filtered measurements $\hat{b}_i$, one can generate a raw control torque by replacing $\hat{b}_i$ in (3.2.3) with the raw measurements b_i. In Figures 3.4.2-(d), -(e), -(f) the torque τ with raw torque τ_n are illustrated. Quaternion stabilization errors are illustrated in Figure 3.4.2-(c), where the trajectory converge to the stable equilibrium. In the case of attitude tracking, all simulation results are illustrated in Figures 3.4.3 and 3.4.4, where the effectiveness and performances of the proposed control solution are highlighted.

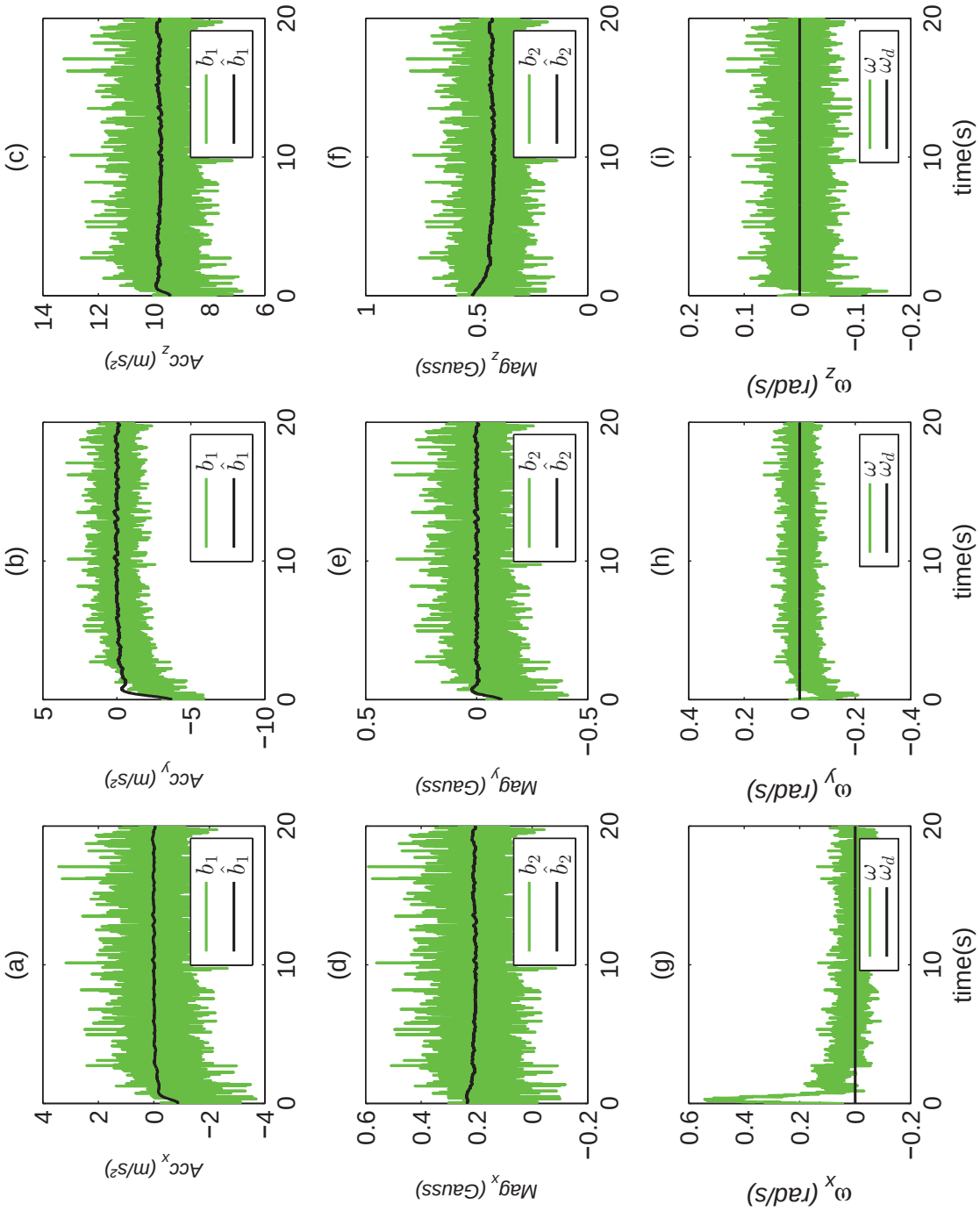

Figure 3.4.1: Inertial vectors and angular velocity results in the case of stabilization

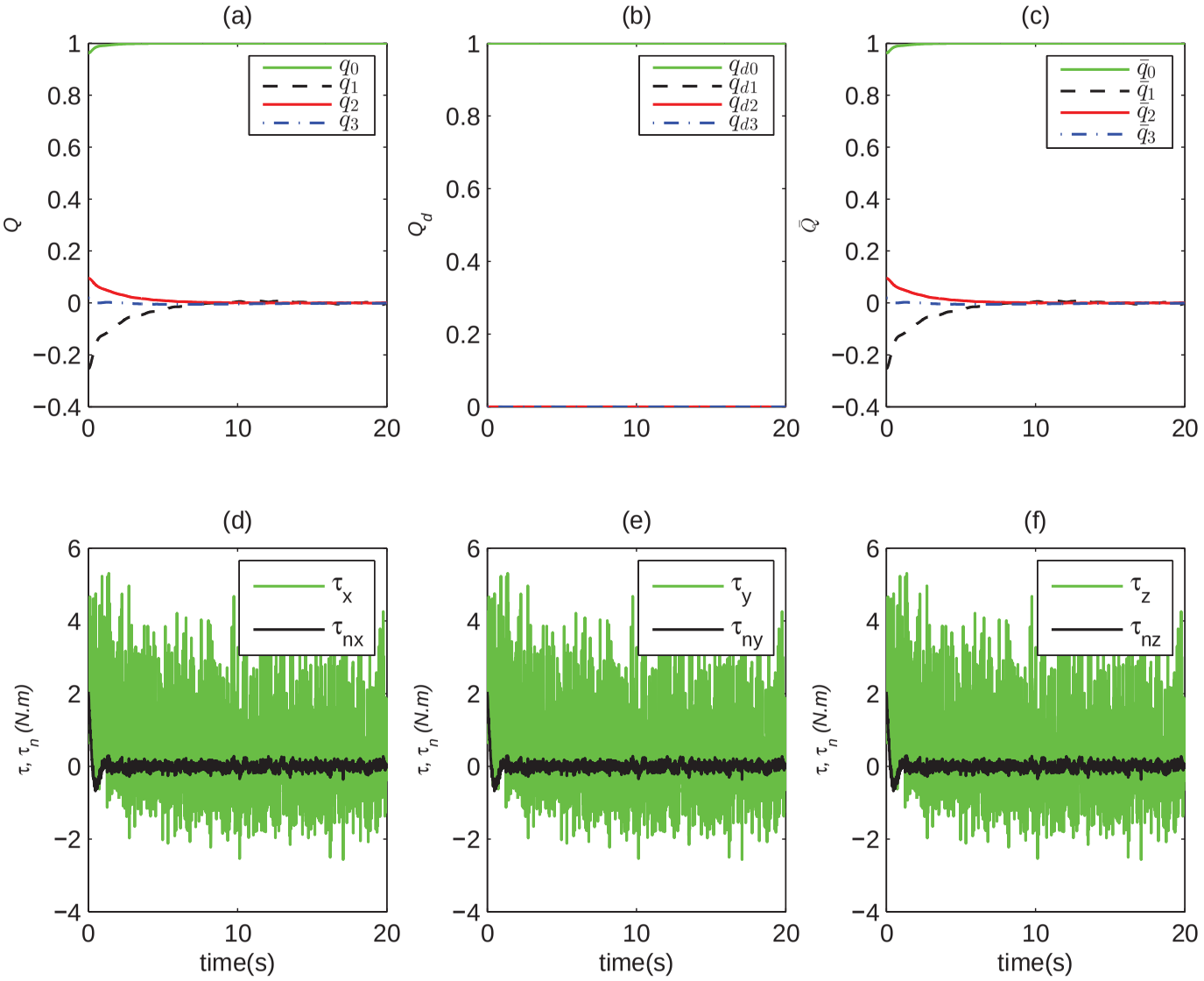

Figure 3.4.2: Attitude and torque in the case of stabilization

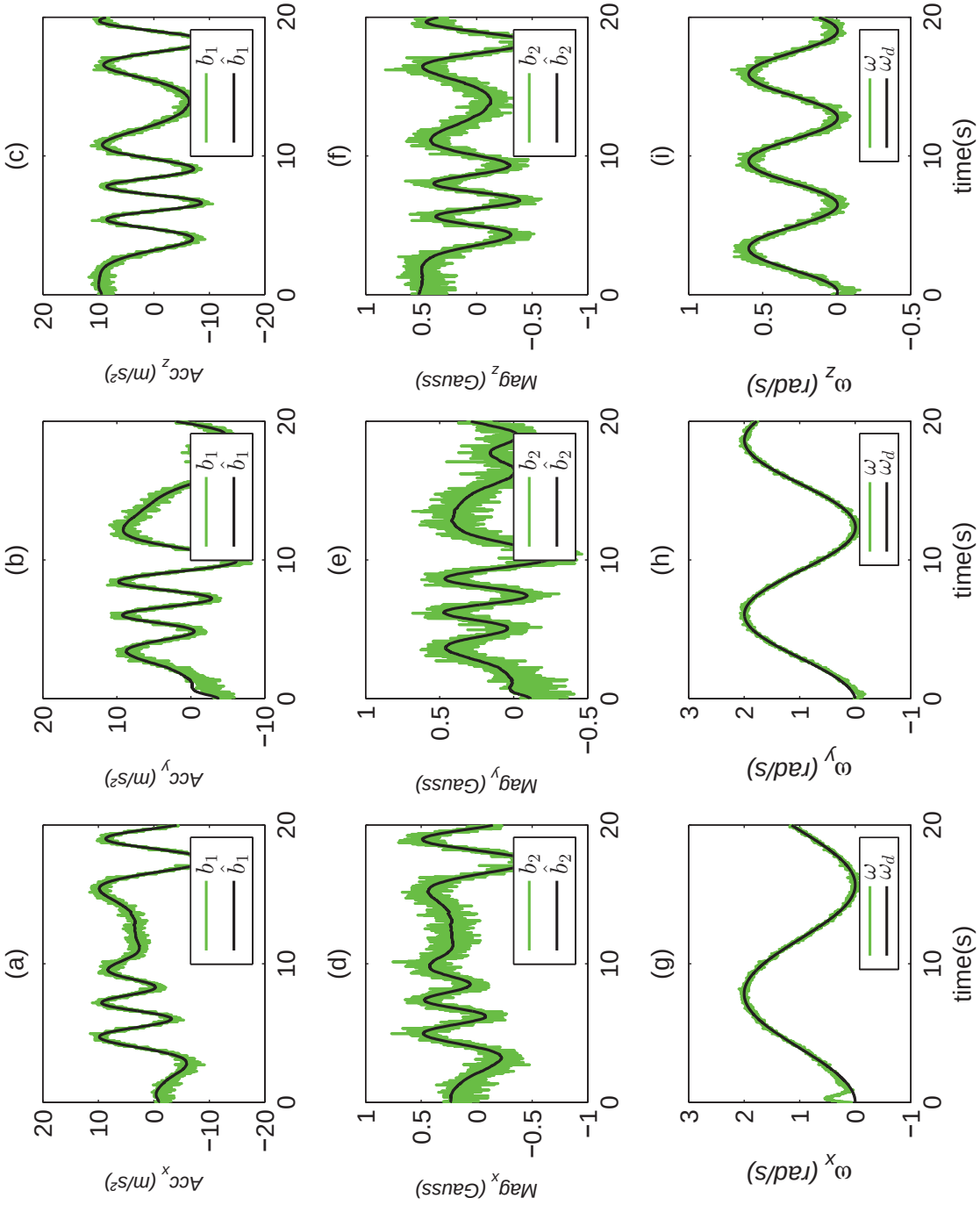

Figure 3.4.3: Inertial vectors and angular velocity results in the case of tracking

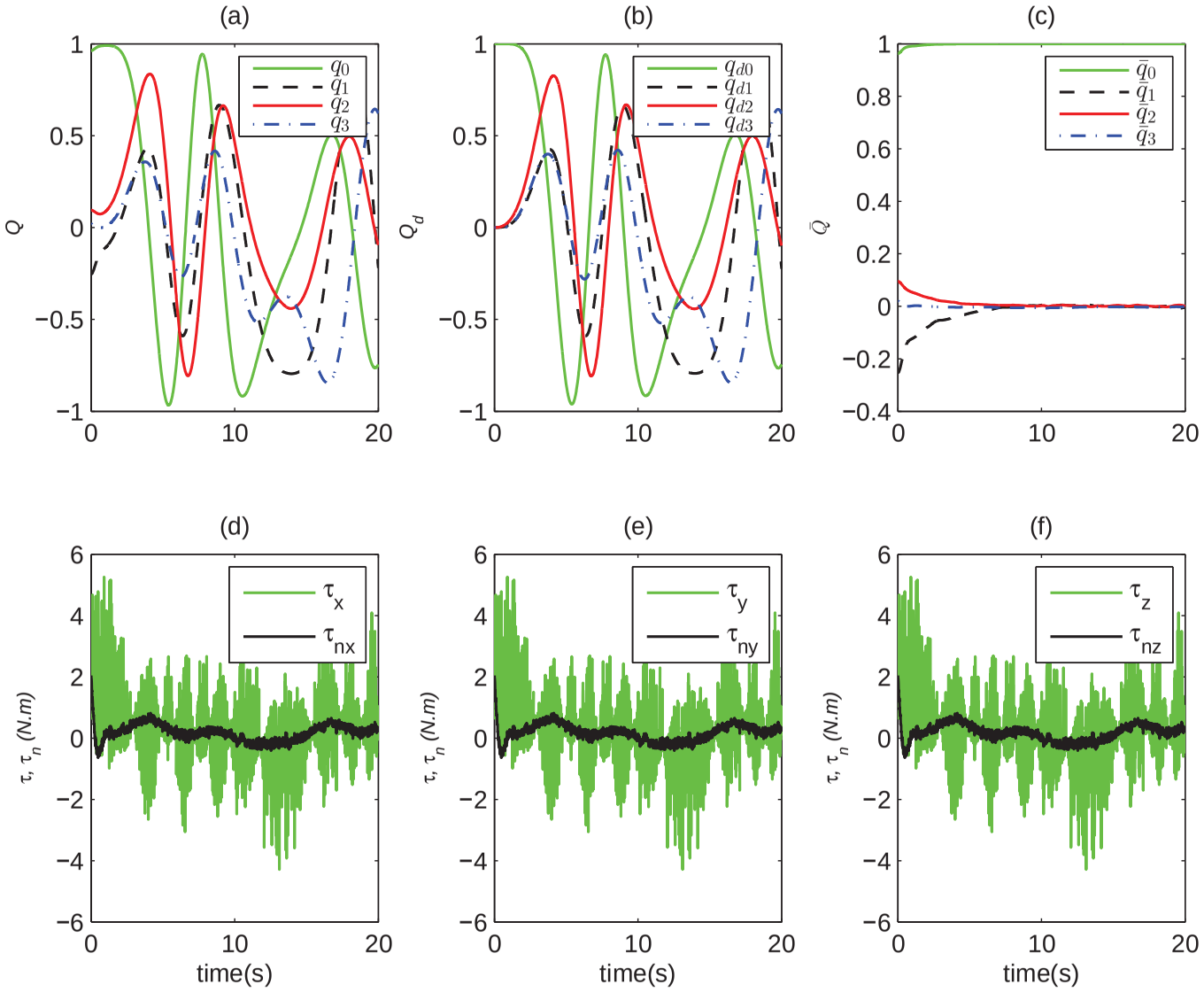

Figure 3.4.4: Attitude and torque in the case of tracking

3.5 Conclusion

As a logical sequel to the proposed attitude estimation solutions, another novelty of this work led in the proposition of new control law for attitude tracking problem. This solution used filtered inertial measurements and rate-gyro measurements to control the attitude of a rigid body without using “attitude measurements”. That were possible by the introduction of a linear-like complementary filter coupled with the control law to ensure an almost global asymptotic stability of the closed loop dynamics. The stability analysis was based on Lyapunov theory and LaSalle’s invariance theorem. Moreover, some previous results were extended to ensure that the case of the closed loop system continuum of equilibria can be always avoided. Also, it was shown that the proposed control law avoid the undesired unwinding phenomena.

Even if the proposed attitude tracking control law ensures the stabilization case, a more simple attitude stabilization control law was presented, in which almost global stability property was also ensured. It was shown that the proposed control laws were very robust to strong additive noise on measurements by a set of simulation results.

It is clear that the availability of at least two non-collinear inertial vector measurements and the angular velocity measurements is required for the proper functioning of the proposed control laws. If angular velocity is lost due to sensor or system failure, the proposed control law in this Chapter exhibits a poor performance. In order to remedy this problem, it is necessary to consider this special case in the design of the control law, which constitute the next contribution.

Chapter 4

Attitude Stabilization Without Angular Velocity Measurements

4.1 Introduction

Attitude stabilization of rotational motion of rigid body is a classical problem. Despite the considerable existing solutions, it remains until today an active research topic. This is due to the large field of applications such as robotics, unmanned aerial vehicles (UAVs), satellites, marine vehicles, etc. Since attitude control and stabilization is as an interesting theoretical and technical problem, many scenarios were studied in the literature (see for instance [72, 75], [93],[53, 69] and [17]). An interesting and challenging scenario is the attitude stabilization without angular velocity. The main goal is to stabilize the attitude without the use of gyroscopes, which can be very expensive or vital to the system, like gyroscopes on Hubble (see, Figure 4.1.1) used for pointing the telescope. They measure attitude when Hubble is changing its pointing from one target (a star or planet) to another, and they help control the telescope's pointing while scientists are observing targets. There are a total of six gyroscopes on board– three serve as backups. In 2009, all six of Hubble's gyroscopes had to be replaced and one can imagine the cost generated. At the light of these problems, it is conceivable to reduce costs and ensure continuity of the mission of the rigid body despite the failure of the gyroscopes when this type of controllers is used. Many works in the literature dealt with attitude control without angular velocity problem (see, for instance [5, 10, 32, 81, 95, 96, 99, 101, 111, 112]), some of them exploited the passivity of the system such as [22, 29, 58, 97, 103].

In almost all results dealing with the case of attitude control without angular velocity, the "instantaneous measurements of the attitude" are used in the control law (see, for instance [5, 94, 96, 103, 104]). As there is no sensor which physically measures the attitude of a rigid

body, the aforementioned velocity-free controllers require some kind of attitude observer relying on the available direction sensors. However, almost all static algorithms based only on body vector measurements are very sensitive to noise (see, for instance [6, 92, 114]). Also, all the most efficient algorithms make use of the inertial vector measurements and the angular velocity information to estimate the attitude of the rigid body (see, for instance [24, 25, 114]). To overcome this problem, a "velocity-free" attitude control scheme, that incorporates explicitly vector measurements instead of the attitude itself, has been proposed for the first time in [95].

Since it is impossible to achieve a global asymptotic stabilization using continuous time invariant state feedback [14], the attitude control scheme presented in this chapter use the notion of "*Almost Global Asymptotic Stability*" of the closed loop system. Therefore, this work and that proposed in [95] present a stronger stability property compared to [99], where the convergence depends on a non trivial condition on initial conditions. The notion of "*almost global stability*" is used in the sense that a dense and open set belonging to the Special Orthogonal Group $SO(3)$ exist, where all trajectories are stable. The proposed solution given here can be regarded as an extension of [95]. The main differences are the following: (a) the use of an auxiliary system in terms of body vector measurements, defined on $\mathbb{R}^3$, rather than that of an auxiliary system defined on $\mathbb{S}^3$; (b) the explicit design of an angular velocity observer-like which is used in the design of the stabilizing feedback; (c) the proposed controller doesn't use the inertial fixed reference vectors. As a consequence, the set of unstable equilibria of the closed loop dynamics with the auxiliary error system is reduced as compared to that of [95]. The quaternion parametrization is used in the main analysis and the final results are rewritten with rotations expressed in $SO(3)$ by simple projection, which guaranteed that the proposed solution avoid the unwinding phenomenon. It is also shown that the introduction of gain matrices improves drastically the controller performance with respect to both [95] and [99]. Finally, in order to adjust properly the controller gains, a non-linear optimal tuning method is used.

This chapter is organized as follow. Section 4.2 presents an intuitive method to handle the lack of angular velocity based on an observer-like design that will be used in the new proposed control law. A rigorous stability analysis is presented in Section 4.3, where the almost global stabilization of the closed loop system is shown. The effectiveness and robustness of the proposed controller is illustrated via simulation results and comparison with the case where the angular velocity is used in the feedback is presented in Section 4.4, where a detailed optimal nonlinear constrained method for tuning gains is also presented. The obtained results in this Chapter were presented in [11].

(a) Angular speed sensor (www.nasa.gov)

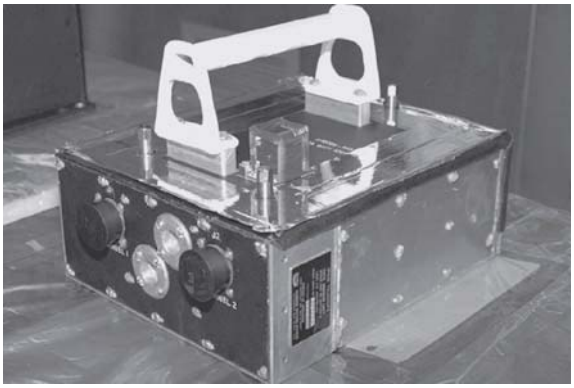

(b) Sensor unit (www.nasa.gov)

Figure 4.1.1: Hubble Gyro

4.2 Handling the lack of angular velocity and Design of the attitude controller

Let $m \geq 2$ be an integer and let $b_i(Q(t)) \in \mathbb{R}^3$ $(i = 1, \cdots, m)$ be a measured vectors expressed in $\{\mathscr{B}\}$. Using (1.3.2), the relation between $b_i(t)$ and their corresponding fixed inertial vectors $r_i \in \mathbb{R}^3$ are given by

$$b_i(Q(t)) = R^T(t) r_i \tag{4.2.1}$$

As a consequence we have $b_i(-Q) = b_i(Q)$ for $1 \leq i \leq m$ and $Q \in \mathbb{S}^3$.

The reduced attitude kinematics (1.4.8) can be rewritten as

$$\dot{b}_i(Q(t)) = -S(\omega(t)) b_i(Q(t)), \, i = 1, \cdots, m. \tag{4.2.2}$$

4.2.1 Angular velocity observer-like system

First of all, it is possible to express the true angular velocity $\omega(t)$ using only the vector measurements by exploiting the reduced attitude kinematic defined in (4.2.2). Let us define $\Gamma = diag(\Lambda_1, \ldots, \Lambda_m)$, where Λ_i, $i = 1, \ldots, m$ are real symmetric positive definite 3×3 matrices, for $1 \leq i \leq m$ and define the symmetric matrix

$$M(t) = \sum_{i=1}^{m} S(b_i(t))^T \Lambda_i S(b_i(t)) \tag{4.2.3}$$

Fact. *If Assumption 2 in Section 1.6 holds, then $M(t)$ is positive definite matrix. It is straight-*

forward to verify this result by using the definition $\forall x \in \left(\mathbb{R}^3\right)^*$, $x^T M(t)x > 0$.

Multiplying (4.2.2) by $S(b_i(t))\Lambda_i$ for $1 \leq i \leq m$ and doing the sum gives

$$\sum_{i=1}^{m} S(b_i(t))\Lambda_i \dot{b}_i(t) = -M(t)\omega(t). \tag{4.2.4}$$

From (4.2.4) the true angular velocity $\omega(t)$ is given by

$$\omega(t) = -M^{-1}(t)\sum_{i=1}^{m} S(b_i(t))\Lambda_i \dot{b}_{i(t)} \tag{4.2.5}$$

Since $\dot{b}_i(t)$ is not a measured quantity, the following new angular velocity observer-like signal is proposed

$$\hat{\omega}(t) = -M^{-1}(t)\sum_{i=1}^{m} S(b_i(t))\Lambda_i \dot{\hat{b}}_i(t), \tag{4.2.6}$$

where the vector $\dot{\hat{b}}_i(t)$ can be viewed as an estimate of the vector $\dot{b}_i(t)$ using the following linear first-order filter on b_i $(i = 1, \cdots, m)$.

$$\dot{\hat{b}}_i(t) = A_i(b_i(t) - \hat{b}_i(t)), \tag{4.2.7}$$

where the constant matrices $A_i \in \mathbb{R}^{3\times 3}$ will be defined later.

Define an error for the linear first-order filter by $\tilde{b}_i(t) = b_i(t) - \hat{b}_i(t)$. Using (4.2.7), (4.2.2) leads to the following error dynamics

$$\dot{\tilde{b}}_i(t) = -A_i\tilde{b}_i(t) + S(b_i(t))\omega,$$

which can be rewritten using the state vector defined by $\zeta(t) := [\tilde{b}_1^T(t), \cdots, \tilde{b}_m^T(t)]^T$, as

$$\dot{\zeta}(t) = -A\zeta(t) + B(t)\omega(t), \tag{4.2.8}$$

where

$$A = \begin{bmatrix} A_1 & 0_3 & \cdots & 0_3 \\ 0_3 & A_2 & \ddots & \vdots \\ \vdots & \ddots & \ddots & 0_3 \\ 0_3 & \cdots & 0_3 & A_m \end{bmatrix}, \; B(t) = \begin{bmatrix} S(b_1(t)) \\ S(b_2(t)) \\ \vdots \\ S(b_m(t)) \end{bmatrix}$$

.

Finally, the angular velocity observer-like signal can be written as

$$\hat{\omega}(t) = M^{-1}(t)B^T(t)\Gamma A\zeta(t). \tag{4.2.9}$$

4.2.2 Controller Design

First, the orientation error is defined by

$$\bar{R}(t) = R(t)R_d^T, \tag{4.2.10}$$

where $R(t)$ is a rotation matrix and R_d is a constant desired rotation matrix. From (1.4.5) and (4.2.10) one can obtain the attitude error dynamics in terms of rotation matrix as follows

$$\dot{\bar{R}}(t) = \bar{R}(t)S(R_d\omega(t)), \tag{4.2.11}$$

$\bar{R}(t)$ corresponds to the quaternion error $\bar{Q}(t) = Q(t) \odot Q_d^{-1}(t) \equiv [\bar{q}_0(t), \bar{q}(t)^T]^T$ whose dynamics is governed by

$$\begin{bmatrix} \dot{\bar{q}}_0(t) \\ \dot{\bar{q}}(t) \end{bmatrix} = \begin{bmatrix} -\frac{1}{2}\bar{q}^T(t)R_d\omega(t) \\ \frac{1}{2}\left(\bar{q}_0(t)I_d + S\left(\bar{q}(t)\right)\right)R_d\omega(t) \end{bmatrix}, \tag{4.2.12}$$

The reduced orientation error is defined by $\bar{b}_i(\bar{Q}(t)) = b_i(Q(t)) - b_i^d$. Therefore, on can get

$$\bar{b}_i(\bar{Q}(t)) = R_d^T(\bar{R}(t)^T - I)r_i, \tag{4.2.13}$$

where $1 \leq i \leq m$ which can be rewritten using (1.3.39) as

$$\bar{b}_i(\bar{Q}(t)) = -2R_d^T(\bar{q}_0(t)I_d - S(\bar{q}(t)))S(\bar{q}(t))r_i. \tag{4.2.14}$$

Now, the following control law is proposed as

$$\tau(t) = z_\rho(t) - M(t)\hat{\omega}(t), \tag{4.2.15}$$

where the term $z_\rho(\cdot)$ was introduced in [95] and is given by

$$z_\rho(t) = \sum_{i=1}^{m} \rho_i S(b_i^d)b_i, \tag{4.2.16}$$

with the coefficients ρ_i's are arbitrary positive constants. Then, it has been shown in Lemma

1 of [95] that one can actually rewrite $z_\rho(\cdot)$ as

$$z_\rho(t) = -2R_d^T(\bar{q}_0(t)I_d - S(\bar{q}(t)))W_\rho\bar{q}(t). \tag{4.2.17}$$

One finally gets that the controller $\tau(\cdot)$ can be expressed as

$$\tau(t) = -2R_d^T(\bar{q}_0(t)I_d - S(\bar{q}(t)))W_\rho\bar{q}(t) - M\hat{\omega}(t). \tag{4.2.18}$$

Using (4.2.8), (4.2.12), (1.4.9) and (4.2.18), leads to the closed loop dynamics which can be

$$\left\{\begin{array}{lcl} \dot{\zeta} & = & -A\zeta + B(\bar{Q})\omega, \\ \dot{\bar{q}}_0 & = & -\frac{1}{2}\bar{q}^T R_d\omega, \\ \dot{\bar{q}} & = & \frac{1}{2}(\bar{q}_0 I_d + S(\bar{q}))R_d\omega, \\ J\dot{\omega} & = & -S(\omega)J\omega - 2R_d^T(\bar{q}_0 I_d - S(\bar{q}))W_\rho\bar{q} - M\hat{\omega}. \end{array}\right. , \tag{4.2.19}$$

The matrices A_i block diagonal of A are chosen as $A_i \triangleq P_i(\Lambda_i)$, for $1 \leq i \leq m$, with P_i positive polynomial on $\mathbb{R}_+^*$ of degree two. As a trivial consequence, one deduces that, for $1 \leq i \leq m$, $R_d A_i R_d^T$ is symmetric positive definite and commutes with Λ_i.

Note. Set $A_d \triangleq diag(R_d A_1 R_d^T, \cdots, R_d A_m R_d^T)$ and $\Gamma_d \triangleq diag(R_d\Lambda_1 R_d^T, \cdots, R_d\Lambda_m R_d^T)$. Then Γ_d and A_d commute ($\Gamma_d A_d = A_d\Gamma_d$).

One can make a further simplification by changing variables as follows:

$$\zeta \rightarrow \xi = \left[\begin{array}{c} R_d\tilde{b}_1(Q(t)) \\ \vdots \\ R_d\tilde{b}_m(Q(t)) \end{array}\right], \quad \omega \rightarrow \bar{\omega} = R_d\omega.$$

By setting

$$B_d := \left[\begin{array}{c} S(R_d b_1) \\ \vdots \\ S(R_d b_m) \end{array}\right] = \left[\begin{array}{c} S(\bar{R}^T r_1) \\ \vdots \\ S(\bar{R}^T r_m) \end{array}\right] = \left[\begin{array}{c} S((I_d - 2\bar{q}_0 S(\bar{q}) + 2S^2(\bar{q}))r_1) \\ \vdots \\ S((I_d - 2\bar{q}_0 S(\bar{q}) + 2S^2(\bar{q}))r_m) \end{array}\right], \tag{4.2.20}$$

and $J_d := R_d J R_d^T$. Therefore, one can end up with the following autonomous differential

equation

$$\left\{\begin{array}{lcl} \dot{\xi} & = & -A_d\xi + B_d\bar{\omega}, \\ \dot{\bar{q}}_0 & = & -\frac{1}{2}\bar{q}^T\bar{\omega}, \\ \dot{\bar{q}} & = & \frac{1}{2}(\bar{q}_0 I_d + S(\bar{q}))\bar{\omega}, \\ J_d\dot{\bar{\omega}} & = & -S(\bar{\omega})J_d\bar{\omega} - 2(\bar{q}_0 I_d - S(\bar{q}))W_\rho\bar{q} - B_d^T\Gamma_d A_d\xi. \end{array}\right. , \tag{4.2.21}$$

Note that J_d is a real symmetric positive definite matrix. If one defines the state $\chi := (\xi, \bar{Q}, \bar{\omega})$ where $\bar{Q} \equiv \begin{bmatrix} \bar{q}_0 \\ \bar{q} \end{bmatrix} \in \mathbb{S}^3$ and the state space $\Upsilon := \mathbb{R}^{3n} \times \mathbb{S}^3 \times \mathbb{R}^3$, one can rewrite (4.2.21) as

$$\dot{\chi} = F(\chi),$$

where F gathers the right-hand side of (4.2.21) and defines a smooth vector field on Υ. Moreover, note that $\bar{Q}$ and $-\bar{Q}$ represents the same physical rotation, implying that (4.2.21) projects on $SO(3)$ as an autonomous differential equation. We will use that fact in Subsection 4.3.2.

4.3 Stability Analysis of the Proposed Controller

In this section, a rigorous analysis using two attitude representations are presented. As often, it turns out that it is simpler for the stability analysis to use unit quaternions for the representation of rotations instead of rotation matrices elements of $SO(3)$, even-though the reformulation of the results in terms of orthogonal matrices is useful. This is why, in a first step the stability analysis is completed and obtain a first theorem (Theorem 4.1) using unit quaternions and, in a second step, the main result in terms of elements of $SO(3)$ is obtained by simply projecting Theorem 4.1 using Rodriguez formula (1.3.39).

Lemma 4.1. *Under the hypothesis* ***(GEN)*** *in Section 3.2, the solutions of equation $z_\rho = \mathbf{0}$ where z_ρ is defined by (4.2.17) are the following: (a) the two points $\pm(1,\mathbf{0})$; the six points $\pm(0,v_i)$, $1 \leq i \leq 3$, with (v_1,v_2,v_3) being an orthonormal basis diagonalizing W_ρ.*

Proof. Let $(q_0,q) \in \mathbb{S}^3$ such that $z_\rho = \mathbf{0}$, i.e.,

$$(q_0 I - S(q))W_\rho q = \mathbf{0}.$$

If $q_0 \neq 0$, it is immediate to see that $q_0 I_d - S(q)$ is invertible and thus $q = \mathbf{0}$, finally implying that $q_0 = \pm 1$.

If $q_0 = 0$, one can obtain the equation $S(q)W_\rho q = \mathbf{0}$. According to the properties of $S(q)$ with $q \in \mathbb{S}^2$, one can get that q is an eigenvector of W_ρ with unit length, which is concluded under hypothesis **(GEN)**. □

4.3.1 Analysis with rotations expressed in $\mathbb{S}^3$

Consider the following non negative differentiable function $V : \Upsilon \to \mathbb{R}^+$

$$V = \xi^T \Gamma_d A_d \xi + 4\bar{q}^T W_\rho \bar{q} + \bar{\omega}^T J_d \bar{\omega}, \tag{4.3.1}$$

which is radially unbounded over Υ since W_ρ and J_d are positive definite matrices. Moreover, since Γ_d and A_d commute, the gain matrix $\Gamma_d A_d$ is symmetric block diagonal positive definite.

Theorem 4.1. *Consider System (1.4.9)-(1.4.16), under Assumptions 1, 2, 4 and 5 in Section 1.6 and the control law (4.2.15) with the auxiliary system given by (4.2.8), then if Hypothesis **(GEN)** in Section 3.2 holds true, one gets that*

(1) *There are eight equilibrium points, given by*

$$\Omega_1^{\pm} = (\mathbf{0}_{3m}, \begin{bmatrix} \pm 1 \\ \mathbf{0} \end{bmatrix}, \mathbf{0}),\ \Omega_{2,3,4}^{\pm} = (\mathbf{0}_{3m}, \begin{bmatrix} 0 \\ \pm v_i \end{bmatrix}, \mathbf{0}),$$

with (v_1, v_2, v_3) is an orthonormal basis diagonalizing W_ρ.

(2) *All trajectories of (1.4.9)-(1.4.16) converge to one of the equilibrium points defined in Item (1).*

(3) *Set $c := 4\lambda_{min}(W_\rho)$, where $\lambda_{min}(W_\rho)$ is the smallest eigenvalue of W_ρ, then the equilibrium point Ω_1^+ is locally asymptotically stable with a domain of attraction containing the set*

$$V_c^+ := \{\chi \in \Upsilon \mid V(\chi) < c \text{ and } \bar{q}_0 > 0\} \tag{4.3.2}$$

and the equilibrium point Ω_1^- is locally asymptotically stable with a domain of attraction containing the set

$$V_c^- := \{\chi \in \Upsilon \mid V(\chi) < c \text{ and } \bar{q}_0 < 0\}. \tag{4.3.3}$$

(4) *The other equilibrium points $\Omega_{2,3,4}^{\pm}$ are hyperbolic and not stable (i.e. the eigenvalues of each of the corresponding linear systems have non zero real part and at least one of them has positive real part). This implies that the system (1.4.9)-(1.4.16) is almost globally asymptotically stable with respect to the two equilibrium points $\Omega_1^{\pm}$ in the following*

sense: there exists an open and dense subset $\Upsilon_0 \subset \Upsilon$ *such that, for every initial condition* $\chi_0 \in \Upsilon_0$*, the corresponding trajectory converges asymptotically to either* Ω_1^+ *or* Ω_1^-.

Proof. Regarding Item (1), one must solve the equation $f(\chi) = 0$, where f is the nonlinear function describing (4.2.21). Two cases can be considered.

Assume first that $\bar{q}_0 \neq 0$. Both matrices $\bar{q}_0 I_d + S(\bar{q})$ and $\bar{q}_0 I_d - S(\bar{q})$ are non singular. Therefore from the third equation of (4.2.21) $\bar{\omega} = \mathbf{0}$ and thus $\xi = \mathbf{0}_{3m}$ from the first equation of (4.2.21). The fourth equation of (4.2.21) reduces to $z_\rho = \mathbf{0}$ and one concludes that $\bar{q} = \mathbf{0}$ and $\bar{q}_0 = \pm 1$ leading to two equilibrium points : $\Omega_1^+ = (\mathbf{0}_{3m}, \begin{bmatrix} 1 \\ \mathbf{0} \end{bmatrix}, \mathbf{0})$ and $\Omega_1^- = (\mathbf{0}_{3m}, \begin{bmatrix} -1 \\ \mathbf{0} \end{bmatrix}, \mathbf{0})$.

Next, assume that $\bar{q}_0 = 0$. Then $\|\bar{q}\| = 1$ and according to the third equation of (4.2.21), one gets that $\bar{\omega}$ is collinear to $\bar{q}$, let say $R_d \bar{\omega} = \mu \bar{q}$ and then μ must be equal to zero according to the second equation of (4.2.21), implying that $\bar{\omega} = \mathbf{0}$. As in the previous case, one deduces that $\xi = \mathbf{0}_{3m}$. The fourth equation of (4.2.21) yields that $\bar{q}$ and $W_\rho \bar{q}$ are collinear, leading to the six points $\Omega_{2,3,4}^{\pm}$.

Regarding Item(2). Recall that $\Gamma_d A_d$ is symmetric block diagonal positive definite, then using the facts that

$$\bar{\omega}^T S(\bar{\omega}) = 0,\ \bar{q}^T W_\rho (\bar{q}_0 I_d + S(\bar{q}))\bar{\omega} = \bar{\omega}^T (\bar{q}_0 I_d - S(\bar{q})) W_\rho \bar{q},\ \bar{\omega}^T B_d^T \Gamma_d \xi = \xi^T \Gamma_d B_d \bar{\omega},$$

the time derivative of (4.3.1) in view of (4.2.21) yields

$$\dot{V} = -\xi^T \Lambda \xi \leq 0, \tag{4.3.4}$$

since $\Lambda = A_d^T \Gamma_d A_d + \Gamma_d A_d^2 = 2\Gamma_d A_d^2$ is symmetric positive definite. One can deduce that all trajectories of (4.2.21) are defined for all times and bounded.

Since (4.2.21) is autonomous and V is radially unbounded, one can use LaSalle's invariance theorem, cf. (4.3.4). Therefore every trajectory converges to a trajectory γ along which $\dot{V} \equiv 0$. Then ξ must be identically equal to zero, implying at once that $B_d \bar{\omega} \equiv \mathbf{0}$ as well. The latter assertion yields that $\bar{\omega}$ must be non-collinear to all the b_i's, which can be true only if $\bar{\omega} \equiv 0$ since there are at least two non-collinear vectors b_i. From the fourth equation of (4.2.21) one can conclude that $z_\rho = \mathbf{0}$ leading to the conclusion by Lemma 4.1.

Regarding Item(3). The proof is given only for Ω_1^+ since the other case is entirely similar. Take an initial condition $\bar{\chi}$ in V_c^+. Since V is non increasing, $V(\chi) < c$ for all times and, for every $t \geq 0$, $\bar{q}(t)^T W_\rho \bar{q}(t) \leq \lambda_{min}(W_\rho)$. This implies that $\|\bar{q}(t)\| < 1$ for every $t \geq 0$ and thus $\bar{q}_0(t) \neq 0$ for every $t \geq 0$, one can deduce that $\bar{q}_0(t)$ keeps the same sign namely that $\bar{q}_0(0)$,

which is positive. Since the trajectory converges to one of the eight equilibrium points, it must be Ω_1^+ since this is the only one contained in V_c^+.

The proof of Item (4) is deferred in Appendix A, where it is shown that the equilibria $\Omega_j^\pm$, $j = 2,3,4$ are unstable.

Finally, there exists an unstable manifold of dimension at least one in neighborhoods of the $\Omega_j^\pm$, $j = 2,3,4$, and since all trajectories converge to an equilibrium point, therefore (4.2.21) is almost globally asymptotically stable with respect to the two equilibrium points $\Omega_1^\pm$. □

Remark 4.1. Denote by $\Psi \subset \Upsilon$ the set composed of the union of stable manifold of the unstable equilibria $\Omega_j^\pm$, $j = 2,3,4$. Therefore, for every initial condition $\chi_0 \in \Psi$, the corresponding trajectory converges to one of the unstable equilibrium point $\Omega_j^\pm$, $j = 2,3,4$.

4.3.2 Main result on $SO(3)$

Recall that (4.2.21) projects to an autonomous differential equation on $\bar{\Upsilon} := \mathbb{R}^{3m} \times SO(3) \times \mathbb{R}^3$. One can deduce at once the theorem given below. To state it, we need the following notations. If v stands for a line corresponding to an eigenvector of W_ρ, let S_v be the rotation of angle π with respect to v and define the projection $\overline{\mathscr{R}} : \Upsilon \longrightarrow \bar{\Upsilon}$ that associate each $\chi = (\xi, \bar{Q}, \bar{\omega}) \in \Upsilon$ a $\bar{\chi} = (\xi, \bar{R}, \bar{\omega}(\bar{R})) \in \bar{\Upsilon}$ such that $\overline{\mathscr{R}}(\chi) = \bar{\chi}$ and $\mathscr{R}(\bar{Q}) = \bar{R}$.

Corollary 4.1. *Consider the projection of system (1.4.9)-(1.4.16) onto $\bar{\Upsilon}$ under Assumptions 1, 2, 4 and 5 in Section 1.6 and the control law corresponding to (4.2.18) with the auxiliary system corresponding to (4.2.8). Then, if Hypothesis* ***(GEN)*** *in Section 3.2 holds true, one gets that*

(1) *There are four equilibrium points, given by : $\Omega_1 = (\mathbf{0}_{3m}, I_d, \mathbf{0})$, $\Omega_v = (\mathbf{0}_{3m}, S_v, \mathbf{0})$ with v a line corresponding to an eigenvector of W_ρ.*

(2) *All trajectories of the projection of (1.4.9)-(1.4.16) onto $\bar{\Upsilon}$ converge to one of the equilibrium points defined in* (1).

(3) *Set $c := 4\lambda_{min}(W_\rho)$, where $\lambda_{min}(W_\rho)$ is the smallest eigenvalue of W_ρ. Then the equilibrium point Ω_1 is locally asymptotically stable with a domain of attraction containing the set*

$$\bar{V}_c := \left\{ \bar{\chi} \in \bar{\Upsilon} \mid V(\chi) < c \text{ with } \bar{\chi} = (\xi, \mathscr{R}(\bar{Q}), \bar{\omega}) \right\}. \tag{4.3.5}$$

(4) *The other equilibrium points Ω_v are hyperbolic and not stable (i.e. the eigenvalues of each of the corresponding linear systems have non zero real part and at least one of them has positive real part). This implies that the projection of system (1.4.9)-(1.4.16)*

onto $\bar{\Upsilon}$ *is almost globally asymptotically stable with respect to the equilibrium point* Ω_1 *in the following sense: there exists an open and dense subset* $\bar{\Upsilon}_0 \subset \bar{\Upsilon}$ *such that, for every initial condition* $\bar{\chi}_0 \in \bar{\Upsilon}_0$*, the corresponding trajectory converges asymptotically to* Ω_1.

4.4 Control Gains Tuning and Simulation Results

This section provides a procedure to have optimal gains usually local but approaching as near as possible to the global solution. The effectiveness of the proposed velocity-free attitude stabilization controller will be shown using simulation results and comparison is done with respect to the controller (3.3.3-3.3.4) that uses angular velocity measurements.

We denote a state vector $\chi = (\begin{bmatrix} \tilde{b}_1 \\ \tilde{b}_2 \end{bmatrix}, Q, \omega)$, where we take two non-collinear vectors b_1 and b_2. For simplicity and without loss of generality, we take $R_d = I_d$, which means that $\bar{q} = q$, $\bar{\omega} = \omega$ and $b_i^d = r_i$. The matrices Λ_1, Λ_2 are chosen diagonal such as $\Lambda_i = diag(\gamma_{i1}, \gamma_{i2}, \gamma_{i3})$ where $i = 1,2$, therefore the matrices A_1 and A_2 will be $A_i = a_{i0}I_d + a_{i1}\Lambda_i + a_{i2}\Lambda_i^2$ where $i = 1,2$.

In what follows, the following parameters are the same: the inertial reference vectors $r_1 = [0,\ 0,\ 1]^T$ and $r_2 = [0.4348,\ 0.0008,\ 0.9005]$, the inertia matrix is selected from [101]

$$J = \begin{bmatrix} 10 & 1.2 & 0.5 \\ 1.2 & 19 & 1.5 \\ 0.5 & 1.5 & 25 \end{bmatrix}, (Kg.m^2)$$

and the simulation sample time is 0.01s with RK4 solver. The notation "With ω" will be used to design the controller (3.3.3-3.3.4) proposed in Chapter 3.

4.4.1 Parameters Tuning

Consider the case when two non-collinear inertial fixed vectors r_1, r_2 (i.e. $m = 2$) are considered and the used quaternion formulation of the closed loop dynamics is given by (4.2.21). Consider now an objective function $g(\kappa)$ such that κ is the vector of all parameters to be tuned. The goal is to find $\min_{\kappa}(g(\kappa))$ with the following constraint $l(\kappa(\cdot)) \leq \kappa(\cdot) \leq u(\kappa(\cdot))$, where $\kappa = [\ \rho_1 \quad \rho_2 \quad a_{1(j-1)} \quad a_{2(j-1)} \quad \gamma_{1j} \quad \gamma_{2j}\ ]^T, (j = 1,\ldots,3, \kappa \in (\mathbb{R}_+^*)^{14}$ is the vector of parameters), $l(\kappa(\cdot))$ and $u(\kappa(\cdot))$ are the lower and upper bounds corresponding to each parameter and $\kappa(\cdot)$ is an element of κ.

Generally, optimization algorithms find a local optimum, which depends on a basin of attraction of the starting point. Also, the effectiveness of existing algorithms depends on the

lower and upper limits. These last values can be determined based on the dominant poles of the linearized system around the stable equilibrium point.

The linearization of (4.2.21) at $\Omega_1^+ = (\mathbf{0}_6, \begin{bmatrix} 1 \\ \mathbf{0} \end{bmatrix}, \mathbf{0})$ can be written as follows

$$\begin{cases} \dot{z}_\xi &= -Az_\xi + Gz_\omega \\ \dot{z}_q &= \frac{1}{2}z_\omega \\ J\dot{z}_\omega &= -G^T\Gamma Az_\xi - 2W_\rho z_q, \end{cases} \tag{4.4.1}$$

where $G = \begin{bmatrix} G_1^T & G_2^T \end{bmatrix}^T$ with $G_i = S(r_i)$, Γ and A are defined in Subsection 4.2.1 and W_ρ is defined in (3.2.10). Setting $Z = (z_\xi^T, z_q^T, z_\omega^T)^T$ with $z_\xi \in \mathbb{R}^6$, $z_q \in \mathbb{R}^3$ and $z_\omega \in \mathbb{R}^3$ are the linearized vectors of ξ, q, ω, respectively. Then the system (4.4.1) can be rewritten as $\dot{Z} = \mathscr{B}Z$, where

$$\mathscr{B} = \begin{bmatrix} -A & 0_{6\times 3} & G \\ 0_3 & 0_3 & I_d/2 \\ -J^{-1}G^T\Gamma A & -2J^{-1}W_\rho & 0_3 \end{bmatrix}.$$

Note that we used the fact that $\dot{z}_{q_0} = 0$. The linearization of the closed loop dynamics is used to determine the upper and the lower limits$u(\kappa(\cdot))$, $l(\kappa(\cdot))$ respectively. Let's take an arbitrary initial condition $Q(0) = \begin{bmatrix} 0.7212, 0.3999, -0.3999, 0.3999 \end{bmatrix}^T$. For an arbitrary chosen fixed $\kappa(m)$, $m = 3, \ldots, 14$ gains values, we start by varying $\kappa(1)$ and $\kappa(2)$. After inspecting the zero-pole map, one can determine an upper and lower bounds for $\kappa(1)$ and $\kappa(2)$ gains based on the location of the dominant pole, if it exists. The same reasoning gives the values in Table 4.4.1.

Objective Functions and Optimal Control Gains Tuning

Since there exist many possibilities to select the objective function. Different objective functions derived from three well known performance index (see section 5.7 of [28]) were tested. The first is Integral of Absolute Error (IAE), the second is Integral of Time-weighted Absolute Error (ITAE) and the last is Integral of Square Error (ISE), with the possibility to minimize energy and attitude error in the same time by choosing $\sigma \in [0\ 1]$. The first conclusion after several simulations is that the most appropriate objective function for our application is the ISE function $g_{ise}(\kappa) = \int_0^\infty \left(\|\bar{q}\|^2 + \sigma\|\tau\|^2\right) dt$ with $\sigma = 0.1$. Indeed, it minimizes convergence time of the quaternion error and gives a comparable energy consumption to the ones of the controller used for comparison, as we will see after. Initial gains vector are chosen arbitrary as $\kappa_0 = [0.599, 0.586, 0.754, 0.368, 0.015, 5.668, 1.963, 0.099, 2.155, 5.561, 0.021, 5.979, 5.464, 5.954]$.

To get an idea of the effectiveness of the optimization used methods, we compare two

methods to calculate gains optimally. The first one uses the Matlab *fmincon* function and the second method is based on the use of the same function with variation of initial conditions of the parameters in a procedure called *global search* (see, for instance [67]) because the locality of the solution essentially depends on the initial conditions. The best one is the third one, i.e., the *global search* method and the final value κ_{final} with criterion ISE is presented in Table 4.4.2. The corresponding gain matrices are presented in Table 4.4.3. Note that the eigenvalues of obtained matrix W_ρ are simple, despite teh fact that it is not included as a constraint in the tuning gains method. Also, during all conducted simulations using two non-collinear reference vectors no selected set of gains led to multiple eigenvalues of W_ρ. This fact is expected since it is stated in Lemma 3.1.

gains	$l(\kappa(m))$	$u(\kappa(m))$
$\rho_i (i = 1,2)$	4	17
$a_{i0} (i = 1,2)$	0.1	0.5
$a_{i1} (i = 1,2)$	0.001	0.05
$a_{i2} (i = 1,2)$	0.00001	0.005
$\gamma_{ij} (i = 1,2, j = 1,2,3)$	20	120

Table 4.4.1: Lower and upper limits

gains	ISE $g_{ise}(\kappa) = \int_0^\infty \left(\|\bar{q}\|^2 + 0.1\|\tau\|^2\right) dt$
$\rho_i (i = 1,2)$	[9.0339, 7.3266]
$a_{1(j-1)} (j = 1,2,3)$	[0.4061, 0.0365, 0.0034]
$a_{2(j-1)} (j = 1,2,3)$	[0.2898, 0.0205, 0.0027]
$\gamma_{1j} (j = 1,2,3)$	[30.7484 104.4165 93.6847]
$\gamma_{2j} (j = 1,2,3)$	[93.4728, 20, 106.8129]

Table 4.4.2: Selected optimal gain values

4.4.2 Simulation results

This subsection shows the impact of the tuned gains on the nonlinear behavior of the new controller and the effectiveness of the proposed controller compared with the controller (3.3.3-3.3.4) named "with ω". For comparison purpose, the gains of the controller (3.3.3-3.3.4) were

parameters	values calculated with ISE criterion
Λ_1	diag([30.7484 104.4165 93.6847])
Λ_2	diag([93.4728, 20, 106.8129])
A_1	diag([4.7430 41.2868 33.6668])
A_2	diag([25.7963 1.7798 33.2838])
W_ρ	$\begin{bmatrix} 14.9750 & -0.0025 & -2.8686 \\ -0.0025 & 16.3601 & -0.0053 \\ -2.8686 & -0.0053 & 1.3851 \end{bmatrix}$
eigenvectors of W_ρ	$v_{\rho 1} = \pm \begin{bmatrix} 0 \\ -1 \\ 0 \end{bmatrix}$, $v_{\rho 2} = \pm \begin{bmatrix} 0.9801 \\ 0.0018 \\ -0.1984 \end{bmatrix}$, $v_{\rho 3} = \pm \begin{bmatrix} -0.1984 \\ -0.0004 \\ -0.9801 \end{bmatrix}$
eigenvalues of W_ρ	$\lambda_{\rho 1} = 16.3601$, $\lambda_{\rho 2} = 15.5558$ $\lambda_{\rho 3} = 0.8044$

Table 4.4.3: Gain matrices

tuned to generate a comparable torque compared to the controller (4.2.15). The chosen gains for the the controller "with ω" are : $\alpha_1 = 1.1234$, $\alpha_2 = 0.9874$, $\delta_1 = 0.9468$, $\delta_2 = 0.9987$, $\rho_1 = 0.3708$, $\rho_2 = 0.4119$ and $k = 0.4770$.

Depending on the attitude initial condition and tacking in consideration or not the measurements noise, forth cases were selected.

- In the first case, the initial attitude is $Q(0) = \begin{bmatrix} 0.7212, 0.3999, -0.3999, 0.3999 \end{bmatrix}^T$ without noise measurements.
- In the second, case the initial attitude is $Q(0) = \begin{bmatrix} -0.7212, 0.3999, -0.3999, 0.3999 \end{bmatrix}^T$ without noise measurements.
- The third case is chosen to be an unstable equilibrium point $Q(0) = \begin{bmatrix} 0, 0, -1, 0 \end{bmatrix}^T$ without noise measurements.
- The forth case use the same initial condition as the first case, but a noise with standard deviation of 0.01 $(normalized)$ is added to the vector measurements b_1 and b_2.

In all cases the initial angular velocity is chosen to be $\omega(0) = [0.005, 0.006, 0.004]^T$ (rad/s).

Remark 4.2. Special care should be taken where dealing with noisy measurements. In the forth case the gain parameters are chosen differently, the gains $a_{1(j-1)}(j = 1,2,3)$, $a_{i1}(i = 1,2)$ and $a_{i2}(i = 1,2)$ remain unchanged (see Table 4.4.2), the selected other gains are $\Lambda_1 = diag([25.7484, 19.4165, 30.6847])$, $\Lambda_2 = diag([30.4728, 15, 10.8129])$ which gives $A_1 =$

$diag([3.6, 2.3966, 4.7274])$, $A_1 = diag([3.4217, 1.2048, 0.8271])$ and $\rho_1 = 6.0339$, $\rho_2 = 4.3266$. This choice is justified by the fact that matrices A_1 and A_2 represent the frequency cutoff of the auxiliary filters.

The evolution of the unit-quaternion trajectories with respect to time for the new and "with ω" controllers are presented in Figure 4.4.1. In which the trajectories converge asymptotically to the equilibrium point Ω_1^+ in the first case illustrated in Figure 4.4.1a, the trajectories converge asymptotically to the equilibrium point Ω_1^- in the second case illustrated in Figure 4.4.1b. Thus, it is clear that the two controllers can avoid the unwinding phenomenon. Note that, in the third case, even if the initial condition is a theoretical unstable equilibrium point, we verified by simulation that the numerical errors push the trajectories far from this point as depicted in Figure 4.4.1c. Figures 4.4.2, 4.4.3 and 4.4.4 show the angular velocity and applied torque in the three cases. It is clear that the introduction of gain matrices gives better results according to each axis separately. Even if measurements are corrupted by noise, Figure 4.4.1d show that the unit-quaternion trajectories converge to the stable equilibrium point. Figure 4.4.5 illustrates the behaviors of angular velocity and applied torques in the forth case, where one can conclude that the proposed control law without angular velocity is more sensitive to noise than the one with angular velocity.

4.5 Conclusions

In this chapter, attitude stabilization controller for rigid body was proposed, in which neither the angular velocity nor the instantaneous measurements of the attitude are used in the feedback. This controller could be of great help (as main or backup controllers) in applications where prone-to-failure and expensive gyroscopes are used. When almost all existing solutions to this problem use the instantaneous attitude measurements, while it is well known that efficient attitude observer use the angular velocity to obtain an accurate results, the approach

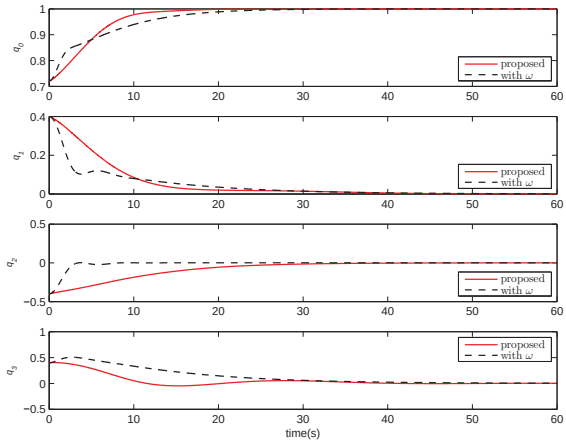

(a) case01

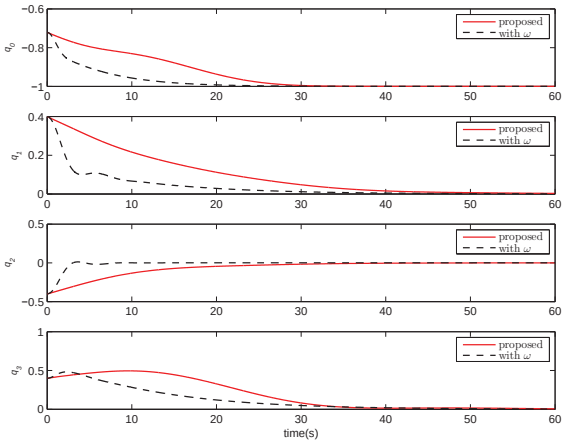

(b) case02

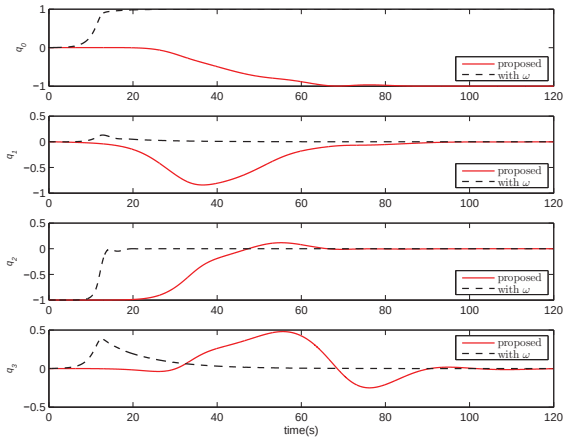

(c) case03

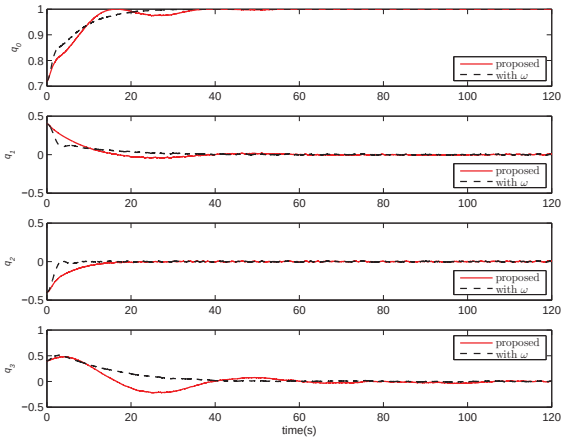

(d) case04

Figure 4.4.1: Quaternions trajectories in all cases

presented in this chapter overcomes totally reconstructing the attitude. It mainly uses an auxiliary system that can be considered as an observer of the angular velocity using only the inertial measurements.

The proposed controller has the following interesting properties :

- It doesn't use the inertial fixed reference vectors.
- It reduces the set of unstable equilibria of the closed loop dynamics with respect to previous proposed controller.
- It provides an almost global asymptotic stability of the desirable equilibrium.
- It avoids the "unwinding phenomenon".

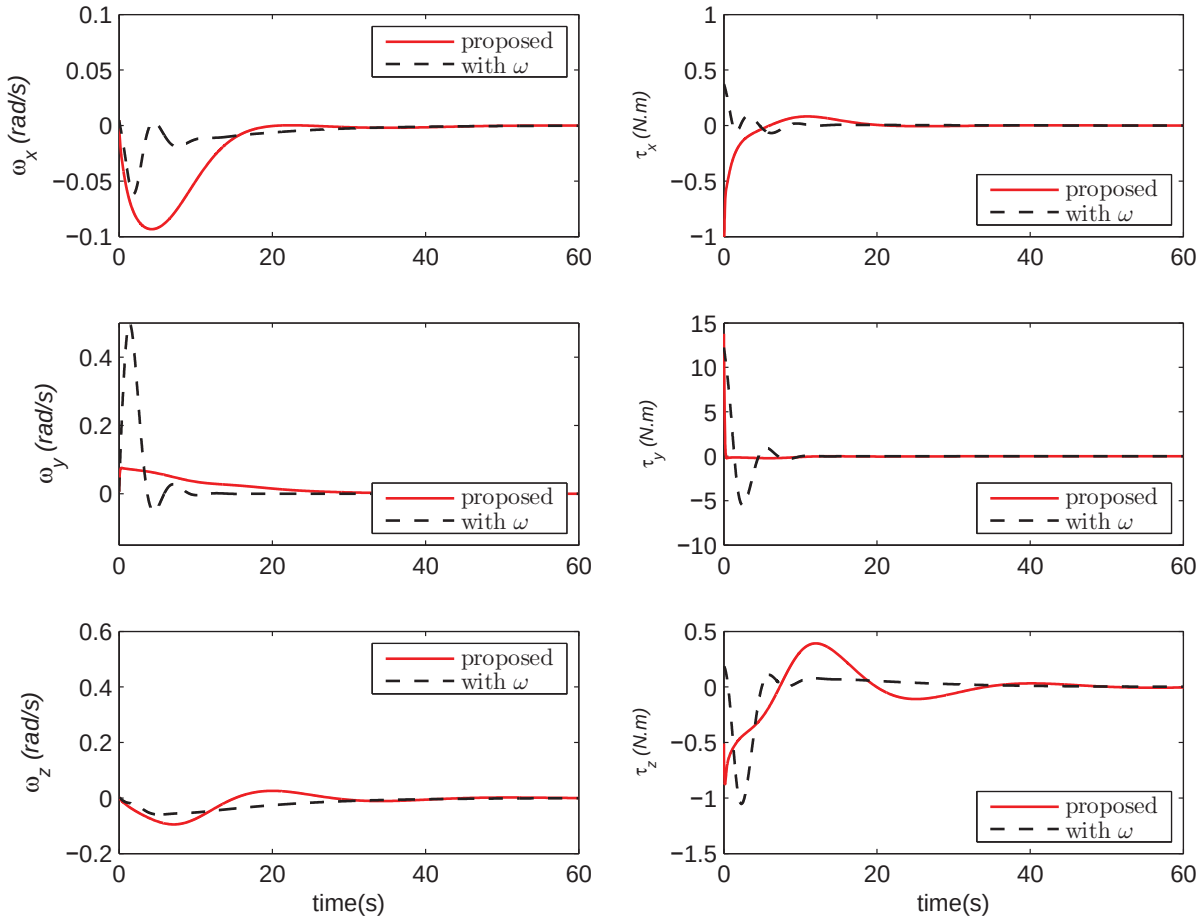

Figure 4.4.2: Angular velocity and applied torques in case 01

In addition, it was shown that the set of control gains leading to a continuum of equilibria of the closed loop system is an algebraic variety of positive co-dimension given at least two non-collinear observed inertial vectors. A non-linear optimal tuning method have been used to adjust properly the controller gains and it was shown via simulations that the introduction of gain matrices leads to good results. The performances and effectiveness of the proposed solution were illustrated via simulation results and compared with respect to the case where angular velocity was used.

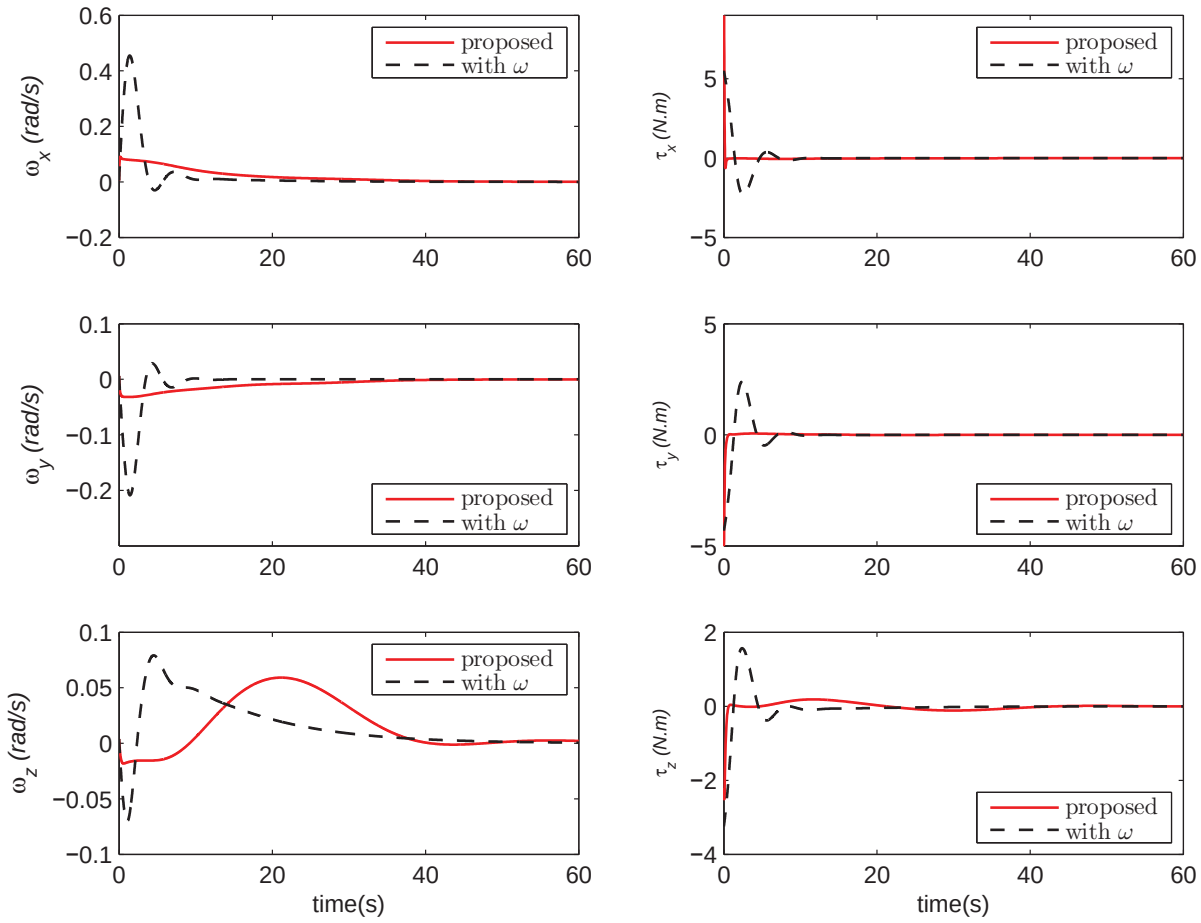

Figure 4.4.3: Angular velocity and applied torques in case 02

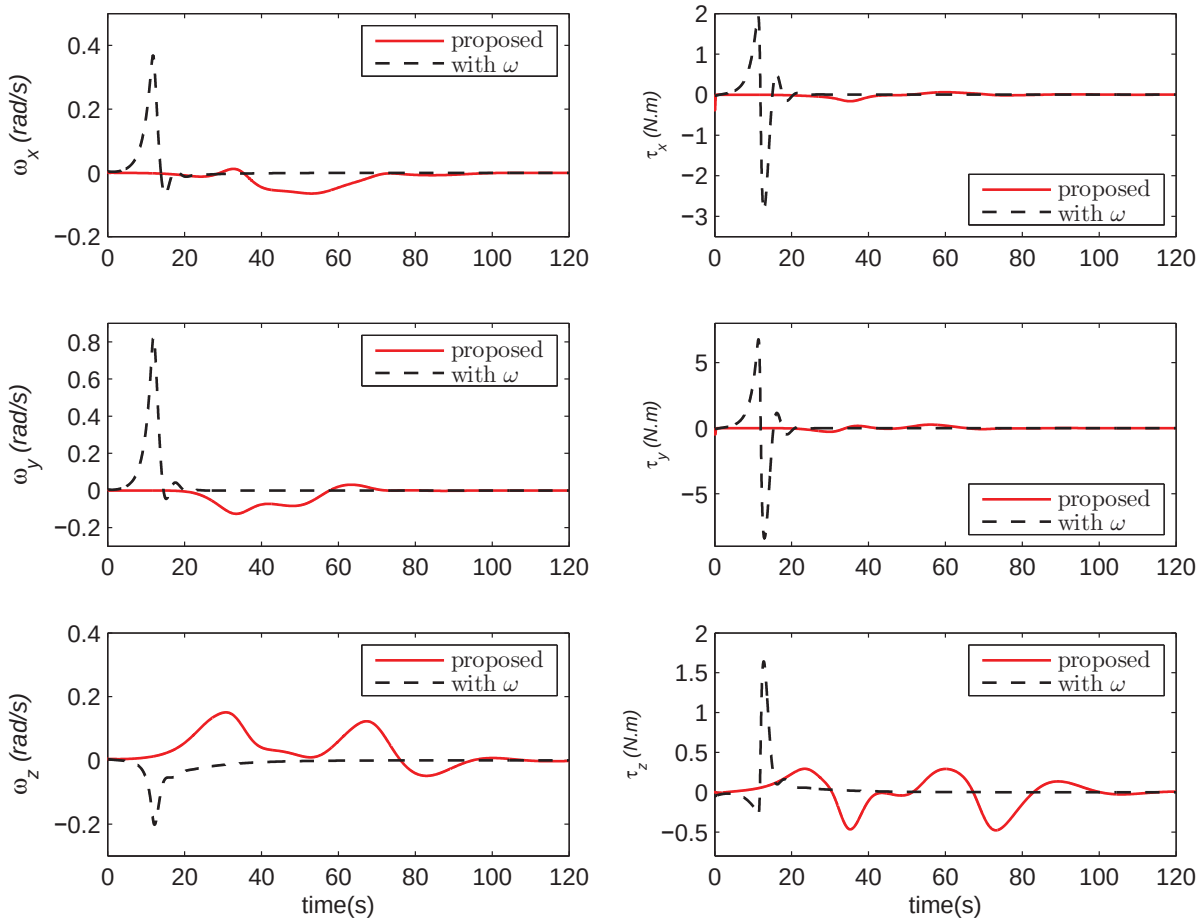

Figure 4.4.4: Angular velocity and applied torques in case 03

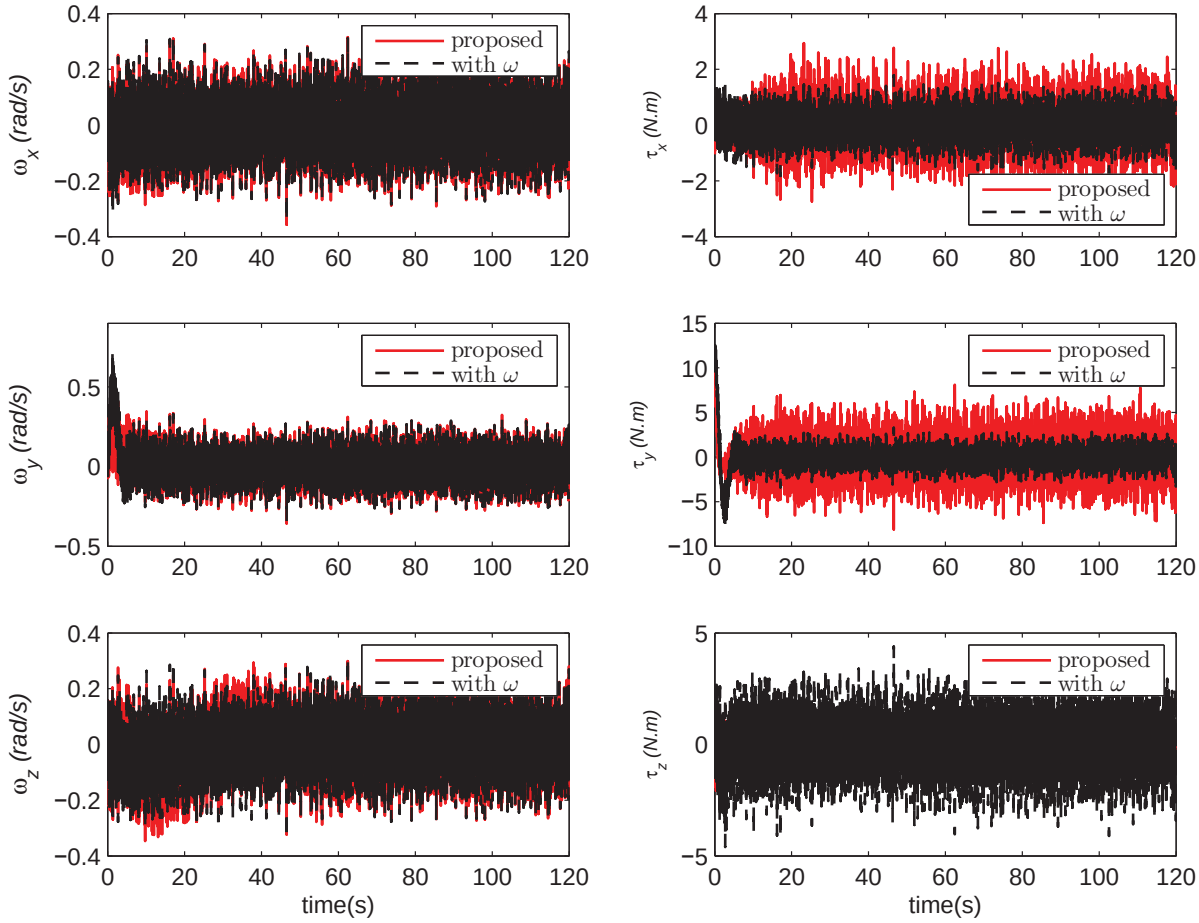

Figure 4.4.5: Angular velocity and applied torques in case 04

Chapter 5

Experimental Validation

5.1 Introduction

One of the most known aerial robot is the quadrotor and probably the most used one as a research platform for experimental tests. Mainly, this is due to their simple structure and low cost. For this, many universities have designed their own quadrotor and an interesting open source projects are growing [57]. The first attempt was the design of a quadrotor with an autopilot based on a Hardware In the Loop board. The goal was to provide a quick implementation method to experiment and validate designated observers and controllers for attitude, which is possible since the user can use Matlab-Simulink to implement the developed model directly on the TMS DSP Board. The result of this work is presented in Figure 5.1.2, where all models required for operating sensors and actuators were developed. This solution took longer time than expected, thus abandoned.

The best way to use such platforms is to start from an open source project. The use of this type of project provides a functional solution with the ability to make any kinds of changes, both hardware and software. One of the most famous open-hardware and open-software multirotor projects is DIY drone project [2]. The open source software code named "ArduCopter" is a generic customized code that can be used for many type of aerial multirotor robots. The hardware is developed and marketed by 3DR [3] and a set of platforms are available, see Figure 5.1.1. The software development follows the evolution of material and two types of autopilots are available, the APM2.6 and PixHawk, that can be used on any platform. The cheaper solution was selected based on DIY Quad and APM2.6 autopilot. The cost of all hardware needed do not exceed 800 Euros.

This chapter presents the experimental used test-bench (see, Figure 5.2.1) and operations performed for turning on the platform such as calibration operations. The effectiveness and the performances of all proposed solutions in this thesis are validated by performing many ex-

periments using this platform. Details about the software used project ArduCopter are differed in Appendix B. Note that partial results in this Chapter were presented in [12].

5.2 Test-bench presentation

Experiments were done based on the open-hardware and open-software DIY drone project [2]. We have used the platform shown in Figure 5.2.1. It is a test-bench with DIY Quad [3] used for indoor tests. Specially, to validate the developed observers and controllers for attitude estimation and control.

The test bench for attitude control and estimation is composed of a support and the DIY Quad. The DIY Quad is a Quadcopter equipped with

1. Holder with rotation ball joint
2. Quad frame
3. Autopilot APM2.6
4. Four electronic speed controllers (ESCs)
5. Four 850Kv brushless motors with propellers
6. Graupner RC receiver
7. 3DR Telemetry Radios
8. u-blox GPS with compass
9. Power distribution board and LiPo battery
10. APM Power module for current consumption and battery voltage measurements

(a) DIY Quad kit

(b) IRIS+

(c) AeroSkywalker

(d) X8+

(e) DIY Y6 kit

Figure 5.1.1: Overview of 3DR solutions(*http://store.3drobotics.com*)

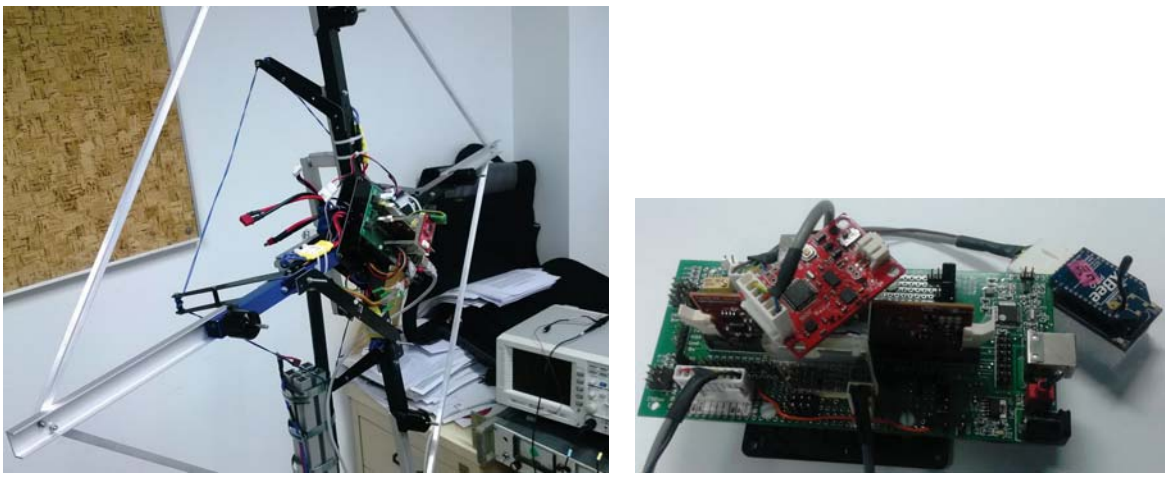

(a) Platform (b) DSP based Autopilot

Figure 5.1.2: First developed HIL platform

Figure 5.2.1: Test-bench DIY Quad equipped with the APM2.6 autopilot

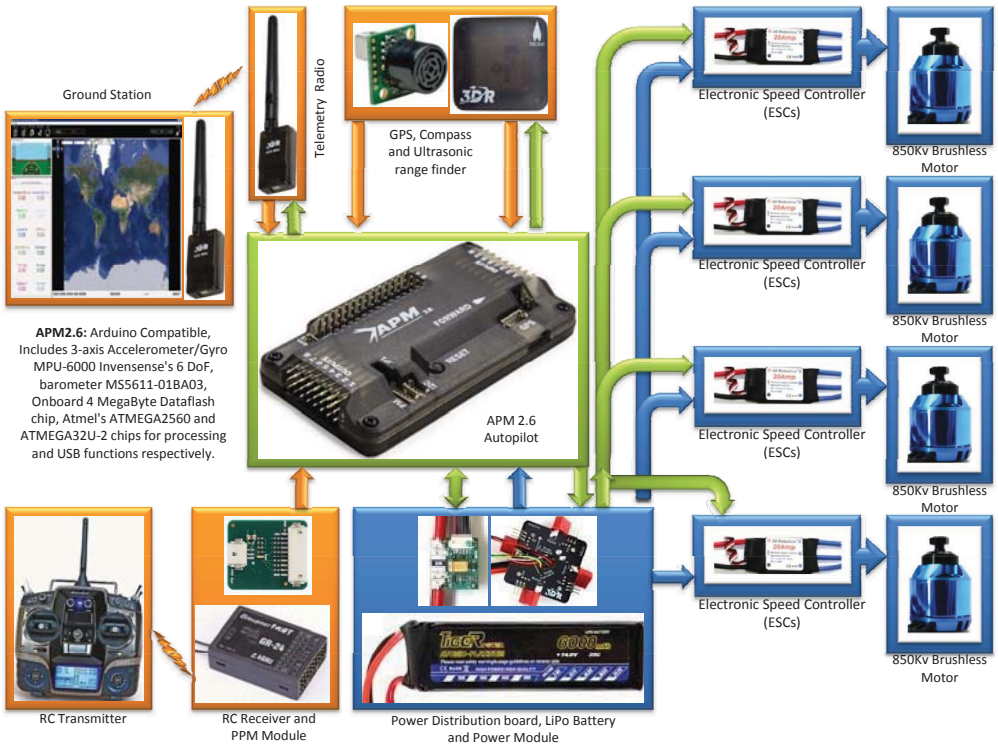

Figure 5.2.2: AMP2.6 Mounting

In addition, the RC transmitter is used to perform manual control and fly mode selection. The open source ground station APM planner is also used to visualize telemetry data and to configure adjustable gains and parameters. See Figure 5.2.2 for AMP2.6 mounting with different other components. The autopilot APM2.6 is based on Atmel ATMEGA2560-16AU using an external clock of 16MHz and ATMEGA32U-2 as a fail-safe processor. The embedded system is equipped with Invensense's 6 DoF Accelerometer/Gyro MPU-6000 and a 3-axis external digital compass HMC5883L-TR.

The open source software project "ArduCopter V3.3-dev" was modified and used to perform different experiments, especially, parts dealing with attitude control. One can found the complete architecture for existing attitude control process in Figure B.0.1. The main loop operating frequency of the firmware is 100Hz. The acquisition of accelerometer and gyros measurements is similar to the main loop while the frequency acquisition of magnetometer measurements is 10 Hz (after an internal filtering).

5.3 Calibrations and inertia matrix determination

5.3.1 Accelerometer calibration and mounting

The accelerometer model (1.5.6) can be rewritten as

$$a_{\mathscr{B}}(t) = a(t) + \eta_a + n_a(t), \tag{5.3.1}$$

where $a(t)$ is the real value of the acceleration vector and $a_{\mathscr{B}}(t)$ is the measured acceleration vector by an accelerometer. The aim of accelerometer calibration is the compensation of the constant offset η_a and scale correction when accelerometer measure the earth gravitational acceleration g. The process is based on placing the quadrotor in positions where all axis of the mobile reference $\{\mathscr{B}\}$ should be collinear to the gravitational earth vector in positive and negative direction. At each position and without moving the quadrotor an accelerometer measurement should be stored. The selected positions allow us to determine the minimum and the maximum accelerometer measurements on each axis. Denote a_{i_min} and a_{i_max} the minimum and maximum measurements on axis i. Then the calibrated measurement for each axis can be evaluated as follow

$$\begin{aligned}
offset_i &= \frac{a_{i_max} + a_{i_min}}{2}, i =' x',' y',' z' \\
scale_i &= \frac{g}{a_{i_max} - offset_i}, i =' x',' y',' z' \\
a_{i_calibrated} &= scale_i(a_{i\mathscr{B}} - offset_i), i =' x',' y',' z' \\
a_{\mathscr{B}}(t)_{calibrated} &= \begin{bmatrix} a_{x_calibrated} & a_{y_calibrated} & a_{z_calibrated} \end{bmatrix},
\end{aligned}$$

where $g = 9.81\,(m/s^2)$.

Now let us focus on the noise $n_a(t)$. Generally, many users mount the autopilot on the frame using a double sided foam tape. An interesting technique was presented in [82], where the author showed that the use of vibration dampening gel rather than a double sided foam tape help reducing a part of the noise $n_a(t)$ due to the vibrations from the motors. This technique was used as illustrated in Figure 5.3.1.

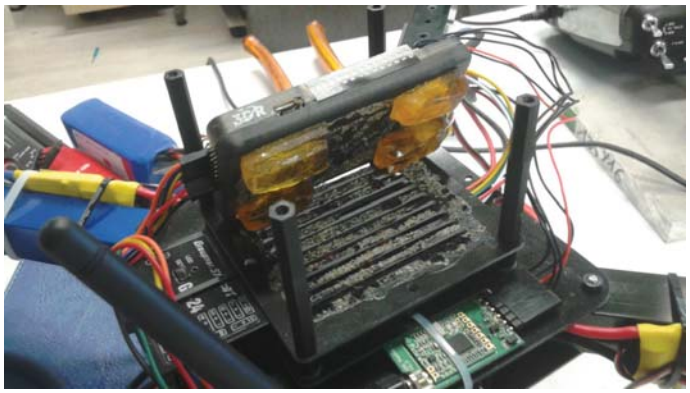

Figure 5.3.1: Used vibration dampening gel

5.3.2 Magnetometer calibration

The magnetometer calibration can be done using a classical method similar to what was presented before for accelerometer calibration. Since magnetometers are sensitive to hard and soft disturbances, obtaining an accurate magnetometer readings is not obvious, specially in indoor tests. A better calibration method to remove the biases, scaling and misalignment errors can be used. Only the model and results are presented here, more details can be found in [82] or in [108]. Consider the following magnetometer raw measurements model

$$m_{\mathscr{B}}(t)_{uncalibrated} = \mathscr{A}\, m_{\mathscr{B}}(t)_{calibrated} + \eta_m, \tag{5.3.2}$$

where $\mathscr{A} \in \mathbb{R}^{3\times 3}$ represents a matrix transformation containing sensor scaling and misalignment errors, η_m represent the measurements offset. After storing a set of measurements uncalibrated data, an ellipsoid that fit to a set of these measurements, see Figure 5.3.2. Thus, $\mathscr{A}$ and η_m can be found and the calibrated data are given by

$$m_{\mathscr{B}}(t)_{calibrated} = \mathscr{A}^{-1}(m_{\mathscr{B}}(t)_{uncalibrated} - \eta_m), \tag{5.3.3}$$

where

$$\mathscr{A}^{-1} = \begin{bmatrix} 0.827786 & 0.0399225 & -0.0296002 \\ 0.0399225 & 0.959383 & 0.0185603 \\ -0.0296002 & 0.0185603 & 0.990549 \end{bmatrix} \text{ and } \eta_m = \begin{bmatrix} 274.308 \\ -84.3697 \\ -20.8206 \end{bmatrix} (mGauss)$$

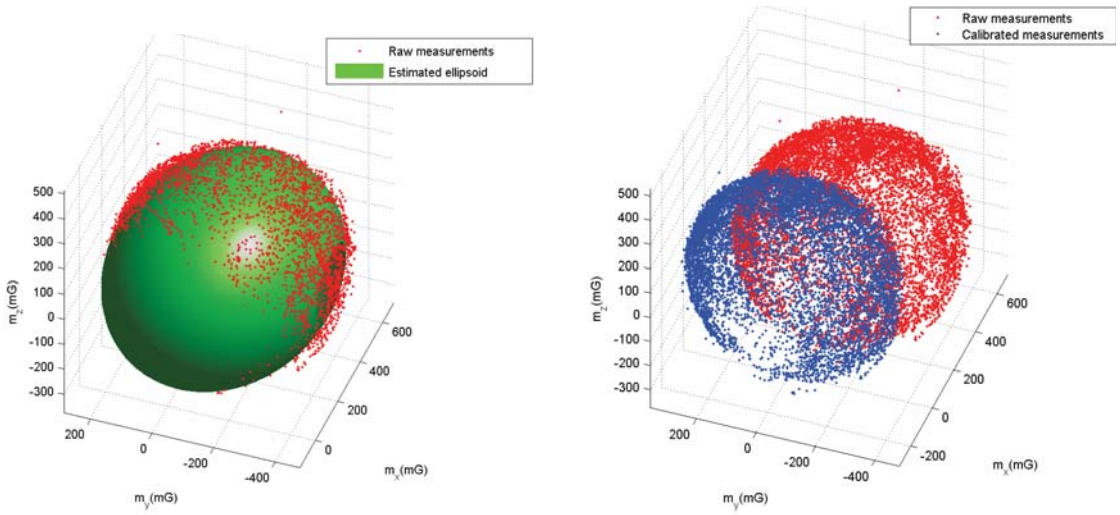

(a) Ellipsoid fit (b) Calibrated measurements

Figure 5.3.2: Magnetometer calibration results

5.3.3 Rate gyro calibration

Rate gyro sensors are very important, especially for attitude estimation. Their calibration is the simplest one, since it is based on storing rate gyro measurements during few seconds without moving the gyro. The average of these measurements constitute a bias that should be compensated.

5.3.4 RC channels and ESCs calibration

The calibration of the RC transmitter/receiver consists in the determination of the minimum, maximum and trim PWM values for each RC channel. The RC Graupner transmitter was configured in mode 2, where left stick controls throttle and yaw and the right stick controls pitch and roll. To control flight mode a three-position switch was attached to RC channel 5. By moving the control sticks and toggle switches to their limits of travel one can obtain the limits presented in Table 5.3.1. After, these limits can be given to the law level controller to allow a symmetric variation in the negative and positive directions for channel 1,2 and 4. It is important to calibrate RC channels without propellers. A complete process of RC and ESC calibration using the ground station APM can be found in [2]. Similarly, ESCs calibration is important, since it allows ESCs to know the PWM limits generated by the autopilot (or flight controller), see [2] for more details.

Channel	Minimum PWM	Maximum PWM	Trim	function
1	1099	1900	1498	pitch
2	1099	1885	1477	roll
3	1100	1899	1100	throttle
4	1099	1900	1500	yaw
5	1099	1900	1500	flight mode

Table 5.3.1: RC channels limits

5.3.5 Inertia Matrix determination

Since the quadrotor is characterized by a symmetric mechanical structure. The inertia matrix can be considered diagonal in the following form

$$J = \begin{bmatrix} J_x & 0 & 0 \\ 0 & J_y & 0 \\ 0 & 0 & J_z \end{bmatrix} (N.m/(rad/s)^2),$$

where $J_x = J_y$.

The process of matrix determination is detailed in [26]. It consists of suspending the quadrotor as depicted in Figure 5.3.3. In each position, one should make a smooth manual rotation around the desired axis and rate gyro can be used to measure the angular velocity from which one can get the oscillation frequency, an example of measured angular velocity is given in Figure 5.3.4. Then, the inertia J_i, $i = 'x','y','z'$ can be determined using the following formula

$$J_i = \frac{mgr^2}{\omega_i^2 l},\ i = 'x','y','z',$$

where $m\,(Kg)$ is the mass of the quadrotor, $g = 9.81\,(m/s^2)$ is the norm of the gravitational earth vector, $r\,(m)$ is the distance from the wire attachment to the axis of rotation (see Figure 5.3.3-a), $l\,(m)$ is the length of the wires (see Figure 5.3.3-b) and $\omega_i = 2\pi f_i\,(rad/s)$ is the oscillation frequency around axis i. Note that it is possible to use Discrete Fourier Transform to get directly f_i.

Finally, the inertia matrix of the quadrotor in Figure 5.3.3 is $J = diag([\ 9.7701 \quad 9.7701 \quad 20.3906\ ]) \times 10^{-4}$, $(N.m/(rad/s)^2)$.

(a) Supporting wires position for x and y axis

(b) Supporting wires position for z-axis

Figure 5.3.3: Inertia matrix determination

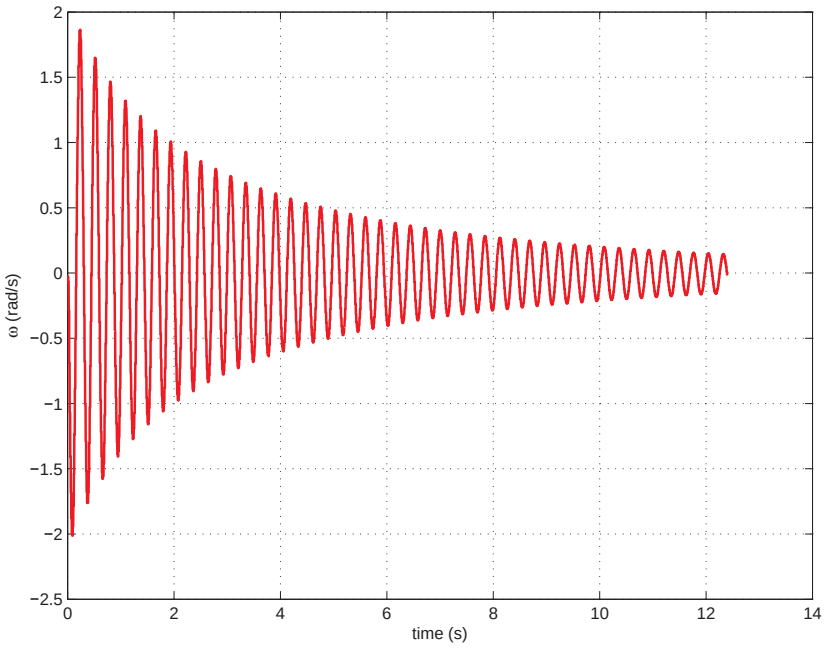

Figure 5.3.4: Gyro rate measurements for a rotation around x-axis

5.4 Experimental validation of proposed attitude estimation and control methods

All operations detailed in previous sections are needed to make possible experimental use of the quadrotor. In this section, we present some experimental results showing the effectiveness and the performances of the proposed solutions.

For experiments, the following parameters are used:

(1) The measurements are given in the mobile frame as shown in Figure 5.2.1.

(2) The first normalized reference fixed inertial vector is $r_1 = [0, 0, 1]^T$ corresponding to the normalized vector of the gravitational earth vector in North East Down "NED" reference frame.

(3) The second normalized reference fixed inertial vector is $r_2 = [0.4348, 0.0008, 0.9005]^T$ corresponding to the normalized vector of the earth magnetic filed in NED reference frame at Vélizy-FRANCE.

For experimental validation, two main experiments were done. The first one was made to evaluate the performance of our attitude observer using the well known Xsens MTi AHRS, as illustrated in Figure 5.4.1. In this experiment, the attitude measurements provided by the MTi is considered as a reference signal. Note that, Kalman filter is implemented inside this IMU. The second experiment consists in the implementation in C/C++ user code of our attitude

controller directly on the autopilot APM2.6.

5.4.1 Attitude estimation

For simplicity, only first order *"Direct"* and *"Passive"* filters presented in Section 2.3 were implemented in experimental tests by using first order Euler integration. The choice of the first order filters is due to real time implementation consideration. Indeed, they are faster and simpler filters. As described above, the attitude measurements delivered by the Xsens MTi will be considered as a reference signal for the comparison of results. This reference is obtained with an internal Kalman filter implemented inside MTi. For comparison purpose, the explicit observer presented in [61] with quaternion formulation was implemented and will be termed as *"MHP"* observer.

From Table 2.4.1, one can rewrite

$$\begin{cases} \dot{\hat{b}}_i &= -S(\omega_m - \hat{\eta})b_i + \gamma_{i1}(b_i - \hat{b}_i) \\ \dot{\hat{\eta}} &= \Gamma_1 \sum_{i=1}^{m} S(b_i)\hat{b}_i \end{cases}, \tag{5.4.1}$$

for the first order *"Direct"* filter and

$$\begin{cases} \dot{\hat{b}}_i &= -S(\omega_m - \hat{\eta})\hat{b}_i + \gamma_{i1}(b_i - \hat{b}_i), \\ \dot{\hat{\eta}} &= \Gamma_2 \sum_{i=1}^{m} S(b_i)\hat{b}_i, \end{cases}, \tag{5.4.2}$$

for the first order *"Passive"* filter.

Remark 5.1. The first order *"Direct"* and *"Passive"* filters given by (5.4.1) and (5.4.2) were implemented using first order Euler integration, where we take $i = 1,2$, $b_1 = a = [\ a_x \quad a_y \quad a_z\ ]^T\ (m/s^2)$ for accelerometer measurements and $b_2 = m = [\ m_x \quad m_y \quad m_z\ ]^T\ (normalized)$ for magnetometer measurements.

For implementation, the following gains were chosen: $\gamma_{11} = \gamma_{21} = 1$ and $\Gamma_1 = \Gamma_2 = 0.003 I_d$ for both two filters while for *"MHP"* observer, the gains presented in [61] were used : $k_P = 1$ and $k_I = 0.3$. The measured initial attitude condition given by MTi was $Q(0) = [0.998043, -0.030992, -0.028809, -0.046046]^T$, which was used as initial condition for *"MHP"* observer and the equivalent initial conditions for 'Direct' and 'Passive' proposed filters were $a(0) = [0.7708, -0.7963, 9.6520]^T$ and $m(0) = [0.0491, 0.0157, -0.2630]^T$.

For reporting results, we first consider the performance of the data fusion obtained by implemented complementary filters. Then, figures 5.4.2 and 5.4.3 show experimental results for the direct and passive filters. One can observe that the two complementary filters have similar performance which corroborates the fact that asymptotic stability were demonstrated

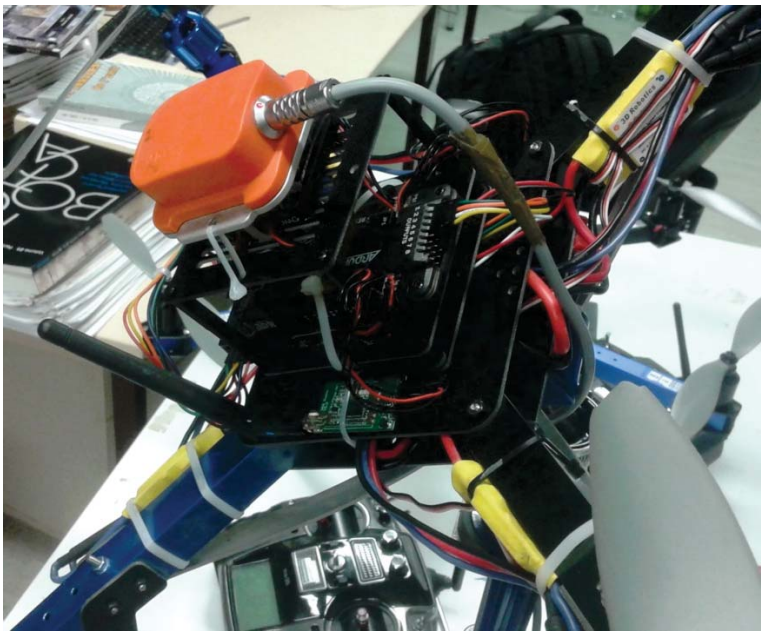

Figure 5.4.1: The Inertial Measurements Unit Xsens mounted on the test-bench

for both filters. As explained before, the passive filter is less sensitive to noise. This can be illustrated in Figure 5.4.2. Note that the raw magnetometer measurements are not very corrupted by noise as illustrated in Figure 5.4.3 and this is due to the fact that they were already filtered inside the MTi. Thereafter, the outputs of theses filters are used to estimate attitude using TRIAD algorithm as illustrated in Figure 5.4.4. In this figure, the estimated attitude using fused data is compared to that obtained with the raw measurements and improvement is observed for the estimation by the proposed method with the TRIAD.

The comparison presented in Figure 5.4.5 illustrates the effectiveness of the proposed observer compared to Kalman filter (implemented inside MTi) or *"MHP"* observer. If we consider the attitude measurements given by the MTi as a reference signal, it is clear that the performance of the proposed passive observer is better than *"MHP"* observer. In Figure 5.4.6, the gyros bias estimation from both observers is shown and both two observers give roughly similar results. Note that in this test, the constant component of the bias was canceled by preprocessing in the MTi.

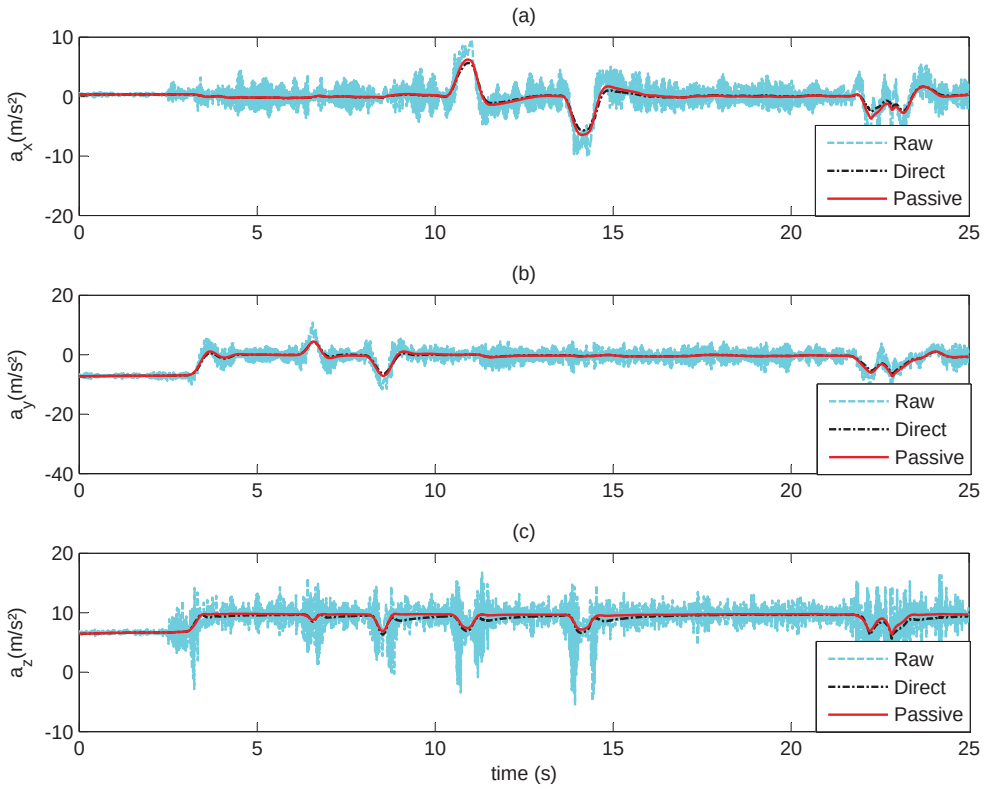

Figure 5.4.2: Complementary Accelerometer filters experimental results

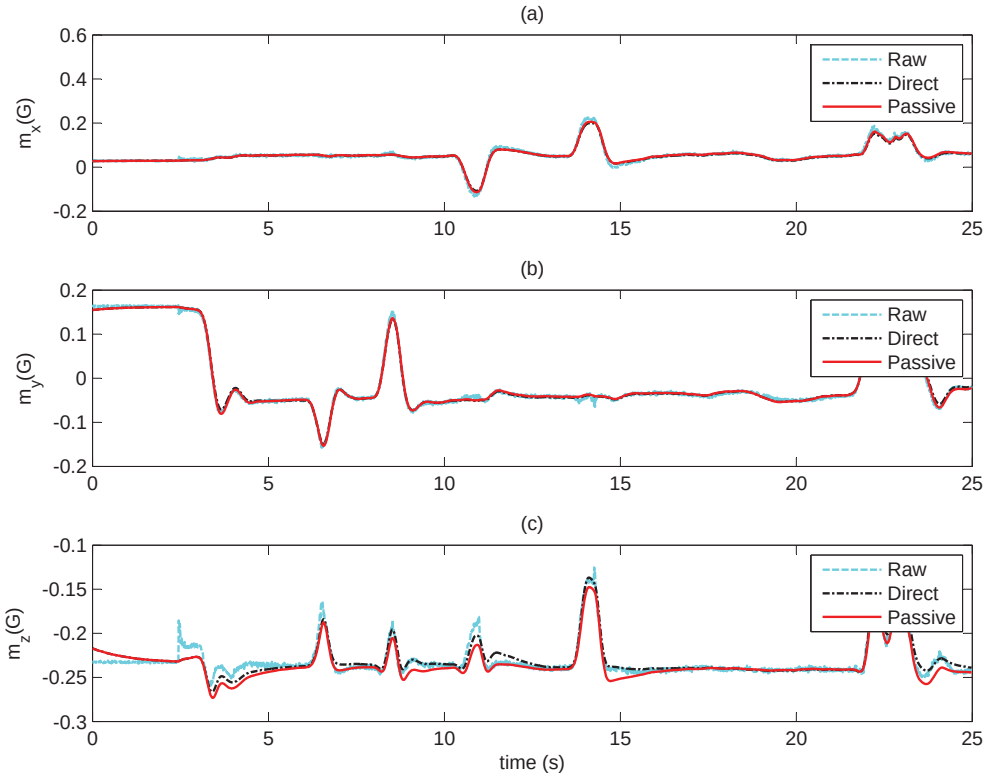

Figure 5.4.3: Complementary Magnetometer filters experimental results

5.4.2 Attitude stabilization

For this test, we considered for simplicity and without loss of generality the special case of stabilization of attitude. The experiment was done using the test-bench shown in Figure 5.2.1. The controller (3.3.2) was implemented using the following notations and parameters : $\hat{b}_1 = \hat{a}\,(normalized)$, $\hat{b}_2 = \hat{m}\,(normalized)$ are the estimates of the inertial vector measurements given by the accelerometers and magnetometers, respectively and $\omega(t)\,(rad/s)$ is the rate gyro measurements. The gains corresponding to accelerometer and magnetometer measurements are $\rho_1 = 1.66$ and $\rho_2 = 0.1161$ (for the axis x and y), respectively, and $\rho_{1z} = 0.05$ and $\rho_{2z} = 0.03$ (for the axis x and y). The damping gain $k = 0.2621$ and the filter gains are $\alpha_1 = 6$ and $\alpha_2 = 10$.

The main loop for attitude stabilization is running at 100Hz. At each loop the measurements of accelerometers and magnetometers are normalized after each iteration. As desired attitude is $R_d(t) = I$, the desired vectors are: $b_1^d = r_1$ and $b_2^d = r_2$. Due to the poor quality of

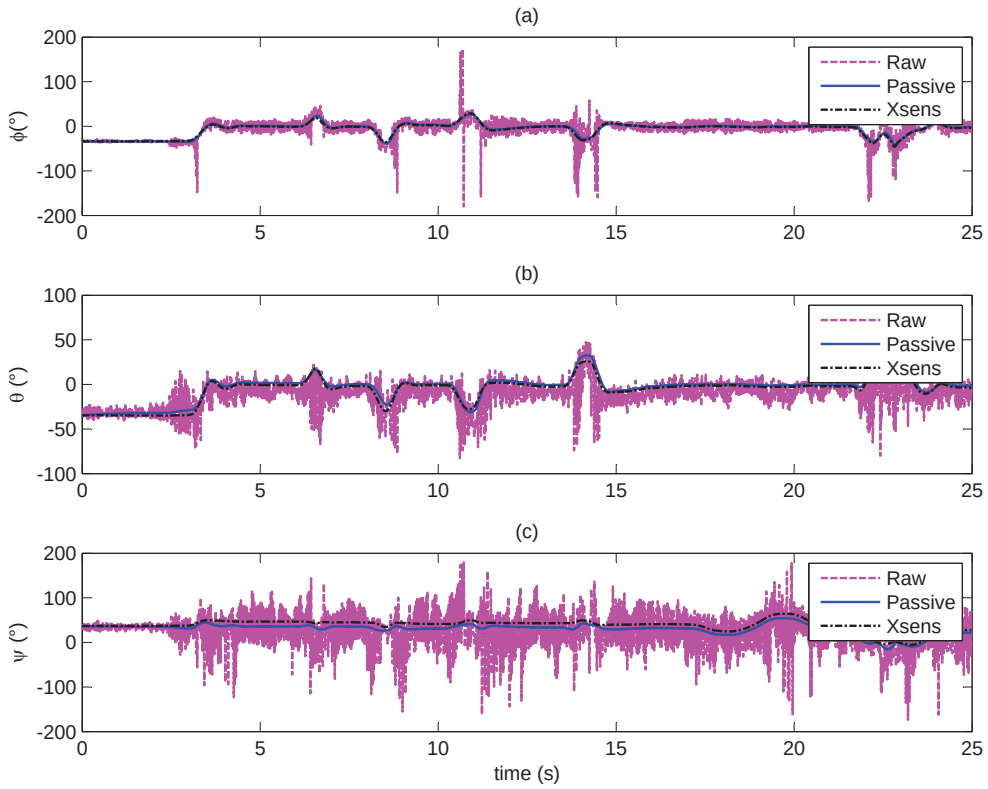

Figure 5.4.4: Attitude estimation experimental results for the proposed observers

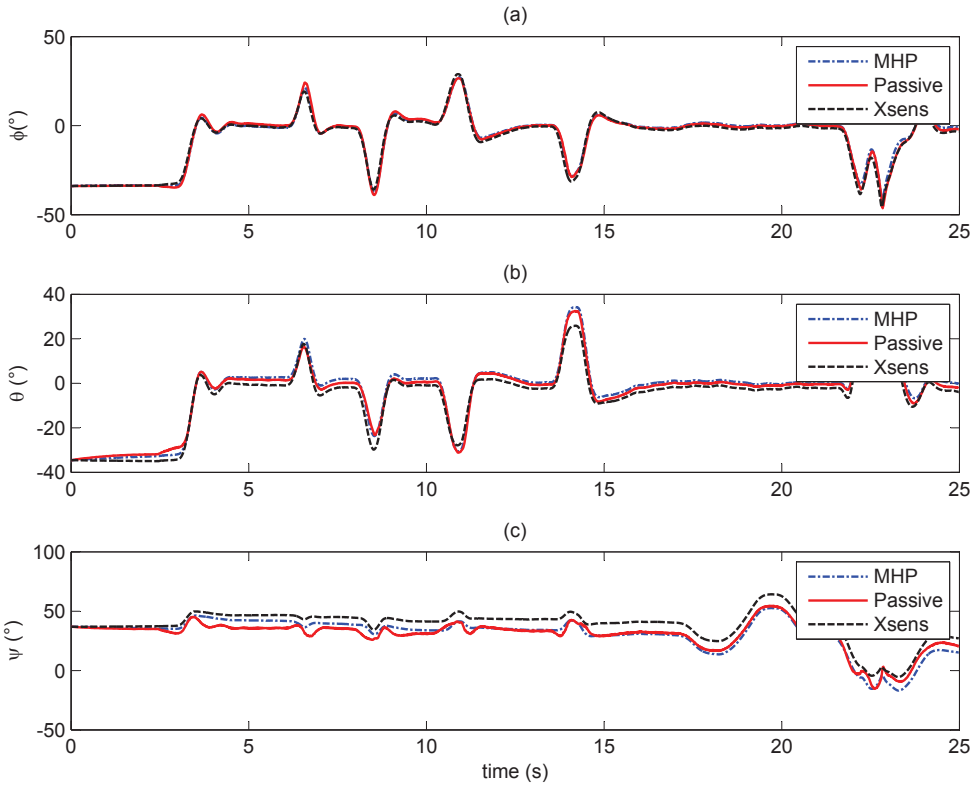

Figure 5.4.5: Attitude estimation experimental results comparison

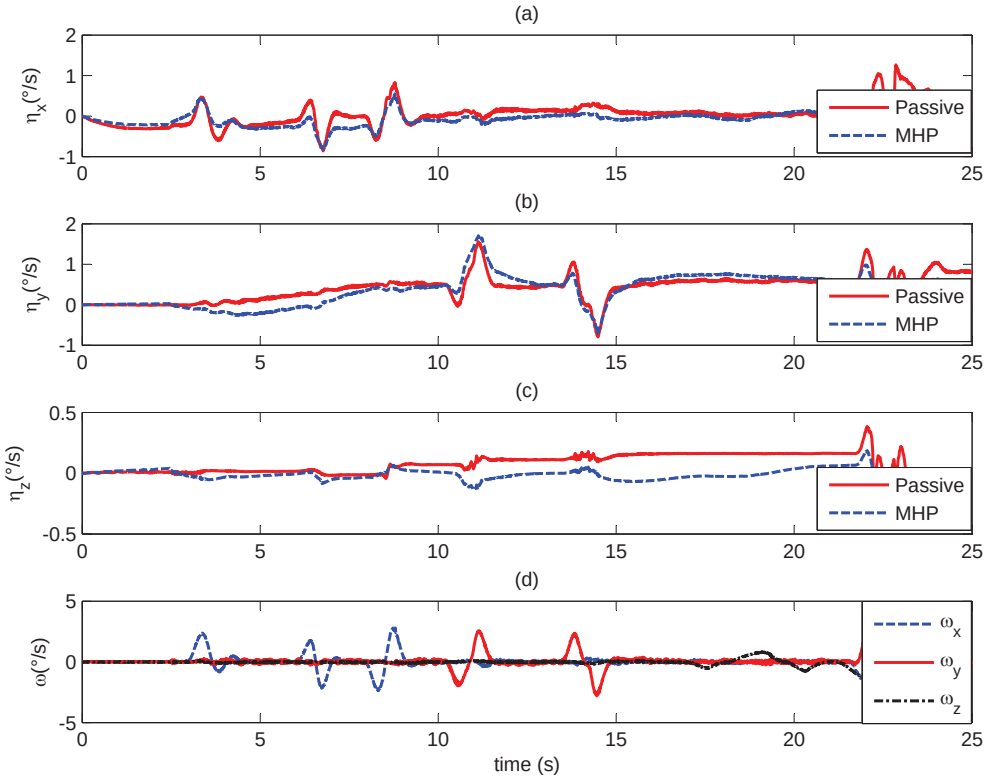

Figure 5.4.6: Rate gyro bias estimation experimental results

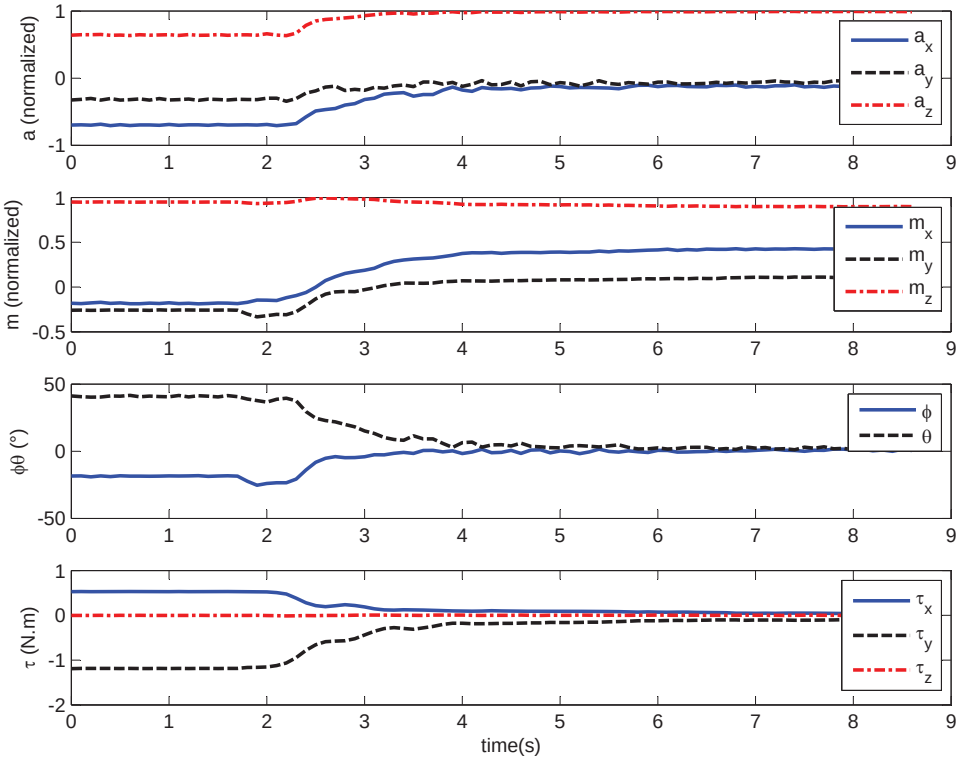

Figure 5.4.7: Attitude stabilization experimental results

magnetometer measurements the gains corresponding to z axis are chosen small. Therefore, the stabilization is done around x and y axis only. Then, starting from an arbitrary measured initial condition in Euler angles $(\phi, \theta, \psi) = (-18.478, 41.192, 2.847)^{\circ}$, the evolution of normalized inertial measurements vectors, torque and Euler angles are shown in Figure 5.4.7. We can see that after transient time, the normalized measurements vectors a and m converge to the desired values $b_1^d = [0,0,1]^T$ and $b_2^d = [0.434, -0.04, 0.899]^T$. Consequently according with the attitude estimate, this corresponds to the roll and pitch angles close to zero which confirms the stabilization of the platform. We can also observe that the control torques are smooth without noise through the use of the complementary filter.

5.5 Conclusion

The Unmanned Aerial Vehicles (UAVs, drones, multirotors, quadcopters) markets are in exponential growth. Especially, due to widening of the civil application fields and high potentials of aerial robotics. Generally, it is hard to use commercial aerial robot for research purposes, due to the fact that researcher should develop his own flight controller to get access to all

needed sensor informations and control correctly the robot. The emergence of the open source projects in this domain resolve this problem. Probably, one of the most known open source project in aerial robots community is ArduCopter project. Sponsored by 3DRobotics, the project offer a complete open source solution to control various types of aerial robots. For this reason, we used this project as a start point to make experimental research.

ArduCopter project was modified and used successfully to validate research theoretical results. Indeed, the proposed attitude estimation and control solutions were validated using DIY Quadcopter hardware and ArduCopter software project. A test-bench for attitude control was assembled using holder with rotation ball joint for security purposes. The obtained experimental results show the effectiveness and performances of the proposed solutions. These results can be improved in future by using the new advanced autopilot system PixHawk rather then the used one (for instance, the APM2.6). Actually, with APM2.6 controls are generated at 100Hz as main loop frequency. PixHawk will allow us to increase this frequency four times, which means 400Hz as a main loop running frequency. Thus, stability will be better and more reliable measurements will be available for other experimental tests.

Conclusion

Despite the considerable number of solutions and due to their importance, attitude estimation and control problems are still relevant. In fact, this thesis gave some contributions on rigid body attitude estimation and rigid body attitude control problems. There are especially three majors contributions presented in this dissertation :

The first one was given in chapter 2, where the notion of complementary linear-like filter was introduced and used with algebraic algorithms (such as TRIAD, Quest, etc.) to give an attitude estimation solution. The novel solution led to several possibilities of implementation considering *n-order direct* or *passive* forms of the complementary filters and the estimation of gyro bias. A complete stability analysis concluded that all trajectories of the closed loop system converge globally asymptotically to the desired equilibrium point. The obtained results were validated and compared to efficient existing solutions by simulations and experiments using a Quadrotor aerial robot and an external reliable Inertial Measurements Unit.

The second contribution of this dissertation was presented in Chapter 3, in which a novel attitude tracking control law coupled with a new linear-like complementary filter were proposed. Only inertial vector measurements and rate-gyro measurements were used to control the attitude of a rigid body without using "attitude measurements". Based on Lyapunov method and Invariance LaSalle's theorem, it was shown that the closed loop error dynamics are almost global asymptotic stable and by a suitable choice of control gains, the closed loop system can not have continuum of equilibria. The designated controller avoids the undesired unwinding phenomena and exhibits noticeable robustness to noise. This was illustrated by simulations and real time implementation on a quadrotor autopilot.

The third contribution was presented in Chapter 4, where a new rigid body attitude stabilization control law was presented, in which neither the angular velocity nor the instantaneous measurements of the attitude are used in the feedback. The unavailability of the angular velocity is handled by the use of an observer-like based on an auxiliary system represented by a first order linear filter of inertial vector measurements. The originality of the proposed controller is that it doesn't use the inertial fixed reference vectors, it reduces the set of unstable equilibria of the closed loop dynamics with respect to previous proposed controllers, it provides

an almost global asymptotic stability of the desirable equilibrium and avoids the "unwinding phenomenon". Also, it was shown that by an adequate choice of control gains, continuum of equilibria of the closed loop system does not exist given at least two non-collinear observed inertial vectors. To correctly set the controller gain matrices, a non-linear constrained optimal tuning method have been used. The performances and effectiveness of the proposed solution were illustrated via simulation results and compared with existing work.

Throughout the completion of this work, several future challenges were identified. The first one related to the proposed high order passive second form, in which the stability analysis remains an open problem when the order is higher than two. The passive second order filter could be of great help to enhance the low sampling frequency of magnetometer measurements compared to that of accelerometer. This seems possible by the introduction of the sensor model as a low pass filter in the complementary filter disign. Also, an interesting work will be the use of vision sensors as source of at least two or more non-collinear observed vectors.

Another possible future work is the extension of the methods presented in this thesis related to attitude control to the case of absolute position control problem of aerial vehicles. Another major contribution would be the generalization of attitude stabilization control without angular velocity to the case of tracking, where the desired attitude and desired angular velocity are time varying. This property makes the stability analysis very challenging.

Appendix A

Proof of Item 4 of Theorem 4.1

Proof. First of all notice the equilibrium points $\Omega_i^{\pm}$, $i = 2,3,4$, cannot be locally asymptotically stable. Indeed let Ω be one of these points and U any open neighborhood of Ω in Υ. Define

$$V_{\Omega}^{-} := \{\chi \in \Upsilon \mid V(\chi) < V(\Omega)\}, \tag{A.0.1}$$

and set $U^{-} := (V_{\Omega}^{-} \cap U)$. The set U^{-} is obviously non empty since it contains points of the type $\lambda\Omega$ with $|\lambda| < 1$ close enough to 1. Moreover, for every $\chi \in U^{-}$, the trajectory of (4.2.21) does not converge to Ω since V is non increasing.

We next prove that the linearization of (4.2.21) at Ω is hyperbolic and admits an eigenvalue with positive real part. We first perform a change of variables. If $\bar{q}_0 = 0$ then $\bar{q} = \sigma v_\rho$, where $\sigma = \pm 1$ and v_ρ is an eigenvector of W_ρ. Let us use the following change of variable (cf. Bullo and Lewis [16], Chaturvedi et al. [20], Mahony et al. [61])

$$X = \begin{bmatrix} x_0 \\ x \end{bmatrix} = \begin{bmatrix} 0 \\ -\sigma v_\rho \end{bmatrix} \odot \begin{bmatrix} \bar{q}_0 \\ \bar{q} \end{bmatrix} = \sigma \begin{bmatrix} v_\rho^T \bar{q} \\ -\bar{q}_0 v_\rho - S(v_\rho)\bar{q} \end{bmatrix} \tag{A.0.2}$$

From (A.0.2) we have

$$\begin{bmatrix} \bar{q}_0 \\ \bar{q} \end{bmatrix} = \begin{bmatrix} 0 \\ \sigma v_\rho \end{bmatrix} \odot \begin{bmatrix} x_0 \\ x \end{bmatrix} = \sigma \begin{bmatrix} -v_\rho^T x \\ x_0 v_\rho + S(v_\rho)x \end{bmatrix} \tag{A.0.3}$$

Recall that v_ρ is a unit eigenvector of W_ρ with associate eigenvalue λ_ρ. The term $\Xi = -(\bar{q}_0 I_d - S(\bar{q}))W_\rho \bar{q}$ function of the new variable can be evaluated as follows. First using the fact that $\sigma^2 = 1$, $W_\rho v_\rho = \lambda_\rho v_\rho$, $S\left(S(v_\rho)x\right) = S(v_\rho)S(x) - S(x)S(v_\rho)$ and $S(v_\rho)v_\rho = \mathbf{0}$, one can obtain

$$\begin{aligned}\Xi &= -\sigma^2\left(\left(-v_\rho^T x\right) I_d - S\left(x_0 v_\rho + S(v_\rho)x\right)\right) W_\rho \left(x_0 v_\rho + S(v_\rho)x\right)\\ &= \lambda_\rho x_0 v_\rho^T x v_\rho + v_\rho^T x W_\rho S(v_\rho)x + x_0 S(v_\rho) W_\rho S(v_\rho)x\\ &\quad + \left(S(v_\rho)S(x) - S(x)S(v_\rho)\right) W_\rho \left(x_0 v_\rho + S(v_\rho)x\right),\end{aligned} \tag{A.0.4}$$

then, using the fact that $x^T v_\rho = v_\rho^T x$, and $S^2(v_\rho) = v_\rho v_\rho^T - v_\rho^T v_\rho I_d = v_\rho v_\rho^T - I_d$, one can get that

$$v_\rho^T x v_\rho = v_\rho v_\rho^T x = \left(S^2(v_\rho) + I_d\right) x, \tag{A.0.5}$$

using the fact that $S(v_\rho)S(x) = x v_\rho^T - v_\rho^T x I_d$ and $v_\rho^T S(v_\rho) = \mathbf{0}$, then

$$S(v_\rho)S(x)W_\rho S(v_\rho)x = -v_\rho^T x W_\rho S(v_\rho)x, \tag{A.0.6}$$

using the fact that $W_\rho v_\rho = \lambda_\rho v_\rho$ and $S(x)v_\rho = -S(v_\rho)x$, then

$$x_0 S(v_\rho)S(x)W_\rho v_\rho = -\lambda_\rho x_0 S^2(v_\rho)x \tag{A.0.7}$$

Finally, using (A.0.3), (A.0.4), (A.0.5), (A.0.6) and (A.0.7), one can rewrite (4.2.21) function of the new variable as

$$\begin{cases} \dot{\xi} &= -A_d \xi + B_d(X)\bar{\omega}\\ \dot{x}_0 &= -\frac{1}{2} x^T \bar{\omega}\\ \dot{x} &= \frac{1}{2}\left(x_0 I_d + S(x)\right)\bar{\omega}\\ J_d \dot{\bar{\omega}} &= -B_d^T(X)\Gamma_d A_d \xi - S(\bar{\omega}) J_d \bar{\omega}\\ &\quad +2\left(x_0 I_d - S(x)\right)\left(\lambda_\rho I_d + S(v_\rho) W_\rho S(v_\rho)\right) x \end{cases} \tag{A.0.8}$$

Therefore, the tangent space of $\mathbb{S}^3$ at $\begin{bmatrix} 1 \\ \mathbf{0} \end{bmatrix}$ is given by the equation $x_0 = 0$ and the linearization of system (A.0.8) at $\Omega = (\xi, X, \bar{\omega}) = (\mathbf{0}_{3m}, \begin{bmatrix} 1 \\ \mathbf{0} \end{bmatrix}, \mathbf{0})$ is given by

$$\dot{Z} = \mathscr{A} Z, \; with \; \mathscr{A} = \begin{bmatrix} -A_d & 0_{3m\times 3} & H \\ 0_{3\times 3m} & 0_3 & I_d/2 \\ -J_d^{-1} H^T \Gamma_d A_d & 2J_d^{-1} G & 0_3 \end{bmatrix},$$

where $Z = (z_\xi^T, z_x^T, z_\omega^T)^T$ with z_ξ, z_x, z_ω are the linearized vectors of $\xi, x, \bar{\omega}$, respectively. The matrices $G = \lambda_\rho I_d + S(v_\rho) W_\rho S(v_\rho)$ and $H = \begin{bmatrix} H_1^T & \cdots & H_m^T \end{bmatrix}^T$ with $H_j = S\left(R_d\left(I_d + 2S^2\left(v_\rho\right)\right) b_j^d\right)$

were evaluated as following : recall that an element B_{di} of B_d is defined as

$$\begin{aligned} B_{di} &= S(R_d b_i) \\ &= S(R_d R^T r_i) \\ &= S(\bar{R}^T r_i) \\ &= S\left(\left(I_d - 2\bar{q}_0 S(\bar{q}) + 2S^2(\bar{q})\right) r_i\right) \qquad \text{(A.0.9)} \\ &= S\left(\left(I_d + 2v_\rho^T x S\left(x_0 v_\rho + S(v_\rho)x\right) + 2S^2\left(x_0 v_\rho + S(v_\rho)x\right)\right) r_i\right) \\ B_{di}\Big|_\Omega &= S\left(\left(I_d + 2S^2\left(v_\rho\right)\right) r_i\right) \\ &= S\left(\left(I_d + 2S^2\left(v_\rho\right)\right) R_d b_i^d\right) \qquad \text{(A.0.10)} \end{aligned}$$

Since Ω is not locally asymptotically stable, it is enough to show that $\mathscr{A}$ does not admit any eigenvalue with zero real part. Reasoning by contradiction, we thus assume that $\mathscr{A}$ has an eigenvalue il, $i^2 = -1$, $l \geq 0$, with $Z^l = (z_1^T, z_2^T, z_3^T)^T \in \mathbb{C}^{3n+6}$ a corresponding eigenvector. One gets the linear system of equations

$$\begin{cases} -A_d z_1 + & Hz_3 & = il z_1, \\ & z_3/2 & = il z_2, \\ -J_d^{-1} H^T \Gamma_d A_d z_1 + & 2J_d^{-1} G z_2 & = il z_3. \end{cases} \qquad \text{(A.0.11)}$$

If $l = 0$, one gets $z_3 = z_1 = 0$ (since A_d is positive definite) and $J_d^{-1} G z_2 = 0$. Recalling that W_ρ is real symmetric with distinct eigenvalues, we have that

$$W_\rho = \lambda_\rho v_\rho v_\rho^T + \lambda_1 v_1 v_1^T + \lambda_2 v_2 v_2^T,$$

where (v_ρ, v_1, v_2) is an orthonormal basis of $\mathbb{R}^3$ made of eigenvectors of W_ρ. By using the properties of $S(v_\rho)$, one gets that

$$G = \lambda_\rho v_\rho v_\rho^T + (\lambda_\rho - \lambda_2) v_1 v_1^T + (\lambda_\rho - \lambda_1) v_2 v_2^T,$$

implying that $\det(G) = \lambda_\rho(\lambda_\rho - \lambda_1)(\lambda_\rho - \lambda_2) \neq 0$ and thus $z_2 = 0$. Then the eigenvector Z is equal to zero, which is impossible.

We deduce that $l > 0$. One deduces that $z_1 = (A_d + il I_{3n})^{-1} H z_3$, $z_2 = -\frac{i}{2l} z_3$ and

$$(i(J_d l + G/l) + H^T \Gamma_d A_d (A_d + il I_{3n})^{-1} H) z_3 = 0 \qquad \text{(A.0.12)}$$

Note that

$$\begin{aligned} H^T\Gamma_d A_d(A_d+i\,lI_{3n})^{-1}H &= \sum_{j=1}^{m} H_j^T R_d\Lambda_j A_j R_d^T(R_d A_j R_d^T+ilI_d)^{-1}H_j \\ &= \sum_{j=1}^{m} H_j^T R_d\Lambda_j A_j R_d^T(R_d(A_j+ilI_d)R_d^T)^{-1}H_j \\ &= \sum_{j=1}^{m} H_j^T R_d\Lambda_j A_j R_d^T((R_d^T)^{-1}(A_j+ilI_d)^{-1}(R_d)^{-1})H_j \\ &= \sum_{j=1}^{m} (R_d^T H_j)^T\Lambda_j A_j(A_j+ilI_d)^{-1}(R_d^T H_j), \end{aligned} \tag{A.0.13}$$

For $j=1,\ldots,n$, let (y_{j1},y_{j2},y_{j3}) be an orthonormal basis diagonalizing Λ_j and Y_j the corresponding orthonormal matrix such that $\Lambda_j = Y_jL_jY_j^T$, where $L_j = diag(\lambda_{j1},\lambda_{j2},\lambda_{j3})$ with $\lambda_{jk}\in\mathbb{R}_+^*$, $j=1,\ldots,n$, $k=1,2,3$. Therefore, $P_j(\Lambda_j) = Y_jP_j(L_j)Y_j^T$, where $P_j(L_j) = diag(P_j(\lambda_{j1}),P_j(\lambda_{j2}),P_j(\lambda_{j3}))$.

Recall that $A_j = P_j(\Lambda_j)$, $j=1,\ldots,n$ where P_j is a positive polynomial of degree two on $\mathbb{R}_+^*$, one deduces that

$$\begin{aligned} \Lambda_j A_j(A_j+ilI_d)^{-1} &= \Lambda_j P_j(\Lambda_j)(P_j(\Lambda_j)+ilI_d)^{-1} \\ &= Y_jL_jP_j(L_j)(P_j(L_j)+ilI_d)^{-1}Y_j^T \\ &= \sum_{k=1}^{3}\frac{\lambda_{jk}P_j(\lambda_{jk})}{P_j(\lambda_{jk})+il}y_{jk}y_{jk}^T, \end{aligned} \tag{A.0.14}$$

where the results on functions of matrices of Chapter 6 and section 6.2 in Horn and Johnson [40] have been used.

Multiplying Eq. (**??**) on the left by $(z_3^*)^T$ and using Eq. (A.0.14), yields

$$i(z_3^*)^T(lJ_d+G/l)z_3 + \sum_{j=1}^{n}\sum_{k=1}^{3}\frac{\lambda_{jk}P_j(\lambda_{jk})(P_j(\lambda_{jk})-il)}{P_j(\lambda_{jk})^2+l^2}((T_j^*)^T y_{jk})(y_{jk}^T T_j) = 0, \tag{A.0.15}$$

where $l>0$, $T_j = R_d^T H_j z_3$ for $j=1,\ldots,n$ and T_j^* is the conjugate of the complex vector T_j. Since $(z_3^*)^T(lJ_d+G/l)z_3$ is a real number, one gets by taking the real part of Eq. (A.0.15)

$$\sum_{j=1}^{n}\sum_{k=1}^{3}\frac{\lambda_{jk}P_j(\lambda_{jk})^2}{P_j(\lambda_{jk})^2+l^2}\left|y_{jk}^T T_j\right|^2 = 0, \tag{A.0.16}$$

where $|\cdot|$ denotes the modulus of a complex number. One deduces at once that $T_j = R_d^T H_j z_3 = 0$ for $j=1,\ldots,n$. Therefore, $S\left(\left(I_d+2S^2\left(v_\rho\right)\right)r_j\right)z_3 = 0$ for $j=1,\ldots,n$. Since at least two vectors r_j are not collinear, one gets that $z_3=0$ and finally $Z=0$, which is again a

contradiction.

If $\mathscr{A}$ does not have eigenvalues with positive real part, it would have only eigenvalues with negative real part and thus $\mathscr{A}$ would be Hurwitz, implying that (4.2.21) would be locally asymptotically stable with respect to Ω. Since this is not true, $\mathscr{A}$ does admit at least one eigenvalue with positive real part. Thus, there exists an unstable manifold of dimension at least one in neighborhoods of the $\Omega_j^{\pm}$, $j = 2,3,4$, and since all trajectories converge to an equilibrium point, therefore (4.2.21) is almost globally asymptotically stable with respect to the two equilibrium points $\Omega_1^{\pm}$. □

Appendix B

Attitude Control in ArduPilot Project Code

The ArduPilot Project Code 3DRobotics [1] is a full open source project, designated for Copter, Rover and Plane robots. The total code base are about 700 thousands lines including libraries. The project make use of external support open source code, such that MAVLink micro air vehicle marshaling-communication library and the core NuttX Real Time Operating System, etc. The code is well documented and can be used for experimental tests. For this purpose, we used the version "ArduCopter V3.3-dev" and made many modifications to create our proper flight mode for attitude control. The class "attitude_control" and other part of the code were modified to accept our controllers, the hole original process for attitude control is depicted in Figure B.0.1.

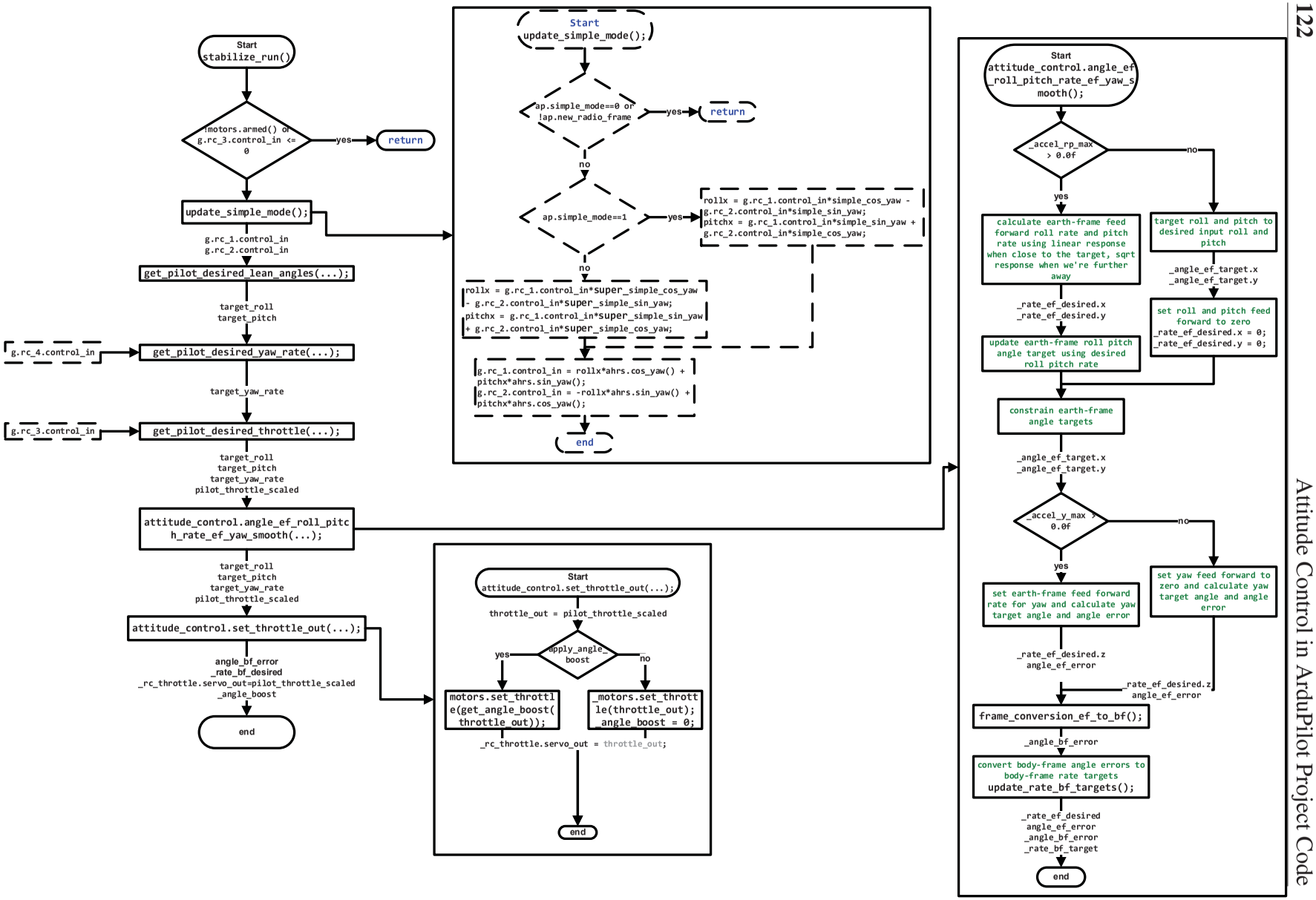

Figure B.0.1: Overview of Attitude control existing code

Appendix C

List of Publications

C.1 Relevant Journal Publications

1. Lotfi Benziane, Abdellaziz Benallegue, Yacine Chitour and Abdelhamid Tayebi, "Inertial Vector Based Attitude Stabilization of Rigid Body Without Angular Velocity Measurements". In International Journal of Robust and Non Linear Control, arXiv preprint arXiv:1501.04767, Article in review.

2. Lotfi Benziane, Abdelhafid El Hadri, Ali Seba, Abdellaziz Benallegue, Yacine Chitour, "Attitude Estimation and Control Using Linear-Like Complementary Filters: Theory and Experiment", In International Journal of Control, arXiv preprint arXiv:1503.02718, Article in review.

C.2 Relevant Conference Publications

1. Lotfi Benziane, Abdellaziz Benallegue and Abdelhafid El Hadri, "A globally asymptotic attitude estimation using complementary filtering". In Proceedings of IEEE International Conference on Robotics and Biomimetics (ROBIO), pages 878-883, Guangzhou, China, 11-14 Dec. 2012. DOI:10.1109/ROBIO.2012.6491079.

2. Lotfi Benziane, Abdellaziz Benallegue and Abdelhamid Tayebi, "Attitude Stabilization Without Angular Velocity Measurements". In Proceedings of IEEE International Conference on Robotics & Automation (ICRA), pages 3116-3121, Hong Kong, China, May 31 2014-June 7 2014. DOI:10.1109/ICRA.2014.6907307.

C.3 Other Publications

1. Ali Seba, Abdelhafid El Hadri, Lotfi Benziane and Abdellaziz Benallegue, “Multiplicative Extended Kalman Filter based on Visual Data for Attitude Estimation”. In IEEE ICRA Workshop on Modeling, Estimation, Perception and Control of All Terrain Mobile Robots, Hong Kong, China, May 31-June 7 2014.

2. Ali Seba, Abdelhafid El Hadri, Lotfi Benziane and Abdellaziz Benallegue, “Attitude Estimation Using Line-Based Vision and Multiplicative Extended Kalman Filter”. In International Conference on Control, Automation, Robotics and Vision (ICARCV), Marina Bay Sands, Singapore, Dec 10-12 2014.

References

[1] 3DRobotics. Ardupilot project http://dev.ardupilot.com/wiki/learning-the-ardupilot-codebase/, March 2015.

[2] 3DRobotics. Arducopter projet http://copter.ardupilot.com/, March 2015.

[3] 3DRobotics. http://store.3drobotics.com/, March 2015.

[4] I. Ahmad, A. El Hadri, and A. Benallegue. Sliding mode based attitude estimation for accelerated aerial vehicles using gps/imu measurements. In *IEEE International Conference on Robotics and Automation (ICRA)*, Karlsruhe, Germany, May 2013.

[5] Maruthi R. Akella. Rigid body attitude tracking without angular velocity feedback. *Systems & Control Letters*, 42(4):321–326, Apr. 2001.

[6] P. Batista, C. Silvestre, and P. Oliveira. Sensor-based globally asymptotically stable filters for attitude estimation: Analysis, design, and performance evaluation. *IEEE Transactions on Automatic Control*, 57(8):2095 – 2100, Aug. 2012.

[7] Ramaprakash Bayadi and Ravi N. Banavar. Almost global attitude stabilization of a rigid body for both internal and external actuation schemes. *European Journal of Control*, 20(1):45–54, Jan. 2014.

[8] A. Benallegue, A. Mokhtari, and L. Fridman. High-order sliding-mode observer for a quadrotor uav. *International Journal of Robust and Nonlinear Control*, 18(4-5):427–440, 2008. ISSN 1099-1239.

[9] L. Benziane, A. Benallegue, and A.E. El-Hadri. A globally asymptotic attitude estimation using complementary filtering. In *IEEE International Conference on Robotics and Biomimetics (ROBIO)*, pages 878–883, Guangzhou, China, Dec 2012.

[10] L. Benziane, A. Benallegue, and A. Tayebi. Attitude stabilization without angular velocity measurements. In *IEEE International Conference on Robotics & Automation (ICRA)*, pages 3116–3121, Hong Kong, China, May 31-June 7 2014.

[11] L. Benziane, A. Benallegue, Y. Chitour, and A. Tayebi. Inertial vector based attitude stabilization of rigid body without angular velocity measurements. *arXiv:1501.04767 [math.OC]*, 2015.

[12] L. Benziane, A. El Hadri, A. Seba, A. Benallegue, and Y. Chitour. Attitude estimation and control using linear-like complementary filters: Theory and experiment. *arXiv:1503.02718v1 [math.OC]*, 2015.

[13] Sylvain Bertrand. *Commande de drone miniature a voilure tournante*. PhD thesis, Nice Sofia Antipolis University, 2007.

[14] Sanjay P. Bhat and Dennis S Bernstein. A topological obstruction to continuous global stabilization of rotational motion and the unwinding phenomenon. *Systems & Control Letters*, 39(1):63–70, Jan. 2000.

[15] Peter. Van. Blyenburgh. Uas: The global perspective with a focus on light uas. In *National UAS Conference*, Sao José dos Santos, Brazil, October 2010.

[16] F. Bullo and A.D Lewis. *Geometric Control of Mechanical Systems : modeling, analysis, and design for simple mechanical control systems*. 2005.

[17] Christopher I. Byrnes and Alberto Isidori. On the attitude stabilization of rigid spacecraft. *Automatica*, 27(1):87–95, Jan. 1991.

[18] L.R.G. Carrillo, A.E.D. Lopez, R. Lozano, and C. Pegard. *Quad Rotorcraft Control, Vision-Based Hovering and Navigation*. Springer-Verlag London, 2013.

[19] P. Castillo, P. Albertos, P. Garcia, and R. Lozano. Simple real-time attitude stabilization of a quad-rotor aircraft with bounded signals. In *45th IEEE Conference on Decisionand Control (CDC)*, pages 1533–1538, December 2006.

[20] N.A. Chaturvedi, A.K. Sanyal, and N.H. McClamroch. Rigid-body attitude control. *IEEE Control Systems Magazine*, 31(3):30–51, Jun. 2011. ISSN 1066-033X.

[21] Peter Corke. *Robotics, Vision and Control Fundamental Algorithms in MATLAB*. Springer-Verlag Berlin Heidelberg, 2011.

[22] B. T. Costic, D. M. Dawson, M. S. de Queiroz, and V. Kapila. Quaternion-based adaptive attitude tracking controller without velocity measurements. *Journal of Guidance, Control, and Dynamics*, 24(6):1214–1222, Nov. 2001.

[23] J.L. Crassidis and Markley F.L. Unscented filtering for spacecraft attitude estimation. *Journal of guidance, control, and dynamics*, 26(4):536–542, 2003.

[24] J.L. Crassidis, F.L. Markley, and F. Cheng. Survey of nonlinear attitude estimation methods. *Journal of guidance, control, and dynamics*, 30(1):12–28, Jan. 2007.

[25] John L. Crassidis and John L. Junkins. *Optimal Estimation of Dynamic Systems*. Chapman & Hall / CRC Applied Mathematics & Nonlinear Science, 2nd edition, 2012.

[26] L. Derafa, T. Madani, and A. Benallegue. Dynamic modelling and experimental identification of four rotors helicopter parameters. In *IEEE International Conference on Industrial Technology (ICIT)*, pages 1834–1839, Dec 2006.

[27] L. Derafa, A. Benallegue, and L. Fridman. Super twisting control algorithm for the attitude tracking of a four rotors uav. *Journal of the Franklin Institute*, 349(2):685 – 699, 2012. ISSN 0016-0032.

[28] Richard C. Dorf and Robert H. Bishop. *Modern Control Systems*. Prentice Hall, twelfth edition, 2011.

[29] O. Egeland and J.-M. Godhavn. Passivity-based adaptive attitude control of a rigid spacecraft. *IEEE Transactions on Automatic Control*, 39:842 – 846, Apr 1994.

[30] A. El Hadri and A. Benallegue. Attitude estimation with gyros-bias compensation using low-cost sensors. In *Joint 48th IEEE Conference on Decision and Control and 28th Chinese Control Conference (CDC-CCC)*, pages 8077–8082, December 16-18 2009.

[31] M. Euston, P. Coote, R. Mahony, J. Kim, and T. Hamel. A complementary filter for attitude estimation of a fixed-wing uav. In *IEEE/RSJ International Conference on Intelligent Robots and Systems (IROS)*, pages 340–345, Acropolis Convention Center, Nice, France, Sept, 22-26 2008.

[32] Nuno Filipe and Panagiotis Tsiotras. Rigid body motion tracking without linear and angular velocity feedback using dual quaternions. In *European Control Conference (ECC)*, 2013.

[33] Emil Fresk and George Nikolakopoulos. Full quaternion based attitude control for a quadrotor. In *European Control Conference (ECC)*, 2013.

[34] H. F. Grip, T. I. Fossen, Johansen T. A., and A. Saberi. Globally exponentially stable attitude and gyro bias estimation with application to gnss/ins integration. *Automatica*, 51(0):158 – 166, 2015. ISSN 0005-1098.

[35] J.F. Guerrero-Castellanos, N. Marchand, A. Hably, S. Lesecq, and J. Delamare. Bounded attitude control of rigid bodies: Real-time experimentation to a quadrotor mini-helicopter. *Control Engineering Practice*, 19(8):790 – 797, 2011. ISSN 0967-0661.

[36] A. Hably and N. Marchand. Global stabilization of a four rotor helicopter with bounded inputs. In *IEEE/RSJ International Conference on Intelligent Robots and Systems(IROS)*, pages 129–134, Oct 2007.

[37] J.K. Hall, N.B. Knoebel, and McLain T.W. Quaternion attitude estimation for miniature air vehicles using a multiplicative extended kalman filter. In *IEEE/ION Position, Location and Navigation Symposium*, pages 1230 – 1237, May 5-8 2008.

[38] Allen Hatcher. *Algebraic Topology*. Cambridge University Press, 2002.

[39] JR. Walter T. Higgins. A comparison of complementary and kalman filtering. *IEEE Transaction On Aerospace And Electronic Sysytems*, AES-1 1(3):321–325, May 1975.

[40] Roger A. Horn and Charles R. Johnson. *Topics in Matrix Analysis*. Cambridge University Press, 1991.

[41] M.-D. Hua, P. Martin, and T. Hamel. Velocity-aided attitude estimation for accelerated rigid bodies. *arXiv:1411.3953*, Nov. 2014.

[42] Minh-Duc. Hua. Attitude estimation for accelerated vehicles using gps/ins measurements. *Control Engineering Practice*, 18:723–732, 2010.

[43] Minh-Duc Hua, T. Hamel, Pascal Morin, and Claude Samson. A control approach for thrust-propelled underactuated vehicles and its application to vtol drones. *IEEE Transactions on Automatic Control*, 54(8):1837–1853, Aug 2009. ISSN 0018-9286.

[44] Minh-Duc Hua, T. Hamel, P. Morin, and C. Samson. Introduction to feedback control of underactuated vtol vehicles: A review of basic control design ideas and principles. *IEEE Control Systems*, 33(1):61–75, Feb 2013. ISSN 1066-033X.

[45] Minh-Duc Hua, Tarek Hamel, Pascal Morin, and Claude Samson. Control of vtol vehicles with thrust-tilting augmentation. *Automatica*, 52(0):1 – 7, 2015. ISSN 0005-1098.

[46] Qian. Hua-ming, Huang. Wei, Qian. Lin-chen, and Shen. Chen. Robust extended kalman filter for attitude estimation with multiplicative noises and unknown external disturbances. *IET Control Theory Applications*, 8(15):1523–1536, Oct 2014. ISSN 1751-8644.

[47] M. Izadi and Amit K Sanyal. Rigid body attitude estimation based on the lagrange-alembert principle. *Automatica*, 50(10):2570 – 2577, 2014. ISSN 0005-1098.

[48] S.M. Joshi, A.G. Kelkar, and J.T.-Y. Wen. Robust attitude stabilization of spacecraft using nonlinear quaternion feedback. *IEEE Transactions on Automatic Control*, 40 (10):1800–1803, 1995. ISSN 0018-9286.

[49] M. Jun, S.I. Roumeliotis, and G.S. Sukhatme. State estimation of an autonomous helicopter using kalman filtering. In *IEEE/RSJ International Conference on Intelligent Robots and Systems (IROS)*, volume 3, pages 1346 – 1353, 1999.

[50] Farid Kendoul. *Modelling and control of unmanned aerial vehicles, and development of a vision based autopilot for small rotorcraft navigation*. PhD thesis, UTC, 2007.

[51] Farid Kendoul. Survey of advances in guidance, navigation, and control of unmanned rotorcraft systems. *Journal of Field Robotics*, 29(2):315–378, 2012. ISSN 1556-4967.

[52] Maryam Kiani and Seid H. Pourtakdoust. Adaptive square-root cubature quadrature kalman particle filter for satellite attitude determination using vector observations. *Acta Astronautica*, 105(1):109 – 116, 2014. ISSN 0094-5765.

[53] Hariharan Krishnan, Mahmut Reyhanoglu, and Harris McClamroch. Attitude stabilization of a rigid spacecraft using two control torques: A nonlinear control approach based on the spacecraft attitude dynamics. *Automatica*, 30(06):1023–1027, 1994.

[54] V. Kubelka and M. Reinstein. Complementary filtering approach to orientation estimation using inertial sensors only. In *IEEE International Conference on Robotics and Automation (ICRA)*, pages 599–605, RiverCentre, Saint Paul, Minnesota, USA, May 14-18 2012.

[55] T. Lee. Global exponential attitude tracking controls on so(3). *IEEE Transactions on Automatic Control*, PP(99):1–1, 2015. ISSN 0018-9286.

[56] Taeyoung Lee. Robust adaptive attitude tracking on so(3) with an application to a quadrotor uav. *IEEE Transactions on Control Systems Technology*, 21(5):1924–1930, 2013. ISSN 1063-6536.

[57] Hyon Lim, Jaemann Park, Daewon Lee, and H.J. Kim. Build your own quadrotor: Open-source projects on unmanned aerial vehicles. *IEEE Robotics Automation Magazine*, 19(3):33–45, Sept 2012. ISSN 1070-9932.

[58] F. Lizarralde and J.T. Wen. Attitude control without angular velocity measurement: a passivity approach. *IEEE Transactions on Automatic Control*, 41(3):468–472, Mar. 1996. ISSN 0018-9286.

[59] T. Madani and A. Benallegue. Control of a quadrotor mini-helicopter via full state backstepping technique. In *IEEE Conference on Decision and Control (CDC)*, pages 1515–1520, Dec 2006.

[60] T. Madani and A. Benallegue. Backstepping control for a quadrotor helicopter. In *IEEE/RSJ International Conference on Intelligent Robots and Systems (IROS)*, pages 3255–3260, Oct 2006.

[61] R. Mahony, T. Hamel, and Pflimlin J.-M. Nonlinear complementary filters on the special orthogonal group. *IEEE Transactions on Automatic Control*, 53(5):1203–1218, Jun. 2008.

[62] R. Mahony, V. Kumar, and P. Corke. Multirotor aerial vehicles: Modeling, estimation, and control of quadrotor. *IEEE Robotics Automation Magazine*, 19(3):20–32, Sept 2012. ISSN 1070-9932.

[63] F. Landis Markley and John L. Crassidis. *Fundamentals of Spacecraft Attitude Determination and Control*. Microcosm Press and Springer, 2014.

[64] P. Martin and Salaun E. An invariant observer for earth-velocity-aided attitude heading reference systems. In *IFAC World Congress*, volume 17, pages 9857–9864, COEX, South Korea, 2008.

[65] P. Martin and E. Salaun. Design and implementation of a low-cost observer-based attitude and heading reference system. *Control Engineering Practice*, 18(7):712–722, July 2010.

[66] K. Masuya, T. Sugihara, and M. Yamamoto. Design of complementary filter for high-fidelity attitude estimation based on sensor dynamics compensation with decoupled properties. In *IEEE International Conference on Robotics and Automation (ICRA)*, pages 606–611, RiverCentre, Saint Paul, Minnesota, USA, May 14-18 2012.

[67] MathWorks. How globalsearch and multistart work, http://fr.mathworks.com/help/gads/how-globalsearch-and-multistart-work.html, April 2015.

[68] Christopher G. Mayhew, Ricardo G. Sanfelice, and Andrew R. Teel. Robust global asymptotic attitude stabilization of a rigid body by quaternion-based hybrid feedback. In *Joint 48th IEEE Conference on Decision and Control and 28th Chinese Control Conference (CDC-CCC)*, pages 2522–2527, Shanghai, Dec. 2009.

[69] P. Morin and C. Samson. Time-varying exponential stabilization of a rigid spacecraft with two control torques. *IEEE Transactions on Automatic Control*, 42(4):528–534, Apr. 1997.

[70] James R. Munkres. *Topology*. Prentice Hall, 2nd edition, 2000.

[71] M. Namvar and F. Safaei. Adaptive compensation of gyro bias in rigid-body attitude estimation using a single vector measurement. *Automatic Control, IEEE Transactions on*, 58(7):1816–1822, July 2013. ISSN 0018-9286.

[72] N. Nordkvist and A.K. Sanyal. Attitude feedback tracking with optimal attitude state estimation. In *American Control Conference (ACC)*, pages 2861–2866, 2010.

[73] J.-M. Pflimlina, P. Binettib, P. Souèresa, T. Hamel, and D. Trouchet. Modeling and attitude control analysis of a ducted-fan micro aerial vehicle. *Control Engineering Practice*, 18:209–218, 2010.

[74] Henry. Plinval, Pascal. Morin, Philippe. Mouyon, and Tarek. Hamel. Visual servoing for underactuated vtol uavs: a linear, homography-based framework. *International Journal of Robust and Nonlinear Control*, 24(16):2285–2308, 2014. ISSN 1099-1239.

[75] P. Pounds, T. Hamel, and R. Mahony. Attitude control of rigid body dynamics from biased imu measurements. In *46th IEEE Conference on Decision and Control (CDC)*, pages 4620–4625, 2007.

[76] P. Pounds, R. Mahony, and P. Corke. Modelling and control of a large quadrotor robot. *Control Engineering Practice*, pages 691–699, 2010.

[77] H. Rifaï, J.-F. Guerrero-Castellanos, N. Marchand, and G. Poulin-Vittrant. Biomimetic-based output feedback for attitude stabilization of a flapping-wing micro aerial vehicle. *Robotica*, 31(6):955–968, Apr. 2013. ISSN 1469-8668.

[78] H. Rifai, J.-F. Guerrero-Castellanos, N. Marchand, and G. Poulin. Bounded attitude control of a flapping wing micro aerial vehicle using direct sensors measurements. In *IEEE International Conference on Robotics and Automation, ICRA*, pages 3644–3650, May 2009.

[79] Andrew Roberts and A. Tayebi. On the attitude estimation of accelerating rigid-bodies using gps and imu measurements. In *50th IEEE Conference on Decision and Control and European Control Conference (CDC-ECC)*, pages 8088–8093, Dec 2011.

[80] Nargess. N. Sadaghzadeh, Javad. Poshtan, Achim Wagner, Eugen Nordheimer, and Essameddin Badreddin. Cascaded kalman and particle filters for photogrammetry based gyroscope drift and robot attitude estimation. *ISA Transactions*, 53(2):524 – 532, 2014. ISSN 0019-0578.

[81] Rune Schlanbusch, Esten Ingar Grøtli, Antonio Loria, and Per Johan Nicklasson. Hybrid attitude tracking of rigid bodies without angular velocity measurement. *Systems & Control Letters*, 61(4):595–601, Apr. 2012.

[82] Kurtis W. Schram. Vision-based control and autonomous landing of a vtol-uav. Master's thesis, Lakehead University, 2014.

[83] A. Seba, A. El Hadri, L. Benziane, and A. Benallegue. Multiplicative extended kalman filter based on visual data for attitude estimation. In *IEEE ICRA Workshop on Modelling, Estimation, Perception and Control of All Terrain Mobile Robots*, Hong Kong, China, May 31-June 7 2014.

[84] A. Seba, A. El Hadri, L. Benziane, and A. Benallegue. Attitude estimation using line-based vision and multiplicative extended kalman filter. In *International Conference on Control, Automation, Robotics and Vision (ICARCV)*, Marina Bay Sands, Singapore, Dec 10-12 2014.

[85] M.D. Shuster. A survey of attitude representations. *The Journal of the astronautical science*, 41(4):439–517, October-December 1993.

[86] M.D. Shuster. The triad algorithm as maximum likelihood estimation. *Journal of the Astronautical Sciences*, 54(1):113–123, January-March 2006.

[87] M.D. Shuster and S.D. Oh. Three-axis attitude determination from vector observations. *Journal of Guidance and Control*, 4(1):70–77, january-february 1981.

[88] J. Simanek, M. Reinstein, and V. Kubelka. Evaluation of the ekf-based estimation architectures for data fusion in mobile robots. *IEEE/ASME Transactions on Mechatronics*, 20(2):985–990, April 2015. ISSN 1083-4435.

[89] Larry Smith. *Linear Algebra*. 3rd edition, 1998.

[90] H. Ersin. Soken and Chingiz Hajiyev. Rekf and rukf for pico satellite attitude estimation in the presence of measurement faults. *Journal of Systems Engineering and Electronics*, 25(2):288–297, April 2014.

[91] Mark W. Spong, Seth Hutchinson, and M. Vidyasagar. *Robot Modeling and Control*. Wiley, 2005.

[92] S. Tanygin and MD. Shuster. The many triad algorithms. In *AAS/AIAA*, pages 81–99, 2007.

[93] A. Tayebi, S. McGilvray, A. Roberts, and M. Moallem. Attitude estimation and stabilization of a rigid body using low-cost sensors. In *46th IEEE Conference on Decision and Control (CDC)*, pages 6424–6429, 2007.

[94] A. Tayebi, A. Roberts, and A. Benallegue. Inertial measurements based dynamic attitude estimation and velocity-free attitude stabilization. In *American Control Conference (ACC)*, pages 1027–1032, San Francisco, CA, USA, June 29 - July 01 2011.

[95] A. Tayebi, A. Roberts, and A. Benallegue. Inertial vector measurements based velocity-free attitude stabilization. *IEEE Transactions on Automatic Control*, 58(11):2893–2898, Nov. 2013. ISSN 0018-9286.

[96] Abdelhamid Tayebi. A velocity-free attitude tracking controller for rigid spacecraft. In *46th IEEE Conference on Decision and Control (CDC)*, 2007.

[97] Abdelhamid Tayebi. Unit quaternion-based output feedback for the attitude tracking problem. *IEEE Transactions on Automatic Control*, 53(6):1516–1520, Jul. 2008.

[98] Abdelhamid Tayebi and Stephen McGilvray. Attitude stabilization of a vtol quadrotor aircraft. *IEEE Transactions On Control Systems Technology*, 14(3):562–571, May. 2006.

[99] Divya Thakur. *Adaptation, Gyro-Free Stabilization, and Smooth Angular Velocity Observers for Attitude Tracking Control Applications*. PhD thesis, The University of Texas at Austin, Aug. 2014.

[100] Divya Thakur and Maruthi R. Akella. Gyro-free rigid-body attitude stabilization using only vector measurements. *AIAA Journal of Guidance, Control, and Dynamics*, pages 1–8, 2014.

[101] Divya. Thakur, Maruthi R. Akella, and Frederic Mazenc. Partial lyapunov strictification: Smooth angular velocity observers for attitude tracking control. *Journal of Guidance, Control, and Dynamics*, 38(3):442–451, 2015.

[102] J. Thienel and R.M. Sanner. A coupled nonlinear spacecraft attitude controller and observer with an unknown constant gyro bias and gyro noise. *IEEE Transactions on Automatic Control*, 48(11):2011–2015, Nov 2003. ISSN 0018-9286.

[103] P. Tsiotras. Further passivity results for the attitude control problem. *IEEE Transactions on Automatic Control*, 43(11):1597–1600, Nov. 1998. ISSN 0018-9286.

[104] Panagiotis Tsiotras. Stabilization and optimality results for the attitude control problem. *Journal of Guidance, Control, and Dynamics*, 19(04):772–779, July-Aug. 1996.

[105] B.L. van der Waerden. *Algebra*. Frederick Ungar Publishing Co., New York, 1970.

[106] J.F. Vasconcelos, C. Silvestre, P. Oliveira, P. Batista, and Cardeira B. Discrete time-varying attitude complementary filter. In *American Control Conference (ACC)*, pages 4056–4061, Hyatt Regency Riverfront, St. Louis, MO, USA, June 10-12 2009.

[107] J.F. Vasconcelos, B. Cardeira, C. Silvestre, P. Oliveira, and P. Batista. Discrete-time complementary filters for attitude and position estimation: Design, analysis and experimental validation. *IEEE Transactions on Control Systems Technology*, 19(1):181–198, Jan 2011. ISSN 1063-6536.

[108] J.F. Vasconcelos, G. Elkaim, C. Silvestre, P. Oliveira, and B. Cardeira. Geometric approach to strapdown magnetometer calibration in sensor frame. *IEEE Transactions on Aerospace and Electronic Systems*, 47(2):1293–1306, April 2011. ISSN 0018-9251.

[109] P. Vernaza and Daniel D. Lee. Rao-blackwellized particle filtering for 6-dof estimation of attitude and position via gps and inertial sensors. In *IEEE International Conference on Robotics and Automation (ICRA)*, pages 1571 – 1578, May 15-19 2006.

[110] J.T.-Y. Wen and K. Kreutz-Delgado. The attitude control problem. *IEEE Transactions on Automatic Control*, 36(10):1148–1162, Oct. 1991.

[111] H. Wong, M.S. de Queiroz, and V. Kapila. Adaptive tracking control using synthesized velocity from attitude measurements. *Automatica*, 37(6):947 – 953, 2001. ISSN 0005-1098.

[112] Bing Xiao, Qinglei Hu, and Peng Shi. Attitude stabilization of spacecrafts under actuator saturation and partial loss of control effectiveness. *IEEE Transactions On Control Systems Technology*, 21(6):2251–2263, Nov. 2013.

[113] F. Yacef, O. Bouhali, and M. Hamerlain. Adaptive fuzzy tracking control of unmanned quadrotor via backstepping. In *23rd IEEE International Symposium on Industrial Electronics (ISIE)*, pages 40–45, June 2014.

[114] M. Zamani, J. Trumpf, and Mahony. Nonlinear attitude filtering: A comparison study. *arXiv:1502.03990 [cs.SY]*, Feb 2015.

[115] Lijun Zhang, Huabo Yang, Heping Lu, Shifeng Zhang, Hong Cai, and Shan Qian. Cubature kalman filtering for relative spacecraft attitude and position estimation. *Acta Astronautica*, 105(1):254 – 264, 2014. ISSN 0094-5765.

[116] Zheng Zhu, Yuanqing Xia, and Mengyin Fu. Adaptive sliding mode control for attitude stabilization with actuator saturation. *IEEE Transactions on Industrial Electronics*, 58: 4898–4907, 2011.

[117] An-Min Zou and Krishna Dev Kumar. Adaptive attitude control of spacecraft without velocity measurements using chebyshev neural network. *Acta Astronautica*, 66:769–779, 2010.